Molecular Markers for the Murine Uterus

Thesis

UNRESTRICTED

Molecular Markers for the Murine Uterus

Laura O'Hara BA, MA (Cantab)

A thesis submitted for the degree of Master of Philosophy (MPhil) in the discipline of Biological Sciences, June 2006.

Based on experiments performed at the Department of Physiology, Development and Neuroscience (formerly Department of Anatomy), University of Cambridge.

DATE OF SUBMISSION 3 JULY 2006
DATE OF AWARD 27 NOVEMBER 2007

ProQuest LLC.
789 East Eisenhower Parkway
P.O. Box 1346
Ann Arbor, MI 48106 – 1346

Table of Contents

Figures and Tables

Chapter 3: Tissue type markers for the pseudopregnant mouse uterus

Chapter 4: Markers specific for uterine sub- component tissues

Abbreviations and acronyms used

6x LB	6x loading buffer
BMAL	Brain-muscle arnt-like
BSA	Bovine serum albumin
cDNA	Complementary deoxyribonucleic acid
CE	Catecholoestrogen
CL	Corpus luteum
CLOCK	Circadian locomotor output cycles kaput
Cox	Cyclo-oxygenase
Cry	Cryptochrome
C_t	Threshold cycle
cy-3	Cyanine 3-dNTP
cy-5	Cyanine 5-dNTP
DEPC	Diethylpyrocarbonate
DNA	Deoxyribonucleic acid
DNase	Deoxyribonuclease
dNTP	Deoxynucleotide triphosphate
E2	Oestradiol
EDTA	Ethylenediaminetetraacetic acid
EGF-R	Epidermal growth factor receptor
EP_2	Prostaglandin receptor E2 subtype EP_2
EP_3	Prostaglandin receptor E2 subtype EP_3
ER	Oestrogen receptor
FRET	Fluorescence resonance energy transfer
FSH	Follicle stimulating hormone
G (or GE)	Glandular Epithelium
GAPDH	Glyceraldehyde-3-phosphate dehydrogenase
gp130	G-protein coupled receptor 130
H&E	Haematoxylin and Eosin
H_2	Histamine
HB-EGF	Heparin-binding epidermal growth factor-like growth factor
HBSS	Hanks's buffered salt solution
HDC	Histidine decarboxylase
HOXA-10	Homeobox gene A-10
JAK	Janus kinase
LE	Luminal epithelium
LH	Leuteinising hormone
LIF	Leukaemia inhibitory factor
LIFRa	Leukaemia inhibitory factor receptor alpha
MAPK	Mitogen activated protein kinase
mRNA	messenger ribonucleic acid
Muc	Mucin
OSF-2	Osteoblast stimulating factor 2
P4	Progesterone
PBS	Phosphate buffered saline
PCR	Polymerase chain reaction
Per	Period
PGH_2	prostaglandin H2
PGI2	prostacyclin
PKC	Protein kinase C

Abbreviations and acronyms used

PPAR	peroxisome proliferator-activated receptor
PR	Progesterone receptor
QRT-PCR	Quantitative reverse transcription polymerase chain reaction
RNA	Ribonucleic acid
RNase	Ribonuclease
rRNA	Ribosomal ribonucleic acid
RT	Reverse transcription
RT-PCR	Reverse transcription polymerase chain reaction
S	Stroma
S&G	Stroma and glands
SAGE	Serial analysis of gene expression
SAM	Significance analysis of microarrays
SCN	Suprachiasmatic nucleus
SDS	Sodium dodecyl sulphate
SEM	Standard error of the mean
SSC	Saline sodium citrate
STAT	Signal transducer and activator of transcription
Tn-c	Tenascin-C
VEGF	vascular endothelial growth factor

Acknowledgements

Firstly, I am indebted to both my supervisors, Martin Johnson and Hilary MacQueen.

Thanks Martin for generously allowing me to do this as a part of my job and for persuading me that I was capable of it. Your encouragement and suggestions have been invaluable.

Thanks Hilary for your regular input, your encouragement and for giving me new perspectives on the experiments and the results.

Thanks to the rest of the Johnson group: Hamid Dolatshad, Catherine Aiken and especially Liz Campbell, who has taught me so many new techniques. Thanks to Andrew Sharkey for teaching me the ins and outs of real-time RT-PCR.

Thanks to Carolynn, Marie, Nora and Sam for being around when I needed an excuse for a cup of tea.

A thousand thanks to Andy, for love and banter.

This thesis is dedicated to my parents, Lynne and Steven O'Hara. For all your support and love throughout the last 25 years.

Abstract

The uterus of a mature female mammal undergoes hormonally initiated morphological and transcriptional changes during early pregnancy, preparing it for the implantation and subsequent nurturing of the developing embryo. Implantation involves a global change in gene expression that has not been fully elucidated. The uterus consists of layers of different types of tissue: the luminal epithelium confronts the uterine lumen and acts as a transducer between the blastocyst and the underlying uterine stroma. The stroma contains areas of glandular epithelium and is surrounded by two myometrial layers: one circular and one longitudinal. Each layer of the uterus is undergoing different transcriptional changes and these changes often involve communicating with the other uterine layers and the embryo.

The aim of this work was to identify and characterise molecular markers for the luminal epithelial, glandular epithelial and stromal layers of the uterus. Samples of uterine luminal epithelium and stroma/glands were obtained from mice on day 4 of pseudopregnancy using an enzyme treatment and mechanical extraction technique. Maternally controlled molecular markers of peri-implantation receptivity in the luminal epithelium (EP_2), glandular epithelium (LIF) and stroma (EP_3 and Tn-c) were characterised using real-time RT-PCR with Taqman® fluorogenic probes. Pure samples of each tissue were then obtained using laser microdissection, and were used first to verify the specificity of the markers, then to run a microarray study to identify more putative markers. Finally, the enzyme treatment and mechanical extraction technique with subsequent real-time RT-PCR using Taqman® was used to investigate the expression of canonical circadian genes (Bmal, Clock, Per1, Per2 and Cry1) in the luminal epithelium and stroma of the uterus. All genes were found to be expressed in the luminal epithelium and the stroma, but did not appear to have a circadian rhythm.

Chapter 1: Introduction

Summary

The uterus is a hollow muscular organ located in the pelvic cavity and posterior abdominal wall of female mammals in which the fertilized egg implants and develops. In rodents the uterus is split into two horns that join at the cervix to enter the vaginal vault, but in humans the two horns have become completely united into a single hollow structure with a single cervical communication to the vagina. The uterus is a complex organ both anatomically and temporally. It consists of layers of different tissue types, all morphologically and biochemically distinct. When mature, the uterus of a mature female mammal undergoes hormonally initiated morphological and transcriptional changes called the oestrous cycle that prepare it first for sperm transport and capacitation. The uterus then becomes prepared for the implantation and subsequent nurturing of the developing embryo, should fertilisation occur. These many layers of complexity have made the uterus difficult to study in the past. This dissertation will focus on the transcriptional changes that take place around the time of implantation.

Implantation is the most important time in early pregnancy. If a fertilised embryo arrives in a uterus that is not prepared for implantation then the pregnancy will fail. This preparation involves a global change in gene expression that has not been fully elucidated. To further complicate matters, each layer of the uterus is undergoing different transcriptional changes and these changes often involve communicating with the other uterine layers and the embryo, as discussed in section 1.2.2. The ultimate aim of this research is to characterise maternally controlled molecular markers of peri-implantation receptivity in the different tissue types in the uterus of the mouse. Ethical and technical problems with experiments into human implantation mean that animal models are generally preferred.

The mouse is a useful model organism in reproductive biology. It is easy to keep in large numbers due to its relatively small size and short reproductive life cycle, yet it is mammalian so resembles human anatomy and physiology sufficiently. It also has an almost completely sequenced genome, which makes it very useful for molecular genetics. Its high fecundity permits large numbers of mice with the same traits to be bred relatively quickly and easily. Inbred strains are also readily available. There are quite large physiological and gross anatomical differences (discussed in section 1.2) between human and mouse uteri. However the genetic control of reproduction seems well conserved in mammals and both species have a similar invasive implantation mechanism. Mouse genetic studies are a powerful tool as its genome is well-characterised and large scale studies are relatively easy to do. This gives the mouse its advantage as a model organism in reproductive biology (Lee and Demayo, 2004).

1.1: Structure of the uterus

The mouse uterus is bicornuate, having two uterine horns and a short stem where the two horns join. The stem leads to the cervix and vagina, the other ends of the horns are continuous with the two oviducts. Spatially the uterus is composed of different tissue types in radial layers (see Figure 1.1). The layers of the uterus can be seen clearly when a transverse section is viewed under the microscope. Each layer has distinct roles but they work together to contribute to the function of the uterus as a whole organ. The circular and longitudinal muscles of the myometrium allow the changes in size, shape and motility of the uterus that occur during the cycle, pregnancy and subsequent parturition. The stroma is the tissue that forms the main decidual interface between the mother and the embryo during pregnancy in mice and humans (but not in the early stages of ungulate development in which the luminal epithelium remains intact). The glandular epithelium secretes fluid into the uterine cavity during the oestrous cycle and pregnancy. This fluid may contain proteins, lymphatic cells, hormones and signalling molecules depending on the endocrine state of the uterus. The luminal epithelium is at the heart of the complexity of the uterus as it confronts the uterine lumen, through which both spermatozoa and embryo must pass before implantation. The cells of the endometrium (mainly the stromal cells) become the decidual cells of the placenta during the early stages of pregnancy.

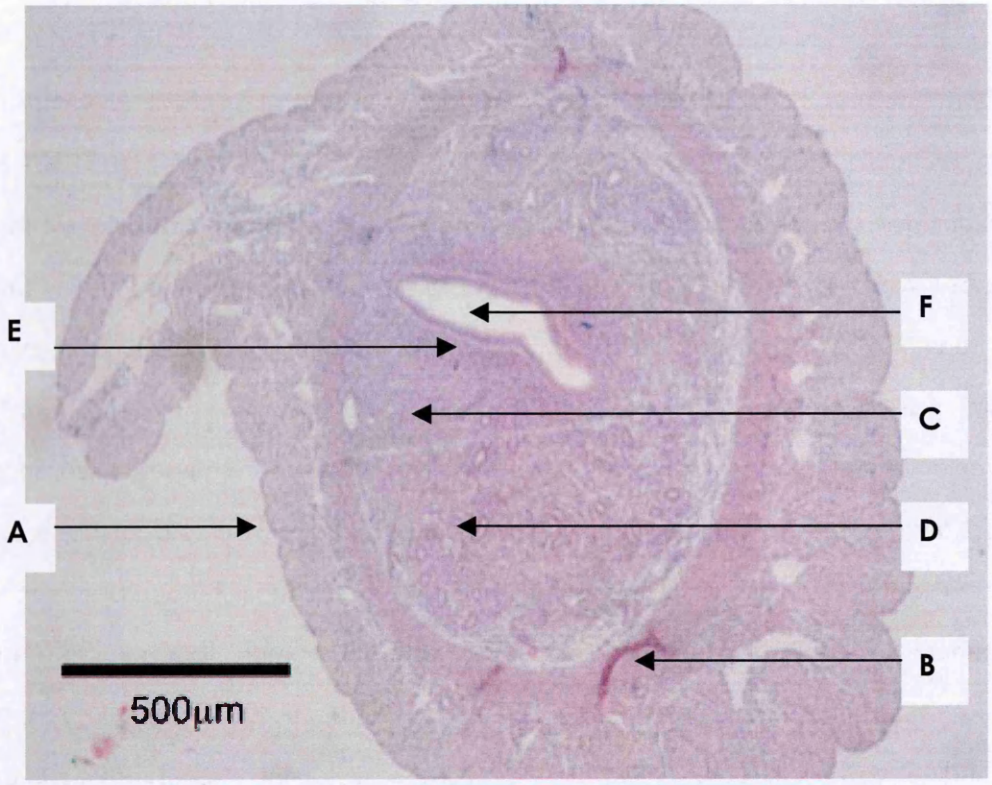

Figure 1.1: Transverse H&E stained section through the murine uterus. *The outer mesenchymal layer (A) interposes between the uterus and the peritoneal cavity and is thickened into a mesometrial layer attaching the uterus to the posterior abdominal wall and through which blood vessels pass. The myometrium (B), situated inside the mesenchyme, is composed first of a layer of longitudinal smooth muscle, then a layer of circular smooth muscle. The endometrium, which lies inside the musculature, consists of a mesenchymal stroma (C) containing glandular invaginations (D) of the innermost l layer, the uterine luminal epithelium (E), which confronts the uterine lumen (F).*

1.2: Temporal changes of the uterus

1.2.1: The oestrous cycle

Over time, the uterus changes under the influence of hormones. The oestrous cycles of mammals are based around changing levels of the hormones luteinising hormone (LH), follicle stimulating hormone (FSH), oestradiol (E2, an oestrogen) and progesterone (P4), as illustrated in Figure 1.2.

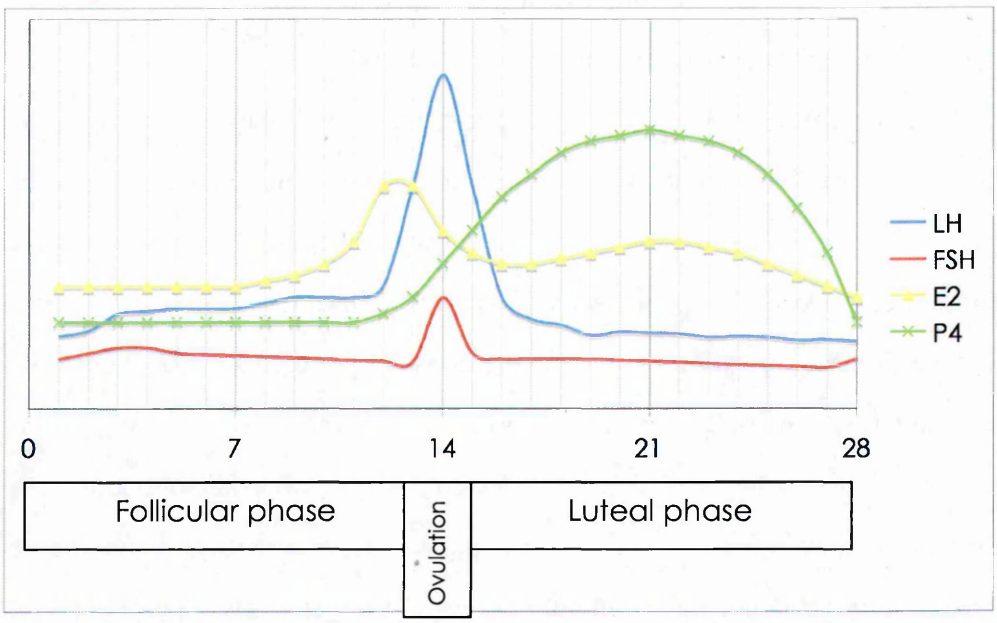

Figure 1.2: Levels of progesterone (P4), oestradiol (E2) follicle-stimulating hormone (FSH) and luteinising hormone (LH) during the human menstrual cycle.

Humans have a 28-day menstrual cycle (Wang and Dey, 2006). Just before menstruation (day 1), E2 and P4 levels are low. Moderate levels of E2 and P4 inhibit LH and FSH so levels of these two gonadotrophins begin to rise. The increasing concentrations of FSH and LH lead to growth of ovarian follicles that are nearing maturity (antral follicles). Maturing antral follicles secrete E2, which has a negative feedback effect on FSH and LH and prevents further rise. Contrary to the inhibitory

effects of small rises in E2 on FSH, a large increase in E2 causes positive feedback and an increase of FSH and LH levels. When a dominant follicle is selected for ovulation a large rise in oestrogen causes a rapid rise in LH and FSH and ovulation occurs. After ovulation, oestrogen levels begin to fall and the corpus luteum ('CL', the post-ovulatory follicle) secretes progesterone. This again represses FSH and LH levels. The CL starts to secrete some oestrogen and levels rise slightly. The combined effect of E2 and P4 stops LH and FSH levels from rising and antral growth from resuming, until the corpus luteum ceases to be functional and secrete these two hormones. Menstruation occurs and the cycle begins again (Johnson and Everitt, 2000).

The mouse has a 4-5 day oestrous cycle where both the follicular and luteal phases are abbreviated if mating does not occur. In the mouse, maturation of ovarian follicles takes place over the course of several cycles because FSH and LH levels do not fall to negligible levels during the luteal phase. The length of luteal phase depends on mating occurring during oestrus. If mating does not occur, the luteal phase is only two to three days long and the corpora lutea secretes a small amount of progesterone only. If a female mates with a vasectomised male she will enter a phase called 'pseudopregnancy' which lasts for approximately 12 days under the duration of the functional corpora lutea. The maternal hormonal changes in early pregnancy and pseudopregnancy are induced by mechanical stimulation of the cervix inducing the release of prolactin by the pituitary gland, which causes maturation of the corpora lutea. The short cycle time maximises the number of opportunities for pregnancy during the short reproductive life of the mouse.

There are four stages of the mouse oestrous cycle: dioestrus, pro-oestrous, oestrus and metoestrus. Each stage lasts for approximately one day. Although the oestrous cycle of rodents is much shorter than that of humans, the temporal relationships of oestradiol, LH and FSH secretion are very similar. The difference is in

the secretion of progesterone, which is rises and falls more rapidly after the LH/FSH surge, then begins to rise again if the animal enters an extended luteal phase. During dioestrus, the uterine epithelial cells are in a quiescent 'G_0' phase as levels of oestrogen begin to increase. The luminal epithelium is not receptive to embryo implantation in this phase. As the level of oestrogen rises, epithelial cells re-enter the cell cycle and begins to replicate their DNA. During this proliferative phase (pro-oestrus), the luminal epithelium increases in surface area and metabolic activity, and secretes proteins into the uterine lumen. The proliferation continues into oestrus (during which ovulation occurs), and results in the uterus becoming distended with fluid; this can be observed macroscopically. These changes prepare the uterus to receive, transport and capacitate spermatozoa (Johnson and Everitt, 2000). The rising oestrogen levels also affect the female's behaviour, making her receptive to males. The surge of LH and FSH takes place between 5 and 7 hours before darkness to ensure that ovulation and the receptive period begin at around midnight, in the middle of the mouse active period. If mating does not occur, after ovulation, the oestrogen level falls, mitosis stops and the uterine wall together with the luminal and glandular epithelia begin to degenerate (metoestrus). The proliferative cycle then begins again. The oestrous cycle can be followed in mice by analysis of the cells lining the vagina (section 2.2.2).

1.2.2: The peri-implantation period

Mating in mice usually takes place during the early hours of the morning. Mating can be confirmed by the presence of a plug of coagulated semen at the entrance to the vagina (see section 2.2.3). The day the plug is seen can be designated day 0, 0.5 or 1 of pregnancy, the notation used depending conventionally (and confusingly!) on the type of study being undertaken. Uterine studies usually designate the day of plug as day 1 and this will be the notation used

in this Thesis. After mating takes place, sperm move through the uterus and meet the egg in the ampulla of the oviduct, where fertilisation occurs. The fertilised embryo then begins to divide and moves down the oviduct to enter the uterus on day 3. There, it becomes a blastocyst and, in preparation for implantation, loses its zona pellucida due to the action of uterine proteases, (Johnson and Everitt, 2000). The hormonal synchronisation of the movement of the embryo and receptivity of the uterus coincides in a 'window of implantation'. In the mouse this begins around 2200-2300 h on day 4 of pregnancy and lasts for around 24 hours. Prior to this window, the uterus is pre-receptive and after it, the uterus loses its receptivity and enters a refractory period where implantation cannot occur (Dey et al., 2004). This restricted period of receptivity has led the uterus to be described as a relatively hostile site for the embryo when it is not receptive. It is thought that this is to protect the mother from the potentially dangerous invasive characteristics of trophoblast, which behaves much like a malignant tumour during implantation (Soundararajan and Jagannadha Rao, 2004).

Implantation in the mouse involves three stages: apposition, adhesion and penetration (Carson et al., 2000). During apposition the trophectoderm of the developing blastocyst becomes closely apposed to the luminal epithelium. Adhesion involves an attachment reaction that results in the inability to dislodge the blastocyst from the luminal epithelium by flushing the uterus. At this stage the luminal epithelium (LE) acts as a transducer signalling the embryo's presence locally to the underlying stroma to initiate the decidual response and increase the local vascularisation. During subsequent penetration, the trophectoderm invades through the LE into the decidualising stroma, which contains and nourishes the embryo. The residuum of the epithelium and the underlying decidualised stroma form the maternal component of the placenta.

The steroid hormones progesterone (P4) and oestrogen work in a spatio-temporal manner to establish the window of implantation (DeMayo et al., 2002).

The major ovarian oestrogen is oestradiol (E2). Steroid hormone receptors are present in the cytoplasm of the cells that express them. The hormone/receptor complex translocates to the nucleus and can regulate transcription of genes by binding to response elements in their promoter regions. There are two different types of oestrogen receptor (ER), oestrogen receptor alpha (ERα) and oestrogen receptor beta (ERβ). ERα is the predominant ER expressed in the uterus. In early pregnancy, ERα is primarily expressed in the luminal epithelium. During the peri-implantation period, expression generally increases in the uterine stroma but levels decrease in the stroma at the site of implantation. The progesterone receptor (PR) exists in two isoforms known as PRA and PRB. Levels of both are low in early pregnancy but increase in both epithelium and stroma during the implantation period. Expression of ER and PR is self-regulated as well as being regulated by the steroid hormones themselves. Both ER and PR null mutant mice are infertile and exhibit pleiotropic reproductive abnormalities (DeMayo et al., 2002).

The pre-ovulatory oestrogen rise causes epithelial cells to proliferate, as described in section 1.2.1. Mating induces the corpus luteum to secrete progesterone via the action of prolactin (Johnson and Everitt, 2000). Rising progesterone levels initiate stromal cell proliferation around day 3 of pregnancy. On day 4 a small amount of oestrogen secreted from the murine ovary (nidatory oestrogen), further stimulates stromal cell proliferation. This secondary release of oestrogen is vital for the timing of the window of implantation, having effects on both the endometrium and the blastocyst. Delayed implantation will occur (and the blastocyst will stop dividing and become dormant) if the ovaries are removed before the morning of day 4 and the uterus is kept primed with systemic injections of progesterone. Implantation can then be re-started with a single injection of oestrogen (Dey et al., 2004). The full effects of progesterone and nidatory oestrogen are not clear but genes affected by ovarian steroids have been identified by: observing reproductive phenotypes of mutant mice, library screening

and (more recently) microarray studies. These studies are discussed in 1.3.2. There is also evidence that catecholoestrogen (CE), a metabolite of nidatory oestrogen, may act directly on the blastocyst itself (Paria et al., 1998b).

The variety of genes involved in implantation includes the genes encoding cytokines, adhesion molecules, growth factors, developmental genes and vasoactive factors. Genes expressed around the time of implantation are either maternally controlled (transcriptionally regulated by oestrogen and progesterone) or controlled by the cross-talk between the blastocyst and the epithelium from the time of blastocyst apposition at the luminal epithelium.

Maternally controlled gene expression:

LIF and its downstream effects

The cytokine Leukaemia Inhibitory Factor (LIF) is vital for the initiation of implantation. Blastocysts cannot implant in the uteri of *LIF* null mutant mice, nor do their uteri undergo decidualisation (Chen et al., 2000). *LIF* is induced by nidatory oestrogen. It is produced by the glandular epithelium on day 4 of pregnancy and secreted into the uterine lumen (Bhatt et al., 1991). It binds to the heterodimeric LIF receptor present on the apical luminal epithelium. Binding of LIF to the transmembrane protein LIF receptor alpha (LIFRα) causes dimerisation of the receptor with gp130 and activation of a number of downstream pathways including the mitogen-activated protein kinase (MAPK) pathway, the protein kinase C (PKC) pathway and the JAK/STAT signalling pathway. The JAK/STAT pathway in the luminal epithelium is thought to be the primary mediator of LIF signalling in implantation. Deletion of the cytoplasmic domain in gp130 selectively abolishes the activation of the JAK/STAT pathway and results in failure of implantation, and luminal epithelium incubated with LIF in vitro selectively activates

the JAK/STAT pathway and not the MAPK pathway. This evidence does not rule out the contribution of the other pathways or tissues to the transmission of LIF signalling during implantation, Binding of interleukin-11 (IL-11) to its receptor also causes its dimerisation with gp130 and activation of the MAPK and JAK/STAT pathways.

Binding of the appropriate ligand ,phosphorylates the signal transducer Stat3 which then enters the epithelial cell nucleus and acts as a transcription factor (Cheng et al., 2001). This signalling cascade induces the expression of many genes involved in early pregnancy, including vitally important ones, as inhibition of Stat3 activation in the endometrium has been shown to prevent implantation (Catalano et al., 2005). *LIF* null mutant mice show absent or aberrant expression of several genes known to be involved in implantation (Song et al., 2000) (Fouladi-Nashta et al., 2005), including *Heparin-binding epidermal growth factor-like growth factor (HB-EGF), Amphiregulin, Cyclo-oxygenase-2 (Cox-2), Homeobox gene A10 (Hoxa-10)* and *Tenascin (Tn-c)* (molecules discussed below). *LIF* null mutant mice also show aberrant uterine physiology: animals fail to develop apical pinopods and have an increased glycocalyx (Fouladi-Nashta et al., 2005). An injection of LIF has been shown to restart delayed implantation as a substitute for oestrogen, implying that the actions of nidatory oestrogen that are vital to implantation are mediated through the *LIF* signalling pathway (Chen et al., 2000).

Hoxa-10 and its downstream effects

Another uterine gene up-regulated by ovarian steroids is *Hoxa-10. Hoxa-10* is a member of the *Homeobox* family of transcription factors, which are important in segmentation patterning in early development; *Hoxa-10* null mutant mice have a transformation of the proximal 25% of the uterus into oviduct (Benson et al., 1996). *Hoxa-10* levels are up-regulated in the stroma by progesterone on late day 3 of pregnancy (Ma et al., 1998) and *Hoxa-10* mutant mice show reduced stromal cell proliferation in response to progesterone, leading to decidualisation defects (Lim et

al., 1999b). This evidence implies that *Hoxa-10* is involved in the regulation of cell cycle gene expression, backed up by studies that showed aberrant expression of cyclins (Yue et al., 2005) (Das et al., 1999) and cyclin dependent kinases (Rahman et al., 2006) in the stroma cells of *Hoxa-10* null mutant mice. Other genes aberrantly expressed in *Hoxa-10* null mutant uteri include *Cox-2* and *Prostaglandin receptor E2 subtypes EP_3 and EP_4* (Lim et al., 1999b), implying that *Hoxa-10* has an effect on lipid signalling pathways during implantation, though this has not been fully investigated. Hoxa-10 is also known to induce the expression of uterine epithelial *b3 integrin* subunit (of which more is discussed below) in human cells *in vitro* (Daftary et al., 2005).

Adhesion factors and glycoproteins on the luminal epithelium:

There are numerous molecules present on both the apical membrane of epithelial cells and the trophoblast of the blastocyst that may mediate the attachment of the embryo to the uterine luminal epithelium. These complex patterns of expression are reviewed in two comprehensive reviews (Aplin, 1997) (Kimber and Spanswick, 2000). Some molecules mediate adhesion, others block it until the uterus is ready. One of the more numerous types of adhesion molecules in implantation is the integrin family. Integrins are heterodimeric transmembrane glycoproteins, consisting of an alpha and a beta subunit, found in both the receptive luminal epithelium and the hatched blastocyst (Bowen and Hunt, 2000). Integrins can bind other integrins and to a wide variety of extra-cellular matrix proteins found on both blastocyst and LE, including Laminin, Heparan sulphate proteoglycan (HSPG) and Oncofetal fibronectin on the trophoblast (Kimber and Spanswick, 2000). The uterine integrin best characterised in implantation is $\alpha v\beta 3$, found in the apical membrane of epithelial cells. *$\alpha v\beta 3$ integrin* is up-regulated by Hoxa-10 (Daftary et al., 2005), and injection of an antibody to block $\alpha v\beta 3$ integrin resulted in reduced implantation (Illera et al., 2000).

Other glycoprotein molecules present on the luminal epithelium have a restrictive role in implantation. Muc-1 is a large glycoprotein found in the apical luminal epithelium during the oestrous cycle and early pregnancy. It prevents embryo apposition at the luminal epithelium due to its large, highly branched structure. *Muc-1* is up-regulated by oestrogen but down-regulated by progesterone, so it is present during the oestrous cycle and early pregnancy when the uterus is not ready for implantation, but is repressed at the beginning of the implantation window to allow apposition to proceed (Surveyor et al., 1995).

Other genes have been found to be regulated by maternal oestrogen and progesterone during the pre-implantation period, but they are often not as well characterised as those discussed above. These genes are discussed more thoroughly in two excellent reviews (Dey et al., 2004) (Lee and Demayo, 2004) and the pathways above are illustrated in Figure 1.3.

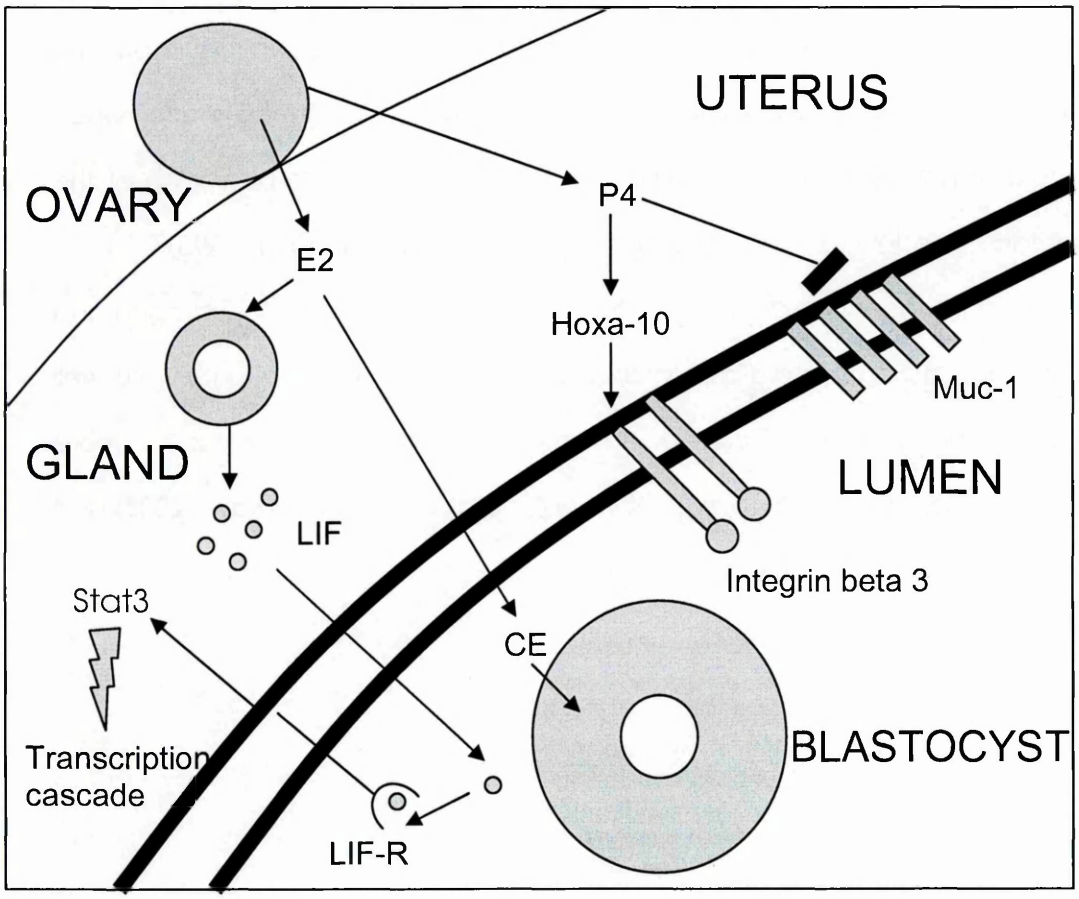

Figure 1.3: A few of the many pre-implantation signalling events in the uterus

E2 also affects the stroma but for clarity this pathway has been omitted from the diagram. Key to abbreviations: CE= catecholoestrogen, E2= oestrogen, LIF= leukaemia inhibitory factor, LIF-R= leukaemia inhibitory factor receptor, Muc-1= mucin1, P4= progesterone, Stat3= signal transducer and activator of transcription 3.

Signalling between blastocyst and uterus during implantation

The interaction of the blastocyst with the luminal epithelium during attachment initiates further molecular signalling between the blastocyst and the epithelium and thereby the stroma. This signalling initiates the invasive procedure of implantation and the massive signalling cascade that is involved in decidualisation of the stroma and the increase in vascular permeability to prepare the uterus for the invasion of the implanting blastocyst.

Heparin-binding epidermal growth factor-like growth factor (HB-EGF)

HB-EGF is thought to be the earliest uterine gene regulated directly by the presence of the blastocyst. It has been found to be expressed in the luminal epithelium surrounding the blastocyst 6-7 hours before the onset of the attachment reaction, but is not expressed in a progesterone-maintained model of delayed implantation, nor in a pseudo-pregnant uterus (Das et al., 1994b). The embryo is still contained within the zona pellucida at the onset of *HB-EGF* expression, ruling out direct interaction as the trigger for expression. These observations led to the conclusion that expression of *HB-EGF* is induced by a factor secreted in the presence of an activated embryo in the luminal epithelium before attachment. The nature of this factor has not been discovered. HB-EGF is known to bind to a receptor called EGF-R, a member of the *ErbB* family of growth factor receptors (Raab et al., 1996) found on the surface of the blastocyst (Paria et al., 1993). Binding to the EGF-R receptor causes its phosphorylation and induces blastocyst hatching and trophoblast outgrowth (Mishra and Seshagiri, 2000). Ovariectomy on the morning of day 4 of pregnancy down regulates the expression of EGF-R on the blastocyst surface (Paria et al., 1993), and HB-EGF in the uterus (Wang et al., 1994). Both are restored with an injection of oestrogen to resume implantation. This evidence implies that HB-EGF binds to blastocyst cells to promote the preparation of the embryo for implantation, but only when the uterus is hormonally prepared.

HB-EGF is found in both a membrane bound precursor form and a mature soluble form, as described in the references above. HB-EGF is present in the luminal epithelium in a membrane bound form around the time of implantation, and blastocysts adhere to cells expressing the membrane bound form, implying that the interaction is important for juxtacrine signalling during apposition. But the mature form must also play a part in paracrine signalling between the embryo and the uterus before apposition, as downstream effects become apparent before the hatching of the blastocyst. The interaction between embryo and uterus via the EGF-R signalling pathway is a good example of peri-implantation cross talk. EGF-R is also found in the stroma of the hormonally prepared uterus (Das et al., 1994a), implying another role for secreted HB-EGF, though this has not been fully investigated. HB-EGF is also found in human endometrium during the window of implantation. Other growth factors such as Beta-regulin, Epiregulin and Neuregulin are induced in the uterus around the time of attachment, slightly later than HB-EGF.

Vasoactive factors

One of the first signs of implantation is an increase in vascular permeability at implantation sites (reviewed in (Dey et al., 2004). Molecules involved in angiogenesis play an important role in forming the placenta during decidualisation of the stroma. Two well-characterised molecules involved in angiogenesis are cyclo-oxygenase (Cox) and vascular endothelial growth factor (VEGF).

Cox is an enzyme that converts arachidonic acid into prostaglandin H_2 (PGH_2). Individual prostaglandin synthases then act on PGH_2 to form several structurally similar yet biologically diverse prostaglandins, which have many functions in female reproduction, including angiogenesis in the decidualising stroma. Cox exists in two forms, both present in the peri-implantation uterus. Cox-1 is a constitutively expressed enzyme, found in epithelial cells pre-implantation but disappearing from the uterus around implantation (Chakraborty et al., 1996). *Cox-1*

null mutant mice are fertile, but have problems with parturition (Lim et al., 1997). Cox-2 is inducible, its expression triggered by the actions of both maternally regulated genes (such as *LIF*), and the presence of the activated blastocyst. It is up-regulated in hormonally activated luminal epithelium and subepithelial stromal cells at the anti-mesometrial pole exclusively surrounding the blastocyst at the time of attachment reaction on day 4 and the morning of day 5 (Chakraborty et al., 1996). *Cox-2* null mutants are infertile, exhibiting pleiotropic reproductive anomalies (including failure of implantation and decidualisation), which have led it to be implicated as an important factor in implantation. These abnormalities are due to the lack of the prostaglandins produced by Cox-2, as fertility was restored with their injection into the uterus (Lim et al., 1997). Prostacyclin (PGI_2) is the most abundant prostaglandin expressed at the implantation site. It exerts its effects through the Peroxisome proliferater-activated receptor-δ (PPAR-δ). Both *PPAR-delta* and *Prostacyclin synthase* are co-expressed with PGI_2 at the implantation site, implying an important role for this signalling pathway in implantation (Lim et al., 1999a).

Cox-2 derived prostaglandins are thought to influence the signalling pathway of vascular endothelial growth factor (VEGF) (Matsumoto et al., 2002). VEGF was known to be a growth factor involved in angiogenesis, so its expression during implantation was investigated. There are low levels of *VEGF* present in the uterus before implantation, but the attachment of the blastocyst induces strong up-regulation of this signal in the luminal epithelium and peri-epithelial stroma. Expression of the VEGF receptor is also induced with the presence of the implanting blastocyst (Chakraborty et al., 1995).

Histidine decarboxylase (HDC) is an enzyme that produces Histamine (H_2) from L-histidine. Histamine is a ubiquitous cell-cell mediator found in a diverse range of biological processes including inflammation, angiogenesis and smooth muscle contraction. Rising levels of progesterone during early pregnancy cause up-regulation of HDC expression in the luminal and glandular epithelia of the uterus.

Levels peak at day 4 and then start to fall during decidualisation. Pseudo-pregnant mice exhibit a similar pattern, proving that the presence of a blastocyst is not needed for expression (Paria et al., 1998a). Despite this, histamine H_2 receptors are present on the surface of embryos, and H_2 antagonists or an HDC inhibitor inhibit hatching and implantation. H_2 receptors are not present on the blastocyst surface during delayed implantation. This suggests that histamine is involved in communication with the blastocyst and induces it to mature in preparation for implantation (Zhao et al., 2000).

The pathways discussed above are just a few of the signalling pathways initiated by cross-talk between the uterus and the blastocyst and are illustrated in Figure 1.4.

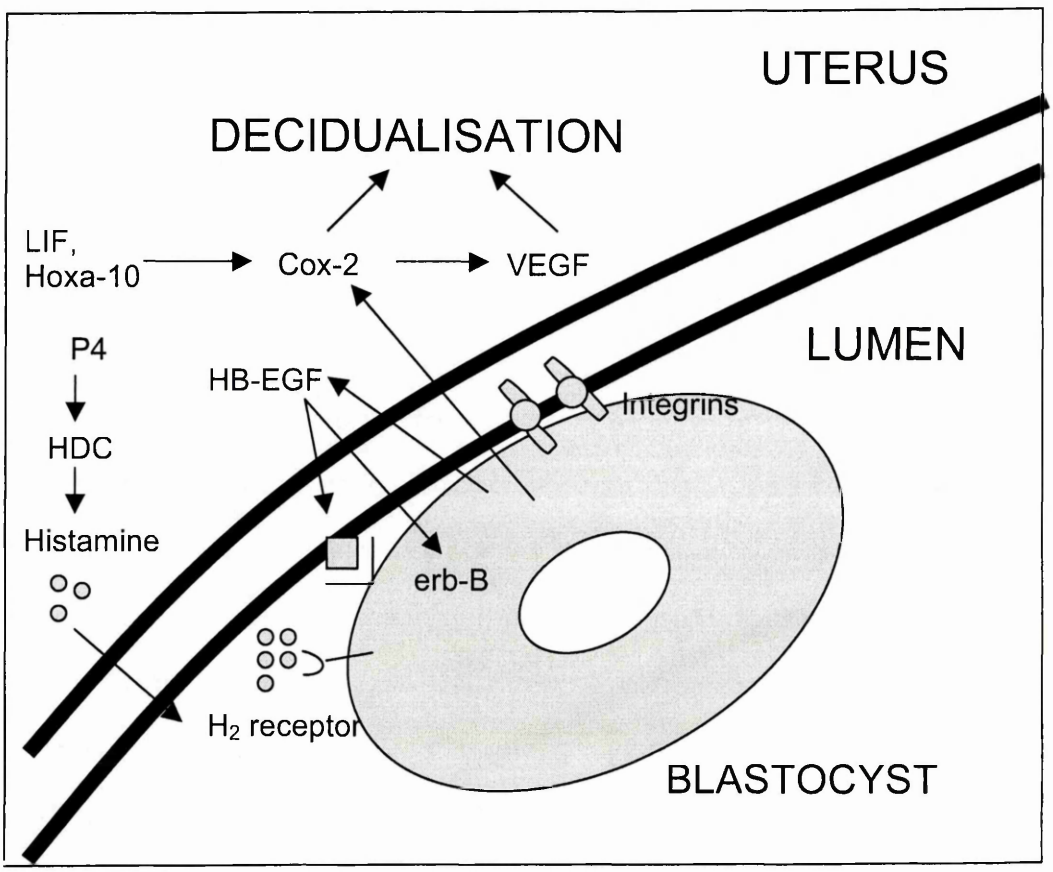

Figure 1.4: A few of the many signalling events during blastocyst attachment and implantation. *Key to abbreviations: Cox-2= cyclo-oxygenase 2, erb B= epidermal growth factor receptor, H_2 receptor= histamine receptor, HB-EGF= heparin-binding epidermal growth factor, HDC= histamine decarboxylase, Hoxa-10= homeobox a-10, LIF= leukaemia inhibitory factor, P4= progesterone, VEGF= vascular endothelial growth factor.*

As described above, the transcriptional changes in the uterus around the time of implantation may be controlled by the hormonal response to mating, initiated by the presence of the embryo at attachment, or in many cases result from a complex interplay between maternal gene expression and interaction with the activated blastocyst. Activation pathways of genes involved in decidualisation are often complex, for example *Cox-2* expression is affected in *LIF* and *Hoxa-10* null mice, as well as being induced by the presence of an activated blastocyst as discussed above. Moreover, both direct and down-stream indirect changes occur in rapid succession, making fine-grained temporo-spatial analysis difficult. To reduce complexity and separate these two responses, pseudo-pregnant mice were used in my studies. Pseudo-pregnant mice are female mice mated with a vasectomised male. The mechanical stimulus of mating causes the mouse to undergo the hormonal changes detailed above, but the absence of fertilised embryos means maternal gene expression pathways initiated by and down-stream of the embryo will not occur. Pseudo-pregnancy can continue for up to 10 days before a normal oestrous cycle is resumed; it is the equivalent of the human luteal phase. The techniques, results and conclusions of some of the previous studies into gene expression in the uterus are discussed below in section 1.3.2.

1.3: Studying changes in transcription in the uterus

When studying gene expression in an organ as complex as the uterus, three broad questions can be asked initially. Where and when are the genes expressed, and at what levels are they expressed in these tissues? Answers to these questions are important for the conduct of experimental studies to address function and regulation.

One of the more traditional methods of investigating both the level and location of expression of a gene of interest is *in situ* hybridisation. Other methods of looking at gene expression involve either homogenising the whole tissue, or dissecting certain parts of the tissue out, before extracting the RNA population of the tissue (either total RNA or just mRNA), then using this RNA in downstream applications described below. These applications are mostly directed towards one or two genes of interest, but if the aim of the study is to identify new genes of interest when none are known already, then microarrays can be used. The methods used can either be semi-quantitative, where an idea of the levels of gene expression can be obtained (even if it is on a scale of absent or present i.e. below or above the detection threshold of the technique) or quantitative, where levels of gene expression in one tissue can be accurately compared to another tissue or even measured absolutely. The range of technical approaches is discussed below, then summarised in Table 1.1. Other studies looking at gene expression in the uterus in a variety of states are also discussed. The techniques, results and conclusions of some of the previous studies into gene expression in the uterus are discussed below in section 1.3.2.

Although looking at transcriptional control in gene expression is fundamental to unravelling the processes of implantation, the control of translation and post-translational modification of the proteins is an important yet relatively neglected area in the research. A gene can be constitutively expressed at the

mRNA level but be translated only under certain conditions, or can be constitutively translated but its activity modified by phosphorylation or cleavage activation under certain conditions. Although this dissertation will not directly address these circumstances, it is important that they are considered when analysing results.

1.3.1 Techniques used in studying gene expression

In whole tissues

In-situ hybridisation

The traditional method of localising gene expression in an organ is *in situ* hybridisation. This involves using radioactive or dye labelled probes for the RNA of interest and hybridising the probe to thin sections of tissue so that specific sites of expression can be identified, even down to the location of transcripts in individual cells. The advantage of this method is that it is very useful when looking at a heterogeneous tissue where the site of expression of your gene of interest is unknown. The disadvantage of this method is that it is often of low sensitivity and probes can bind non-specifically giving false positive results, making *in situ* hybridisation difficult to set up and optimise. The size of the transcript being localised (and thus its processing state and/or actual identity) is also not deducible from the results.

RNA obtained from tissues: known transcript of interest

Northern blotting

Northern blots are used to show whether an RNA species of interest is present in a tissue. RNA is run on a denaturing agarose gel, blotted onto a nitrocellulose membrane, cross-linked, then probed with a labelled hybridisation probe

complementary to the gene of interest. This can be used to show whether a transcript is present in the tissue and the size of the RNA of interest (when compared against size standards run simultaneously). Northern blots can also be used to quantify the relative amount of the transcript present by relating the intensity of the band to the intensity of a normaliser gene such as *β-actin*. Photographs of the gel can be scanned into software that will quantify the brightness of the bands. The values generated can be normalised to brightness of a marker gene run in parallel, which can be difficult if the expression of the gene chosen as a normaliser is highly expressed. Another disadvantage of Northern Blots is that they can give misleading results if the RNA used is even slightly degraded and are less sensitive than many other techniques.

RNase protection assay

The RNase protection assay is another method that relies on the hybridisation of a labelled complementary probe to the RNA of interest. After hybridisation, the remaining, unhybridised, RNA is degraded using an RNase, leaving the double stranded nucleic acids intact. The RNA is then separated using an acrylamide gel. RNase protection assays are more efficient than Northern blots and can tolerate partially degraded RNA. Their disadvantage is their lack of flexibility - the probe must be labelled RNA that is exactly complementary to the region of interest, if not then the region will be degraded along with the non-hybridised RNA.

Reverse-Transcript PCR (RT-PCR)

RT-PCR is a technique based on conventional PCR, but with an added step at the start where mRNA is reverse transcribed into cDNA using a Reverse Transcriptase isolated from a retrovirus. Complementary oligonucleotide primers are then used to designate a region amplified by a thermostable DNA polymerase. This results in exponential amplification of the region of interest. The resulting PCR product is run

on an agarose gel with size standards, stained with ethidium bromide and visualised under UV light. This confirms that the amplification was specific to the region of interest (the size of the band and absence of other bands). The exponential amplification means that the method is very sensitive and can theoretically detect one copy of a transcript, and is ideal for small samples or very low copy transcripts. This advantage can also work as a disadvantage as small amounts of contaminating DNA can also be amplified. Because of this a negative control must always be run simultaneously. RT-PCR also requires a lot of pre-reaction optimisation: the annealing temperature of the primers, the concentration of $MgCl_2$ and the cycle length are only a few of the many variables.

Quantification of RT-PCR results is difficult. Reactions are generally run for a number of cycles that give a saturated (or plateaued) end-point for all samples despite differences in the initial amount of template. For quantitation, ideally the number of cycles should be optimised to give an end point during the exponential phase of amplification (see the section on Quantitative RT-PCR below) so that the brightness of the product when visualised on an agarose gel with ethidium bromide is proportional to the amount of starting template. Analysis of the results is similar to that of a quantitative northern blot. Photographs of the gel can be scanned into software that will quantify the brightness of the bands. The values generated can be normalised to the brightness of a marker gene run in parallel. There are many disadvantages with this method of quantification; primarily the many sources of potential error when running the PCR and gel electrophoresis, photographing the gel and the computer analysis of the image; as well as normalising the results. Quantifying standard PCR in this way has become obsolete with the invention of QRT-PCR, described below.

Real-time RT-PCR

Real-Time RT-PCR (also known as QRT-PCR or quantitative RT-PCR) involves following the exponential amplification of DNA with respect to time, in contrast to other methods, which involve only analysis at the end-point of the reaction (such as running the PCR products on an agarose gel and visualising the bands with ethidium bromide).

Initial amplifications in a PCR reaction will be exponential because reagents are in excess, and template and product are in low enough concentrations that product renaturation does not compete with primer binding. When primer binding begins to occur, the reaction enters the 'plateau' phase where the amplification rate becomes linear with each subsequent cycle. Because the plateau point and the subsequent linear rate of amplification is highly variable, even in duplicate reactions from the same sample, data must be taken from the exponential phase at the beginning of amplification where the level of fluorescence corresponds to initial copy number. Real-time PCR allows the rate of amplification to be viewed after each cycle of replication has finished. There are several technologies that allow the amplification rate to be visualised, all of which are based on the generation of a fluorescent signal. A threshold fluorescence level is set in the exponential amplification phase and the cycle number that corresponds to this threshold is recorded by software running in tandem with the machine. The two most used methods of quantification in Real-Time PCR are SYBR green dye and Taqman® fluorogenic probes.

SYBR green is a dye that selectively fluoresces when bound to double-stranded DNA molecules. As amplicon copies accumulate during the PCR reaction, the level of fluorescence detected by the machine also increases and can be recorded after each cycle. Because SYBR green does not distinguish between the amplicon and any non-specific amplification or primer-dimers, a melting curve must be run at the end of every experiment to ensure that the size of the product(s) formed are as expected. It is often found that there is some non-

specific fluorescence occurring, and this is a major disadvantage of using SYBR green. Sometimes this problem can be overcome if the melt temperature of the contaminant double stranded DNA is higher than that of the desired amplicon by inserting a controlled melt step before each cycle fluorescent reading.

Taqman® is a technology invented and developed by Applied Biosystems. It is like conventional PCR but includes in addition to the primers a 'probe' that binds between the two primers. The probe contains both a fluorescent dye and a quencher. When the intervening length of DNA is short, the quencher quenches the dye's fluorescence by FRET (fluorescence resonance energy transfer). During the PCR reaction, the DNA polymerase cleaves the probe and releases the dye and quencher into solution. The dye can now fluoresce, and fluorescence is proportional to the amplification of the target sequence. The probe has a T_m value of 10°C higher than the primer pair and has a fluorescent dye conjugated at the 5' end and a quencher conjugated at the 3' end. There are differing opinions on the optimum length range for primers and probes, but it is universally agreed that there must not be a G on the 5' end of the probe as it acts as an artificial quencher even after probe cleavage. Because the probe binding is very specific, Taqman® is good for low copy number templates. A melt curve cannot be done on the resulting products as the dye has been cleaved from the probe, so it is difficult to see if any non-specific amplification resulting in fluorescence is occurring. However, the probability of this is very low as the primer-dimers do not contribute towards the fluorescence, and the probability of three oligos all binding within the same region other than the one they were designed for is low. Despite this, random non-specific binding of primers and probe may cause a reduction in the efficiency of the PCR reaction even if it doesn't result in fluorescence. To ensure that consistent amounts of total RNA are present in each sample, the samples are also run using primers for a normaliser gene. Normaliser genes must be consistently expressed in a tissue of

interest under all conditions in the study. Common normalisers include 18s rRNA, β-actin and GAPDH. They are discussed further in section 2.7.4.

The disadvantages of using real-time RT-PCR to quantify gene expression are similar to those of conventional RT-PCTR; since the reaction amplifies very low transcript levels, a negative control must always be run. Pre-reaction optimisation can also be extensive. Each real-time technology has its own advantages and disadvantages, as described above.

RNA obtained from tissues: finding new transcripts of interest

Microarrays

A 'Microarray' is the usual term for solid supports upon which a collection of gene-specific nucleic acids have been placed at defined locations, either by spotting or direct synthesis. In array analysis, a sample of nucleic acids is labelled and then hybridised to the gene-specific targets on the array. Information is gained about the specific nucleic acid composition of the sample based on the amount of probe hybridised to each target spot. Microarrays are often used for differential expression analysis of two or more RNA samples, but may also be used to identify polymorphisms in sequences. The major advantage of gene arrays is that they can provide information on thousands of targets in a single experiment. They are particularly useful if there is no prior information about global gene expression in your sample of interest.

Nucleic acid arrays are most often arranged on glass slides. Depending on the type of array, the target nucleic acids may be oligonucleotides, PCR products or cDNA vectors or purified inserts. The sequences may be representative of a whole genome or a group of related nucleic acids, for example tissue specific genes or functionally similar genes. Arrays can be custom prepared to the user's specification (if the user already knows what genes they're interested in) or a

'standard' array used (if the user is 'fishing' for genes). Glass slide arrays are most often used to compare the expression profiles of two tissues, or two samples of the same tissue that have undergone different treatments. They are often used to compare expression profiles of normal and tumour tissues. More complex multiple sample comparisons can also be undertaken, for example time course studies of naturally occurring or experimentally induced changes.

In a typical experiment the total RNA is isolated from the samples to be compared, converted to cDNA via reverse transcription and each sample is labelled with a distinct fluorescently-labelled nucleotide before both samples (now called probes) are hybridized to the same array. Typically, one sample RNA is labelled with Cyanine 3-dNTP (Cy3) and the other with Cyanine 5-dNTP (Cy5). Each dye produces a different wavelength of fluorescence. The two labelled-RNA populations are hybridized to one glass slide, the excess probe washed off and the array scanned using a fluorescent imager to generate data. The basic principle is that if one of the samples is richer in an RNA transcript than the other, the corresponding spot on the array appears bright for the colour of the dye conjugated to the transcripts from that sample.

Although the above method is common, another method of array analysis also used is Affymetrix's GeneChip technology. The chips are glass slide arrays where the oligonucleotide spots are synthesised directly onto the array substrate (most arrays are printed onto the substrate). RNA samples are converted to biotin-labelled cDNA, and each sample is hybridized to a separate GeneChip. The hybridized cDNA is then stained with a streptavidin-phycoerythrin conjugate and visualised with an array scanner. The chips are designed so that every transcript represented on the chip has between 16 to 20 pairs of targets that match different parts of the 3' end of the mRNA sequence. Every target consists of a pair of 25 residue oligonucleotides: one a perfect match to the transcript, the other a mismatch in which the middle residue has been changed. This probe-pairing

strategy helps minimise the effects of non-specific hybridisation and background signal. All pairs contribute to an average difference score corresponding to the relative level of gene expression of the transcript they represent. Another technique used is one where arrays are spotted on nylon membranes and hybridised with radioactively labelled probes. Microarray technology is progressing quickly and new techniques are emerging all the time.

Array analysis can be a daunting task as a single array experiment can generate thousands of data points. There are many software programmes that can be used to normalise, filter and sort the raw data, generating useful lists of up and down regulated genes. The problem is that there is no standard protocol for array analysis and searching for useful data is often like looking for the golden needle in the haystack. Some array manufacturers offer custom analysis services, where they will take your raw data and send it back in a useful form. Others will perform the whole experimental process for you if you send them your RNA samples.

When useful data have been obtained, differences in expression of specific sequences are often validated by another method of analysis such as RT-PCR, Northern analysis or nuclease protection assays. These same methods can be used for relative or absolute quantification of specific messages of interest identified by array analysis (White and Salamonsen, 2005).

SAGE (Serial analysis of gene expression)

SAGE is based upon the idea that a short sequence tag (10-14bp) contains sufficient information to uniquely identify a transcript provided that the tag is obtained from a unique position within each transcript. To perform SAGE, RNA is first extracted from two cell populations of interest and turned into cDNA. As with microarrays these two populations may be two different tissues or the same tissue under two different conditions. The RNAs are then cut using a restriction enzyme with a 4-base recoginition site, ensuring that every cDNA generated is cut at least

once. The cut DNA is then bound to streptavidin beads by its poly-thymidine end and the cDNA population divided in half. Half are bound to one type of linker, half to another, using their sticky ends generated by restriction digest. A type IIS restriction endonuclease can attach to the linker and bluntly cleaves the cDNA at a defined distance up to 20 base pairs away from its recognition site. Once this is achieved, the cDNA tags bound to linkers A and B are ligated to each other to create ditags. These ditags have linker A on one end, linker B on the other, and both transcript tags are adjacent to one another in the middle. These ditags are then amplified by PCR, using primers that are complimentary to the sequence in either linker. They are then cleaved to remove the modules and leave the sequence from the two tags. All of the ditags generated are then ligated into a 'concatemer': a long string of sequential tags. This collection of tags is then introduced into a vector to be cloned and sequenced. The sequences generated are compared to a SAGE database and matched to their transcript of origin. The number of times a tag is counted is a measure of its relative expression level in that cell population. Tags that are only counted once are generally excluded from an analysis to avoid error. Cell populations can then be compared to each other.

Although SAGE has potential problems, repeating experiments under slightly different conditions can often compensate for them. Certain genes, especially ones from the same family, may generate the same tag. Using longer tag sequences can eliminate this problem. Increasing tag length to 18 bp in an attempt to increase tag specificity has been reported to yield a better representation of DNA expression. Another potential problem is that certain species of mRNAs will not contain the enzyme recognition sequence. These transcripts cannot be cleaved by the enzyme, and consequently, are not included in the analysis. To avoid this problem, two different combinations of anchoring and tagging enzyme can be used and a gene expression profile created for each. The two profiles can then be correlated and compiled to represent accurately the

majority of the genes expressed within a cell.

Technique	Does it localise?	Does it quantify?	Advantages	Disadvantages
In-situ	Yes	Semi	Localises Signal	Low sensitivity, labour-intensive optimisation
Northern	No	Semi	Can visualise size of RNA	Low sensitivity, does not work well with degraded RNAs
Nulease protection assay	No	Semi	Can visualise size, more efficient than Northerns	Lack of flexibility
QRT-PCR	No	Quantitative	Sensitive, accurate	Labour-intensive optimisation
Microarray	No	Quantitative	Discovery of new transcripts present in tissue/condition of interest	Results limited by sequences on array
SAGE	No	Quantitative	Discovery of new transcripts unlimited by array boundaries	May need to run experiments under several different conditions.

Table 1.1: Summary of advantages and disadvantages of some of the techniques used in analysing gene expression, as discussed in section 1.3.1.

1.3.2: Previous studies investigating the mouse uterine luminal epithelium

Before the advent of microarrays, most studies on gene expression in the uterus have looked at single genes. Important genes in implantation have been discovered by several means. The most common is serendipitous observation of reproductive problems in a mutant line, often generated for studies of processes other than implantation. Of the genes discussed in section 1.2.2, *LIF* was discovered to have maternal effects when a knockout line was generated to study embryonic expression, as was *Hoxa-10* in developmental studies. Reproductive problems in *Cox-2* deficient mice confirmed the importance of prostaglandin synthesis for implantation and extended our knowledge of its locus of action to include the LE. Many genes have been characterised in the peri-implantation period by intelligent guesswork: vasoactive factors such as VEGF were initially investigated in the uterus because of the knowledge that decidualisation involves angiogenic processes.

The discovery of an infertile phenotype in a strain of mice carrying a targeted mutation will usually lead to an investigation into the localisation, regulation and temporal expression of that gene. Because of this, the best-characterised genes are usually those that have the most severe effects on implantation, an example being *LIF*. Many other genes are identified as being expressed in the peri-implantation uterus, but mice carrying mutations in those genes often have less severe reproductive problems, so are not yet as well characterised. It may be that the gene in question is a member of a family of genes where expression of others compensates for lack of one, or where different parallel pathways can compensate for deficiencies in each.

Recently a number of microarray studies have been published that detail global gene expression differences between murine uteri under different conditions. These studies are described below. Although human microarray studies

are not discussed in this introduction, murine and human microarray studies (Horcajadas et al., 2004) are compared in Chapter 6.

Progesterone receptor induced genes

To date, only a few genes regulated directly by the progesterone/PR complex have been identified. Further genes have been identified by two recent microarray studies compared in the table below:

Paper	Conditions compared	Experimental Design	Analysis Design
Cheon et al. 2002	Pregnant mice treated at day 3 with PR antagonist vs untreated control. Whole uterus	Affymetrix U74Av2 chips, N=6 for each condition, 3 array replicates of control/test pair.	Score for each transcript is averaged for 3 replicates, 2-fold change applied as threshold, Lists analysed in Genespring.
Jeong et al. 2005	Ovariectomised wild type vs PR null mice, sacrificed either after one progesterone injection, (acute treatment), 4 injections (chronic treatment) or injection with vehicle only. Whole uterus	Affymetrix U74Av2 chips N=5 for each condition, 3 array replicates of each control/test pair	Chips were pre-checked for viability using the MAS5 algorithm, Score for each transcript is averaged for 3 replicates, 1.2-fold change applied as threshold.

Table 1.2: Comparison of two microarray studies searching for genes regulated by progesterone. *Variables are the conditions compared in each array, the experimental design and the analysis design.*

Aims of the studies

Cheon et al. (Cheon et al., 2002) used a progesterone receptor antagonist in pregnant mice to block effects of progesterone through the actions of the PR complex and then compared global gene expression in these two models. In Jeong et al. (Jeong et al., 2005), the study had two aims: to group genes into direct and indirect regulation by progesterone (defined by the expression response time), and to confirm whether the progesterone/PR complex directly regulates the action of progesterone on these genes (defined by its presence or absence in the experimental model).

Differences in design and implementation

Since both experiments used the same microarray chips, the differences in the gene lists generated are due to variation in the experimental design and analysis. In terms of experimental design, both papers have their advantages and disadvantages: Cheon et al. is closer to the conditions in early pregnancy whereas Jeong et al. does not use pregnant mice. Jeong et al. removes the influence of any non-PR effects of progesterone by using knockout mice, whereas Cheon et al. uses an antagonist to PR only. In terms of analysis, Cheon et al. has a higher threshold value for up/down-regulated genes, but Jeong et al. subjects the chips to rigorous test to determine the reliability of the data before even starting to generate lists of genes.

Discoveries, conclusions and comparisons

Cheon et al. found 78 genes to be down-regulated by the PR antagonist RU486 and 70 genes up-regulated. Down-regulated genes included four previously known progesterone targets: *Amphiregulin, Hoxa-11, Proenkephalin* and *Histidine decarboxylase*. The study then selected seven novel genes, confirmed their regulation by progesterone and further investigated their expression over the peri-

implantation period using northern blotting over a time course to determine temporal expression and in-situ hybridization to determine localisation. By pooling data from certain comparisons, Jeong et al. generated lists of genes up-regulated by the progesterone/progesterone receptor complex: 54 genes classed as early response, 13 as intermediate response (expressed in both early and late groups) and 130 as late response. The validity of their observations was confirmed by searching for genes on the lists already known to be up-regulated by P4/PR. *Indian hedgehog* and *Hypoxia inducible factor* were known to be 'early-responsive'; this was confirmed by the study. *Amphiregulin* and *Histidine decarboxylase* were similarly classified as 'intermediate-responsive' genes and found amongst that list, as were *Calcitonin, Calbindin d9k* and *Immune response gene 1*. After functionally grouping the genes identified by this study, three genes involved in retinoic acid synthesis were identified and their expression further investigated using *in-situ* hybridisation and real-time RT-PCR.

Blastocyst regulated genes

Two microarray papers and one SAGE paper have been published that have sought to define a set of genes activated not by the maternal preparation of the uterus for implantation, but by the presence of the blastocyst in the lumen of the uterus at apposition.

Paper	Conditions compared	Experimental Design	Analysis Design
Reese et al. 2001	Manually dissected implantation sites and inter-implantation sites. 11-12 pm on day 4 of pregnancy.	Affymetrix U74A chips N=12 3 array replicates	Genes differentially expressed (more than 2 fold increase/decrease) in 4/9 comparisons were said to be up/down regulated.
Yoon et al. 2004	LE from implantation and inter-implantation sites isolated by laser capture microdissection.	Mouse 6k cDNA chips from Digital genomics (S. Korea), cy dye labelling of cDNAs. N=3 4 array replicates	Data analysed using SAM*, 1.2-fold change applied as threshold.
Ma et al. 2006	Manually dissected implantation sites and inter-implantation sites. Day 5 of pregnancy.	SAGE libraries were created for each experimental condition.	Tags sequenced and compared.

Table 1.3: Comparison of three microarray studies searching for uterine genes regulated by the presence of an activated blastocyst. *Variables are the conditions compared in each array, the experimental design and the analysis design. *SAM= Significance Analysis of Microarrays programme.*

Aims of the studies

The studies by Reese et al. (Reese et al., 2001), Yoon et al. (Yoon et al., 2004) and Ma et al. (Ma et al., 2006) aim to characterise the differences between implantation sites and inter-implantation sites in the murine uterus. All studies rely on the observation that the initial increase in vascular permeability around the site of blastocyst apposition causes injected blue dye to accumulate around

implantation sites in the uterus. Both Reese et al. and Ma et al. manually dissected implantation and inter-implantation sites before flash freezing, whereas Yoon et al. took samples of luminal epithelium at the apposition sites using laser capture microdissection. Because of this, Reese et al. and Ma et al. implantation site samples include the implanting blastocyst as well as the maternal whole uterine tissue, wheras Yoon et al. implantation samples contain maternal LE tissue only.

Differences in design and implementation

The type of arrays used in the two microarray studies are very different; the Reese study uses the Affymetrix U74A array similar to the one used in both the Cheon and Jeong studies, while the Yoon study uses a custom array and Cy dye labelling. Because of this, the two studies are not truly comparable, as the arrays may not contain a similar sample of genes. The analyses are also very different. The Reese study uses a combination of t-test to determine significantly expressed genes, and a statistical approach where each of the three implantation site chips are compared against each of the three inter-implantation chips, and if a gene is found to be significantly expressed in four of the nine possible outcomes then it is classed as up or down-regulated. The study recognises that four out of nine is a low threshold, but notes that if the threshold is increased then many genes known to be expressed at the implantation site are left out of the final lists. The Yoon study used a program called Significance Analysis of Microarray (SAM) program to exclude genes that were calculated to be significantly up or down-regulated, but were also calculated to have a high 'false discovery rate' score as defined by the programme, meaning that although they appear to be significant, statistically they are likely to be a false positive. This is a stringent test, but the results are very reliable, as backed up by the real-time RT-PCR verification.

The Ma et al. study uses the simple yet informative technique of SAGE (described in section 1.3.1) to compare the transcriptome of implantation and

inter-implantation sites. SAGE libraries from implantation and inter-implantation sites were compared using *SAGE2000* software. P values were calculated by *SAGE2000* software using the Monte Carlo simulation method, and represented a crude estimate for the possibility of detecting a difference for given abundances and fold differences between two libraries. Tags that were only found once in a library were not included in the analysis, as were tags that corresponded to more than one gene. SAGE experimental design cannot be compared to microarray experimental design directly, although the conditions used and the results obtained can be compared.

Discoveries, conclusions and comparisons

The Reese study found 36 genes to be up-regulated at implantation sites and 27 down-regulated at implantation sites. 9 of the 36 up-regulated genes including *Tenascin-c* and *Interleukin 1 receptors I and II*, and 6 of the 27 down-regulated genes, including *Prostaglandin E receptor* EP_4, were previously known to be involved in the implantation process. Two up-regulated and two down-regulated genes were verified by *in situ* hybridisation. Because implantation sites taken included all uterine tissues and the blastocyst itself, it is possible that genes up-regulated in one uterine tissue at implantation sites would not have been identified by the microarray because of masking effects of the presence of other tissues and the blastocyst. It is highly likely that this is occurring in this study, since fewer genes were found to be up-regulated compared to the Yoon study, despite the less stringent analysis and the wider range of tissue taken.

The Yoon study found 73 genes highly ranked at implantation sites (53 with known functions) and 13 at inter-implantation sites (5 with known functions). 22 genes from this list with a low 'false discovery rate' score were chosen to be verified using real-time RT-PCR, and 20 of them were confirmed to be up-regulated. The majority of genes identified as up-regulated at the implantation site by this study

were genes related to structural remodelling, and though none of them was previously characterised as being involved in implantation, the authors proposed future study of this possibility. Although the aim and methods of this study were very specific, the lack of genes previously identified to be involved in implantation is interesting. It is possible that the analysis was so stringent that subtle variations in transcript levels were excluded so as not to also allow false positives through.

The Ma et al. study found 100 genes significantly up-regulated at inter-implantation sites and 127 genes significantly up-regulated at implantation sites. This is higher than either the Reese et al. study or the Yoon et al. study. It is likely that this is because the study used SAGE instead of microarrays. Because SAGE does not use arrays, the only limit to the number of genes that can be investigated is the sequencing status of the genome being investigated. This is likely to lead to more transcripts being found to be up-regulated in a SAGE experiment. The lists of genes upregulated at the implantation site included genes previously found to be involved in implantation, including *Follistatin, Igfbp3* and *Igfbp4.* The results were verified using real-time PCR and the transcripts then localised using *in situ* hybridisation on seven up-regulated and seven down-regulated genes. The Ma et al. study has the same complications as the Reese et al. study: the blastocyst is taken as well as the uterus. A combination of laser microdissection and SAGE is likely to yield the most accurate list of genes up-regulated at implantation sites. Comparisons of the lists of genes obtained from these three studies can be found in both Yoon et al. and Ma et al.

Nidatory oestrogen regulated genes

A surge in oestrogen on the morning of day 4 of pregnancy is vital for the uterus to become receptive. This surge is known to upregulate the expression of *LIF* by the glandular epithelium (described in 1.2.2). The downstream targets of LIF have been investigated in another microarray paper (Sherwin et al., 2004). The investigation of

the indirect effect of oestrogen through LIF has been investigated more fully than direct effects of nidatory oestrogen. One paper (Reese et al., 2001), mentioned above, has also looked at global gene expression differences between mice in ovariectomy-induced delayed implantation, and mice where implantation has been restarted by an injection of oestrogen. Mice were ovariectomised on the morning of day 3 of pregnancy and kept in delayed implantation by daily injections of progesterone. On the third day of delayed implantation a single injection of oestrogen was given to the test group (of 6 mice). 12 hours later the test group and a control group not given an oestrogen injection were culled. Microarray analysis using Affymetrix GeneChip technology (as discussed above) showed up-regulation of 128 genes and down-regulation of 101 after termination of delayed implantation. Of the 128 genes up-regulated after termination of delayed implantation, only 3 were previously known to be involved in implantation: *connexins 26* and *43* and *prostaglandin E_2 receptor EP2* subtype. Of the 101 genes up-regulated in delayed implantation, nearly 48% were immune-related genes. The study proposed that further investigation was needed into this phenomenon.

Often, two microarray studies investigating the same pathway will obtain very different comparative gene lists, due to differences in the chips used, the experimental design of the study, the statistical filters used and the interpretation of the results, as discussed above. When designing an analysis strategy for a microarray study, a balance must be struck between obtaining true data and letting through false positives, and this relies on the fine-tuning of analytical methods. As more general studies such as those detailed above are performed, more overlap may be found between outcomes to produce a focus of core genes of interest. However, the gene lists generated from microarrays need dedicated follow-up studies to confirm their validity and assess their significance for the basic mechanisms of implantation. This may involve investigating their spatial and

temporal expression more finely, generating gene knock out lines and observing their reproductive phenotypes.

Gaps in the knowledge

Most studies on peri-implantation mice look at global transcription changes in the uterus as a whole. As discussed in section 1.1, the uterus has morphologically and transcriptionally distinct layers. A transcript may be highly up-regulated in a particular uterine tissue, but if it is highly down-regulated in another of the uterine tissues then it may not be identified in the resulting gene list. More specific investigations are required. Laser microdissection, as used in the Yoon study, is a useful technique for isolating individual uterine tissues and has been used in a recent study (Niklaus and Pollard, 2006) to compare the transcriptomes of glandular and luminal epithelium from pregnant mice. These studies are discussed in Chapter 6. Previous studies are also very restrictive in the timing of the samples that they take. Another recent study has taken samples of uterine luminal epithelium from five time points over the peri-implantation period, compared them to a reference and categorised genes expressed over that period into groups based on the patterns of their expression (Campbell et al.).

This dissertation will attempt to address the relatively neglected issues of uterine tissue heterogeneity and timing of gene expression in the peri-implantation period. An overview of the experiments is presented below.

1.4: Overview of thesis

The general theme of these experiments is the investigation of changes in gene expression of tissues of the murine uterus around the time of implantation with a view to characterising molecular markers for each of the tissues. The work centres on a technique for separating the luminal epithelium from the rest of the uterine tissue using a mild enzymatic (dispase) digestion followed by mechanical extraction (Bigsby et al., 1986). This technique has been used successfully in several previous studies with down-stream techniques including co-culturing of the epithelium and stroma and RNA extraction followed by RT-PCR or northern hybridisation. Papers using this technique are discussed in section 2.2.5.

First (Chapter 3), luminal epithelium and stroma from day 4 and 5 pseudo-pregnant mice were obtained using the dispase method. These tissues were histologically evaluated. Markers for tissues in the peri-implantation uterus (days 4 and 5) were tabulated after a literature search. Possible markers that were specific for uterine luminal epithelium, glands and stroma were identified. A set of paired luminal epithelium and stroma/glands tissues was obtained using the dispase technique and tested for the presence of these markers using real-time RT-PCR with Taqman® probes. In Chapter 4, luminal epithelium, glandular and stromal tissues were taken from peri-implantation mice using laser microdissection, and the markers evaluated in Chapter 3 were confirmed as tissue specific using Real-Time RT-PCR. The tissues were also hybridised to microarray chips and analysed to compare the global expression of genes in each of the three tissue types. In Chapter 5, luminal epithelium and stroma/glands samples were taken at regular time points from day 5 pseudo-pregnant mice, then evaluated for cycling of canonical circadian gene transcripts using real-time PCR.

Chapter 2: Materials and Methods

Summary

2.6.2: PCR primer information

2.6.3: Gel electrophoresis

2.7: RNA extraction and real-time RT-PCR

2.7.1: RNA extraction

2.7.2: Precipitation of nucleic acids

2.7.3: Reverse transcription of RNA for use in real-time RT-PCR

2.7.4: Taqman® assay design

2.7.5: Designing, ordering and storing Taqman® primers and probes

2.7.6: Running real-time RT-PCR

2.7.7: Taqman® data analysis

2.1: Solutions

Material	Notes	Source
PBS tablets	Cat. no.: BR0014G	Oxoid Ltd, UK
18 ohm water	From Elga Purelab Ultra filtration system	Veolia Water, UK
DEPC	Cat. no.: D5758	Sigma-Aldrich, UK
Trizma base	Cat. no.: T1503	Sigma-Aldrich, UK
EDTA	Cat. no.: ED2SS Ethylene diamine tetraacetic acid	Sigma-Aldrich, UK
Boric acid	Cat. no.: B7901	Sigma-Aldrich, UK
Tri-sodium citrate	BDH brand, Cat. no.: 102425M	VWR, UK
Sodium pyrophosphate	Cat. no.: P9146	Sigma-Aldrich, UK
Glycerol	Cat. no.: G5516	Sigma-Aldrich, UK
Bromophenol blue	Cat. no.: B8026	Sigma-Aldrich, UK

Table 2.1: Materials and equipment used in methods detailed in section 2.1
Cat. no. = Catalogue number.

All solutions are given at their stock concentrations. Dilution may be needed to achieve the concentration used in the methods; the appropriate section should be referred to.

10x PBS

Dulbecco's modified calcium and magnesium free phosphate buffered saline (PBS) was made up using tablets. 1 tablet was added to each 100ml of 18 ohm water then autoclaved at 121°C for 15 minutes.

RNAse-free water

Diethyl pyrocarbonate (DEPC) is an alkylating reagent that inactivates any proteins, including RNAses, found in solutions. In a fume hood 1.8ml of DEPC were added to 1.8L of 18 ohm water to give 0.1% DEPC-treated water. The bottle was shaken vigorously and left overnight in the fume hood with the lid slightly loose to

avoid accumulation of carbon dioxide. The water was then autoclaved to inactivate the DEPC.

10x TBE

108 g Trizma base, 55 g Boric acid and 40 ml 0.5M EDTA (pH 8 using hydrochloric acid) were made up to 1 L with DEPC-treated water

20X SSC

175.3 g sodium chloride and 88.2 g Tri-sodium citrate were made up to 1 L with DEPC-treated water, then autoclaved.

Hybridization buffer

20ml formamide, 5ml Denhart's solution (50x stock), 12.5ml 20x SSC, 0.5ml sodium pyrophosphate (100mM stock), 2.5ml Tris pH 7.4 (1M stock) and 0.5ml SDS (10% stock) were made up to 50ml with DEPC-treated water, then filtered using a 0.22µm filter and stored in 1.5ml aliquots at -20°C

6 x loading buffer (6x LB)

6ml glycerol and 0.05g bromophenol blue were made up to 20ml using DEPC-treated water then filtered using a 0.22µm filter and stored in aliquots at -20°C

2.2: Mouse husbandry and tissue isolation

Material	Notes	Source
230mm glass Pasteur pipettes	Volac brand, Cat. no.: Z310727	Sigma-Aldrich, UK
Superfrost slides	BDH brand, Cat. no.: 032K3483	VWR, UK
Methylene blue	Cat. no.: M9140	Sigma-Aldrich, UK
Dispase	Cat. no.: 165859 Neutral protease, grade II from *Bacillus polymyxa* EC 3.4.24.4	Boehringer Mannheim, UK
Hanks's Buffered Salt Solution (HBSS)	Cat. no.: 14170. No calcium, no magnesium	InVitrogen, UK
Trizol®	Cat. no.: 15596-026	Invitrogen, UK
Dissecting microscope		Wild Heerbrugg (now Leica, UK)

Table 2.2: Materials and equipment used in methods detailed in section 2.2, *Cat. no. = Catalogue number.*

2.2.1: Maintenance of experimental mice

MF1 mice were kept in a 12 hour:12 hour Light:Dark regime. 'Light' periods used a bright white light (500-700 lux) and 'Dark' periods a dim red light (5-20 lux). Where reverse-lighting has been used the mice were left for 2 weeks to adjust to the new lighting before experiments began. Food and water were available *ad libitum.* Mice were maintained under conditions specified in the Animals (Scientific Procedures) Act, 1986 and all experiments had local ethical approval. No Home Office licensed procedures were performed.

2.2.2: Vaginal flushing

230 mm glass pasteur pipettes were shortened by cutting the tip of the pipette and flaming until a smooth round end was formed. Approximately 0.25 ml autoclaved PBS was taken up in the tip of the pipette. The mouse was placed on top of the cage and its tail lifted to expose the vagina. The tip of the pipette was inserted into the vagina and the PBS squeezed into the vagina then refluxed a few times before being taken back into the pipette. The liquid was dropped onto a pre-prepared slide marked out using a wax pen to keep each sample separate. The samples

were air dried, stained with 1% methylene blue and rinsed under tap water once or twice. The slides were then allowed to dry before being viewed under a light microscope. The days of the oestrous cycle were scored as follows (Rugh, 1990): Day 1 (oestrus): smear is just squamous epithelial cells. In early oestrus some cells may still have nuclei and seem stringy. Day 2 (metoestrus): approximately equal numbers of leukocytes and epithelial cells, the epithelial cells are large, folded and often with transparent nuclei. Day 3 (dioestrus): almost exclusively leukocytes with some nucleated epithelial cells. There may also be mucus present. Day 4 (proestrus): largely nucleated, some cornified epithelium. There may also be some leukocytes.

2.2.3: Establishment of pseudopregnancy

Female mice were placed into the cages of vasectomised male MF1 mice, just after lights-out. The next morning, before 10am, the female mice were checked for the presence of a vaginal plug of coagulated semen to indicate mating. If a plug was present, the female was removed from the cage and caged separately away from other males. If no plug was present the female was placed back in the cage and left with the male for another 24 hours before being checked again. Day of plug was designated Day 1 of pseudopregnancy.

2.2.4: Dissection and mechanical isolation of uterine tissues (Bigsby et al., 1986)

0.5% dispase in HBSS was made up no more than 1 hour in advance of the procedure. Mice were killed by cervical dislocation. The abdomen was opened after spraying the fur with 70% ethanol and peeling back the skin. The inner abdominal musculature was cut open, taking care not to snip the internal organs. The uterus was located after pushing the coils of gut to the side. The first horn,

oviduct and ovary was separated from the posterior peritoneal wall and any associated fat, mesentery and blood vessels by gripping the ovarian fat pad under the kidney with one set of forceps, whilst cutting away the horn with the other. The horns were then cut across the vaginal vault, so that the two horns remain joined. Any residual mesentery/fat/blood vessels were then trimmed away from the remaining horn, and the ovary cut away from the fat pad, so the uterus and ovaries were still joined.

The dissected uterine horns (approx. 1 cm long and not slit open) were placed into 1x sterile PBS, where any remaining cleaning dissection was completed. Once the uterine horns were in the PBS, they were trimmed into two separate horns whilst being viewed under a dissecting microscope. The ovaries and oviducts were removed by cutting the uterus just before the oviduct/uterus junction. One horn was cut away from the cervix, then the other. If the mouse had been mated, the ovaries were checked for the presence of corpora lutea (dark pink spots seen on the pale pink ovaries) to confirm ovulation induction. Any uteri from mice lacking corpora lutea were discarded. The horns were then placed in 3 ml of 0.5% dispase in HBSS in a small petri dish, and incubated at room temperature for 2.5 to 3 hours. During this time, any remaining mesentery/fat was trimmed from the horns under a dissecting microscope.

After incubation, the endometrial tissues were removed under a dissecting microscope by holding one end of the uterine horn with forceps and applying pressure along the horn with a sealed glass Pasteur pipette bent into a right angle. The resulting extrudate was separated using forceps into stroma and epithelium based on its appearance. Each tissue was transferred into sterile 1x PBS by mouth pipetting with a flame-polished Pasteur pipette. The tissue was washed in the PBS then transferred in minimal PBS to a labelled 1.5 ml Eppendorf tube containing 100 µl Trizol. The tubes were immediately frozen in liquid nitrogen then stored at -80 °C.

2.2.5: Discussion of previous studies utilising the dispase isolation technique

The dispase treatment and mechanical separation technique described in section 2.2.4 (Bigsby et al., 1986) has provided the means of removing and separating epithelial and stromal cells that have been used in several downstream techniques. RNA extracted from these tissues has been used successfully in many of the techniques described in section 1.3.1, including northern blotting (Cheng et al., 2001; Kurita et al., 2001; Kurita et al., 2000; Sidhu and Kimber, 1999), conventional RT-PCR (Illingworth et al., 2000; Tong et al., 1996), real-time RT-PCR (Catalano et al., 2005), ribonuclease protection assays (Cheng et al., 2001) and microarrays on both pseudopregnant (Campbell et al., 2006) and neonatal (Hu et al., 2004) tissue. Protein extracted from these tissues has been assessed by western blotting (Catalano et al., 2005; Cheng et al., 2001; Illingworth et al., 2000) and used in enzyme assays (White and Kimber, 1994).

Populations of intact cells have been cultured successfully, including experiments where the epithelium of a mouse of one genotype is recombined with the stroma of a mouse of another genotype and grafted onto the renal capsule of a host mouse (Buchanan et al., 1998; Cooke et al., 1997; Kurita et al., 2000; Kurita et al., 1998; Mericskay et al., 2004; Miller and Sassoon, 1998; Pavlova et al., 1994). In one study RNA was extracted from the tissue recombinants after removal of the graft and used in northern blotting experiments (Buchanan et al., 1999). Sheets of intact epithelium have also been fixed on a slide, immunostained then viewed under a confocal microscope (Illingworth et al., 2000).

2.3: Histological analysis of fixed tissue sections

Material	Notes	Source
Bouins fix	Gift	Physiology department, Cambridge University
Xylene	BDH brand, Cat. no.: 102936H	VWR, UK
Haematoxylin	Cat. no.: H 9627	Sigma-Aldrich, UK
Eosin	BDH brand, Cat. no.: 341972Q	VWR, UK
DPX	BDH brand, Cat. no.: 360294H	VWR, UK

Table 2.3: Materials and equipment used in methods detailed in section 2.3, *Cat. no. = Catalogue number.*

2.3.1: Dehydration and paraffin embedding of tissues

After dissection, tissues were placed in a 7 ml glass squat tube containing a 50:50 mix of Bouin's fix and 70% ethanol. The tissue was then left overnight at room temperature. The fix was replaced serially for 2 hours each by 100% methanol, 100% ethanol, and finally xylene to clear the tissue. The tissues were then placed, using forceps, into small glass dishes and molten paraffin wax pipetted onto each sample until it was covered. The samples were then placed in an incubator at 60°C and the wax changed every half hour for two hours. A plastic pipette was used to remove old wax. Plastic moulds were taken and their bases lined with a little molten wax, which was then allowed to solidify slightly. The tissue was removed from its molten wax bath in the incubator and oriented on its end in the mould. More molten wax was then added until the sample was covered. The samples were labelled and then left to cool and fully solidify.

2.3.2: Sectioning embedded tissues

The sample was removed from its plastic mould and the block trimmed to give a cuboid structure using a hot scalpel or razor blade. The sample was attached to the microtome block by melting a little wax onto the block and orienting the sample so the leading face was a flat plane. The samples were cut in ribbons at a

thickness of 8 µm, then the ribbons cut into smaller segments of approximately 6 samples. Samples were taken at regular intervals so enough samples were mounted to get 10 slides, each with 2 segments (of 6 samples each). The samples were mounted by picking up each segment of ribbon by a corner using a scalpel, then placing it gently onto the surface of a pre-heated 50 °C water bath using a rolling motion. The wax was allowed to melt slightly and then was caught from underneath using a glass slide. This was repeated for another segment so two ribbon segments were mounted on each slide. The slides were left to drain on a slide rack and then placed in a 37 °C incubator overnight to dry.

2.3.3: Haematoxylin and Eosin staining of histological samples

The slides were placed in slide racks of up to 25 at a time, and then sequentially transferred to large glass baths containing: first xylene for 15 minutes, then 100% ethanol for 10 minutes, then through dilutions of methanol at 100%, 70%, 50% and 30% for 2 minutes each followed by distilled water for at least 5 minutes (up to an hour). The racks were then transferred to a Haematoxylin bath for 3 minutes, washed under running tap water for 5 minutes, then transferred to an acidic ethanol bath for 15 seconds. To counter-stain the slides were left in a bath of 1% eosin for 30 seconds, before being washed with distilled water. The slides were then dehydrated by being sequentially transferred through methanol baths of increasing concentrations for 30 seconds each. The slides were then transferred to a 100% ethanol bath for 5 minutes then xylene for 5-10 minutes. After at least 5 minutes in xylene, the slides were taken two at a time and mounted with coverslips using DPX.

2.4: Laser microdissection of frozen tissue sections

Material	Notes	Source
OCT	Sakura Tissue-Tek brand	Bayer, UK
LCM staining kit	Cat. no.: 1935 Cresyl violet	Ambion, UK
PicoPure™ RNA extraction kit	Cat. no.: KIT0214	Arcturus, UK
Cryostat		Leica, UK
Nanodrop spectrophotometer	Model ND-1000	Labtech, UK
RNaseZap® Wipes	Cat. no.: AM9786	Ambion, UK

Table 2.4: Materials and equipment used in methods detailed in section 2.4, *Cat. no. = Catalogue number.*

2.4.1: RNase-free technique

RNases are ubiquitous and very difficult to remove from lab equipment and plasticware. All plasticware and tips used were certified DNase and RNase free and all bench areas, pipettes and racks wiped with RNase Zap then rinsed with DEPC-treted distilled water. All water used was treated with DEPC before use. The degradation of RNA by RNases is a time and temperature dependent reaction, so all procedures were performed as quickly as possible and samples were kept on ice. Freezing of RNA samples was avoided where possible by performing reverse transcription reactions immediately after RNA extractions, but when freezing was unavoidable the samples were frozen at -80 °C and allowed to thaw on ice to minimise damage by fast thawing. Gloves were worn at all times during contact with the material and plasticware.

2.4.2: Sectioning tissues on cryostat

The samples were removed from the -80 °C freezer and kept on dry ice to avoid thawing. The sections were mounted longitudinally in OCT on pieces of chilled aluminium foil, and then placed on dry ice for the OCT to freeze. Samples were mounted on a cryostat block with additional OCT, then left to equilibrate inside the

cryostat chamber for 20 minutes. Sections were cut at thicknesses of 12 µm and the initial sections containing no uterus tissue or only mesentery/myometrium were discarded. Sections were mounted on membrane slides, and allowed to dry. A maximum of 3 slides with 8-12 sections on each was taken for each sample. Slides were then kept at -20 °C if not needed for immediate use.

2.4.3: Discussion of the techniques of laser microdissection and laser capture microdissection

Laser microdissection and laser capture microdissection are techniques that allow the fine dissection of specific areas of tissue when viewed as thin sections under a microscope. The laser capture system uses a heat sensitive membrane placed over a slide on which sections of the tissue of interest have been mounted. An infrared laser causes the membrane to distort and attach to a user-defined area of the tissue: this can be a single cell or a larger area of tissue. The membrane is then removed with the area of tissue attached. To facilitate the removal of the membrane and subsequent downstream applications, it can be attached to the inside of a specially designed 0.5 µl tube lid. Because the laser is infra-red and the membrane absorbs most of the energy, there is little damage to the cell macromolecules using this technique (Arcturus, 2004). Laser microdissection is a slightly different technique, this time using an ultra-violet laser to ablate the tissue around an area of interest, causing the tissue in that area to become loosened from the slide and either drop into the lid of an Eppendorf tube situated below the inverted slide, or be catapulted by the action of the laser into a lid situated above a non-inverted slide.

Laser microdissection appeared to be well suited to the task of obtaining pure samples of uterine tissues, particularly glands and stroma, which cannot be obtained by conventional dissection. Laser microdissection has been recently used successfully to isolate pure samples of stroma and luminal epithelium (but not

glands) from secretory-phase human biopsies for use in a microarray (Yanaihara et al., 2005) and luminal and glandular epithelium (but not stroma) from peri-implantation pregnant mice (Niklaus and Pollard, 2006), studies discussed further in Chapter 6

2.4.4: Cresyl Violet staining

Tissues were stained using the Ambion LCM staining kit. Cresyl Violet is a basic synthetic dye that binds acidic components such as RNA-rich ribosomes, nuclei, and nucleoli. This histological stain has been used to stain neurological tissues and is especially useful for allowing researchers to identify cellular morphology and tissue architecture. All alcohol solutions were made using nuclease-free water. All plasticware was either certified RNase free and came with the kit, or was treated with RNase Zap prior to use. The slides were taken through the protocol 4 at a time. The slides were first washed in 95% ethanol for 30-40 seconds, then immediately taken to 75% ethanol for another 30-40 seconds before washing in 50% ethanol for 25-30 seconds. In all three of these steps the slides were agitated gently in the solutions by moving up and down using a pair of tweezers to grip the frosted end of the slide. The slides were then drained on an absorbent lint-free tissue and the area to be stained marked with a barrier pen. 300 µl of cresyl violet stain were pipetted onto each slide and left for 40 seconds. Excess cresyl violet was drained from the slide, then the slides washed with 50% and 75% alcohol for 25-30 seconds each. The slides were not agitated during these steps. The slides were then washed once in 95% ethanol and twice in 100% ethanol. The slides were then agitated in xylene, then left for 5 minutes in a second tube of xylene. The slides were removed from the xylene and left in a fume hood to dry. When dry, the slides were immediately taken for laser microdissection.

2.4.5: Laser microdissection of tissues

Laser microdissection was performed using a Leica LMD6000. The LMD6000 is an inverted laser microdissection set-up. Up to four 0.2 ml tubes may be suspended with the inside of their caps facing up underneath the inverted slide. The laser is first calibrated on the objective intended for use when cutting the samples, in this case the x40 objective. The slide is moved until the section of interest is in view on the computer monitor. The appropriate tube cap for collection is selected, the machine will then move the cap directly underneath the area of the slide being visualised on the computer monitor. The 'close line' tool is used to draw around the region of interest, then the 'combined mode' cut tool is used to cut around the region of interest before pulsing the tissue with the laser to loosen it from the slide and allow it to fall into the tube lid below. The 'collector' tool is used to change the microscope to x10 objective and focus on the tube lid to check the progress of section collecting. The area obtained with each laser cutting is recorded in the 'shape list' window and can be copied and pasted into a Microsoft Excel™ spreadsheet to keep note of the total area recorded.

2.4.6: RNA Extraction from tissues obtained by laser microdissection

This protocol was modified from the Arcturus PicoPure RNA extraction kit protocol. All reagents and plastic-ware used were from the kit.

Immediately after a tissue sample had been collected using laser microdissection, the 0.2 ml Eppendorf tube was frozen at -20 °C for 30 minutes. The tube was then briefly pulse spun. 50 µl of Extraction Buffer (XB) were pipetted onto the cap and the tube was spun again before being incubated at 42 °C for 30 minutes, then frozen at -80 °C until needed.

When all samples had been collected, the RNA purification columns were pre-conditioned by pipetting 250 µl of Conditioning Buffer (CB) onto the purification column filter membrane and incubating for 5 minutes at room temperature. The

columns were then spun at 16,000 x g for one minute to remove the CB. 50 µl of 70% ethanol were added to the cell extract/extraction buffer mix and pipetted up and down a few times to mix. The cell extract/ethanol mixture was then pipetted into the pre-conditioned purification column and centrifuged for 2 minutes at 100 x g, to bind the RNA to the column then 16,000 x g for 30 seconds to remove flow-through. 100 µl of Wash Buffer (W1) were pipetted into the purification column and the column centrifuged for one minute at 8,000 x g. 100 µl of Wash Buffer 2 (W2) were pipetted into the purification column and centrifuged for one minute at 8,000 x g, followed by another 100 µl of Wash Buffer (W2) and centrifuged for two minutes at 16,000 x g. The purification column was checked for any residual wash buffer and re-centrifuged at 16,000 x g for one minute if any remained. The purification column was transferred to a new 0.5 ml microcentrifuge tube and 11 µl of Elution Buffer (EB) pipetted directly onto the membrane of the purification column. The purification column was then incubated for one minute at room temperature, before being centrifuged for one minute at 1,000 x g to distribute EB in the column, then for one minute at 16,000 x g to elute RNA. The concentration of the isolated RNA was then quantified using a Nanodrop spectrophotometer then stored at -80 °C until use. Yields are discussed in Chapter 5.

2.5: Microarrays

Material	Notes	Source
Amplitaq DNA polymerase	Cat. no.: N8080171	Applied Biosystems, UK
PCR machine	Techne, Model: 'Genius'	VWR, UK
SMART™ PCR cDNA Synthesis Kit	Cat. no.: K1052-1Kit contains SMART™ CDS Primer IIA, SMART™ TS Primer, SMART IIA Oligonucleotide	BD Bioscience Clontech UK,
BioPrime DNA Labeling System	Cat. no.: 18094-011 Kit contains Klenow, random primer, buffer, low c dNTP, STOP buffer.	Invitrogen, UK
dNTPs	Cat. no.: 27-2035-01	Amersham, UK
PowerScript Reverse Transcriptase	Cat. no.: 8460-1 Kit contains: buffer, DTT	BD Bioscience Clontech UK
Cy3-dCTP	Cat. no.: PA53023	Amersham, UK
Cy5-dCTP	Cat. no.: PA55023	Amersham, UK
Auto-seq G50 columns	Cat. no.: 27-5340-02	Amersham, UK
Cot-1 DNA	Cat. no.: 18440016	Invitrogen, UK
PolyA	Cat. no.: 27-7988	Amersham Bioscience, UK
Denhardt's solution	Cat. no.: D2532 1 mM sodium pyrophosphate, 50 mM Tris pH 7.4,	Sigma-Aldrich, UK
Yeast tRNA	Cat. no.: R5636	Sigma-Aldrich, UK
Bluefuse		Cambridge Blue Gnome, UK
Axon scanner	Model: Genepix 4000	Molecular devices, UK
Genespring		Agilent Technologies, UK
Microarrays	Array name: RFCGR_HGMP_Mouse_Mm_SGC_Av2 from MRC RFCGR Microarray Programme	(Hinxton, UK)

Table 2.5: Materials and equipment used in methods detailed in section 2.5, *Cat. no. = Catalogue number*

2.5.1: Microarray - SMART™ based protocol

All SMART™ reagents used are from the SMART™ PCR cDNA Synthesis Kit

1st strand synthesis

0.5 µg total RNA, 1 µl 3' SMART™ CDS Primer IIA (10 µM), 1 µl SMART™ TS Primer (10 µM), were made up in a sterile thin walled 0.2 ml tube and nuclease-free water

added to 5 µl. The tube was vortexed, pulse spun, then incubated at 72 °C for 2 minutes, before being placed on ice. 2 µl of 5 x First Strand Buffer, 1 µl of 20 mM DTT, 1 µl of 10 mM dNTPs and 1 µl of Powerscript RT were then made up to a master mix and 5 µl aliquotted into each tube. The tube was vortexed, pulse spun, then incubated for 60 minutes at 42 °C (in a pre-heated block), placed on ice and stored at -20 °C if not immediately needed.

cDNA amplification

75 µl of RNase-free water, 10 µl of 10 x PCR Buffer II, 2 µl of 10 mM dNTPs, 4 µl of IIA Primer, 5 µl of 25 mM $MgCl_2$ and 2 µl of AmpliTaq (5 U/µl) were made up to a master mix. The tube was vortexed, pulse spun and then 98 µl added to tubes containing 2 µl 1st Strand synthesis product. The tubes were then vortexed and pulse spun again before being placed on a pre-warmed 95 °C PCR hot block. The cDNA was amplified on a Techne Genius PCR machine first for 1 minute at 95°C to activate the enzyme, then 14 cycles of 95 °C for 5 seconds, then 65 °C for 5 seconds, and finishing with 68 °C for 6 minutes.

Klenow labelling

Klenow labelling was performed using reagents from the Bioprime labelling system kit (2.1.2), 21 µl of amplified cDNA were taken and added to 20 µl of 2.5 x Random Primer Buffer in a sterile thin wall 0.2 ml tube. The tubes were mixed, pulse spun, incubated at 95 °C for 5 minutes then placed on ice. 5 µl of 10 x Low C-dNTPs, 2 µl of Cy3 or Cy5-dCTP and1 µl of Klenow polymerase (40 U/µl) were added to the mix individually and the tube incubated at 37 °C for 2 hours. After 2 hours, 5 µl of STOP Buffer were added to each tube to stop the reaction.

Purification of labelled cDNA using G50 columns

The G50 columns were prepared two at a time by first vortexing to resuspend the resin. The cap was then loosened and the bottom closure snapped off. The column was placed in a 1.5 ml tube and spun at 2,000 x g for 1 minute. The column was then transferred to a new tube. 1 µl of the eluate was taken for cDNA quantification using a Nanodrop spectrophotometer. The rest of each sample was applied to the centre of the column and spun at 2,000 x g for 1 minute. The purified Cy3 and Cy5 labelled products were combined (using a light tight container). 2 µl of Human Cot-1 DNA (used as a carrier), 10 µl of 3M sodium acetate (pH 5.2), and 250 µl of 100% ethanol were added to each tube. The tubes were inverted to mix, and the DNA precipitated for a minimum of 2 hours (overnight if possible) at -20 °C. The tubes were spun at 12,000 x g for 15 minutes at 4 °C, then washed with 750 µl of 75% ethanol, then spun at 12,000 x g for 5 minutes. The supernatant was discarded and the pellet allowed to air dry in the dark.

Hybridisation

Coverslips stored in 70% ethanol were cleaned by wiping gently with 70% ethanol, rinsed under a tap of distilled water, then were rinsed twice in Millipore filtered water, and once in isopropanol and left to air dry. The hybridisation buffer was warmed to 50 °C then vortexed and pulse spun. The coverslip was placed 1 mm from the bottom edge of the slide, then 50 µl of buffer pipetted onto the gap between coverslip and slide, allowing it to flow underneath the coverslip by capillary action. The slides were pre-hybridised for 2 hours at 50 °C (with buffer but no Denhart's solution) in a humidified box placed in a water bath. The coverslips were removed by immersing slides in 2 x SSC then washed as described above. The slides were washed once in 2 x SSC then rocked for 5 minutes, twice in Millipore filtered water and once in isopropanol, then air dried. The probe was re-suspended in 50 µl of warm hybridisation buffer containing 2 µl of human Cot-1 DNA (as a

carrier) (1 µg/µl), 1µl of poly(A) (8 µg/µl), 1 µl of yeast tRNA (4 µg/µl). The probe mix was incubated for 95 °C for 5 minutes then spun for 5 minutes at 13,000 x g. The coverslip was applied to the slide and the probe added to the slide. The arrays were then hybridised for 16-18 hours at 50 °C in a humidified box placed in a water bath.

Washing slides

The coverslips were removed by immersing slides in 2 x SSC. The slides were washed in the dark on a rocking platform, twice for 5 minutes in 2 x SSC, twice for 5 minutes in 0.1 x SSC, 0.1% SDS, twice for 5 minutes in 0.1 x SSC. The slides were then rinsed twice in 0.1 x SSC, once in Millipore water and once in isopropanol. They were then dried immediately by centrifugation at 100 x g for 2 minutes.

2.5.2: Post-hybridisation data analysis

Post washing and drying, the hybridised microarray was kept in an opaque slide box in the dark. Slides were scanned on an Axon scanner and imported into Bluefuse for analysis. Bluefuse generates fluorescence readings for each address and flags data by checking that the fluorescence at each address is homogenous and not a smudge or artefact on the array chip. The address is assigned a confidence level between 0 and 1 (highest). The resulting data were uploaded to http://www.obgyn.cam.ac.uk/RMRG/analysis.html for normalisation using the per-spot, per-chip intensity dependent Loess algorithm. The purpose of the normalisation is to compensate for the differences in levels of fluorescence of each dye due to quenching of the fluorophore. The log2 ratio of cy3 to cy5 was then calculated for each address. Data were imported into GeneSpring where Condition Tree analysis was performed to check that the two tissue chip replicates were more similar to each other than they were to the other chips. The Condition Tree is an algorithm in GeneSpring that extracts meaningful patterns from large

quantities of data by grouping similar samples/conditions together based on similar expression profiles. It then displays gene similarities as a dendrogram, a tree-like structure made up of "branches". Smaller branches nest within larger ones until eventually one stem joins all branches. This nested structure forces all genes to be related at a certain level, with larger branches representing the more distantly related genes.

The data were then filtered. Addresses where the raw fluorescence did not exceed 150 arbitrary units for either cy3 or cy5 channels were removed, as were addresses with confidence levels below 0.5. Filtering using the raw fluorescence levels is to prevent false positives where the log2 ratio cy3/cy5 appears to be significant even if the raw levels imply there is little or no binding to the address. This process of elimination has been previously used with a fluorescence cut off point of 250 arbitrary units and a flag cut-off of 0.5 as defined by BlueFuse (Campbell et al., 2006).. but because the overall fluorescence level of these arrays appeared to be low, the lower cut-off was proposed. Genes with less than a twofold difference to the reference were removed and the resulting lists classed as 'up-regulated' and 'down-regulated'.

2.6: PCR and Gel Electrophoresis

Material	Notes	Source
MacVector		Accelrys, UK
BIOTAQ™ DNA Polymerase	Cat. no.: 21040 Includes buffer	Bioline, UK
Agarose	Low melting point Cat. no.: 15517-022	Invitrogen, UK
Ethidium bromide	Cat. no.: E1510	Sigma-Aldrich, UK
Gel tank		Bio-Rad, UK
UV transilluminator	BioDoc-IT system	UVP, UK
1KB ladder	Cat. no.: N32325	NEB, UK

Table 2.6: Materials and equipment used in methods detailed in section 2.6, *Cat. no. = Catalogue number.*

2.6.1 PCR

PCR mastermix specific for the number of samples was made up to 24 µl for each reaction using 1x Bioline buffer (2.5 µl of Bioline 10x buffer), 0.5 mM dNTPs (1.25 µl of 10 mM total dNTPs), 2.5 mM $MgCl_2$ (2.5 µl of 25 mM $MgCl_2$), 0.5 µM 5' primer (0.5 µl of 25 µM 5' primer), 0.5 µM 3' primer (0.5 µl of 25 µM 3' primer) and 16.75 µl of sterile Millipore water. The master mix was vortexed, spun down and aliquotted. 20 ng DNA in a volume of 0.5 µl was added to each tube, followed by 0.5 µl of Bioline Taq polymerase. The tubes were gently vortexed, spun down and cycled on a PCR machine for 95 °C for 1 minute, followed by 40 cycles of 95 °C for 30 seconds, 67 °C for 30 seconds and 72 °C for 90 seconds, then an incubation at 72 °C for 5 minutes.

2.6.2: PCR primer information

Primers were designed using Accelrys MacVector and ordered from Sigma Genosys. Primers were resuspended to a stock concentration of 100 mM then diluted to a working concentration of 25 µM using nuclease-free water.

EP_2

Sequences: 5':GATGCTCCTGCTGCTTATCGTG,

3': GCAAAGATTGTGAAAGGCAAGG, Product size: 243 bp

EP_3

Sequences:5':CAATCAGATGTCGGTTGAGCAATG,

3': GCTGGAAGCATAGTTGGTGTGG, Product size: 187 bp

2.6.3: Gel electrophoresis

The percentage (w/v) agarose was determined by the size of the product: 3% for 100-200bp, 2% for 200-1000bp, 1.5% for 1000-1500bp or 1% for >1500bp. The relevant weight of agarose powder was poured into a conical flask containing 1x TBE and plugged with tissue. The flask was then heated in a microwave for periods of 1 minute, mixing between each, until no solid agarose or viscous fluid movement could be seen. The flask was allowed to stand for a few minutes until cool enough to pour.

The agarose was carefully poured into a gel tank with inserted combs and allowed to set for 30 minutes at 4 °C. The combs were then eased out of the set gel and the gel placed in the running tank containing 1x TBE. More 1x TBE was poured into the tank until the gel was covered. 10 µl of PCR product was mixed with 2 µl of Loading buffer and pipetted into its designated well. One well at either end of each comb was loaded with 10 µl of NEB 1KB ladder. The samples were loaded as quickly as possible, then run at max (200A) current and 100V (120V with larger gel tank) until the blue dye front had reached the end of the gel. The gel was placed in a sealed box containing 0.5 mg/ml ethidium bromide solution for 5 to 10 minutes, then de-stained in distilled water for the same length of time. The gel was then viewed in a UV transilluminator and photographed for reference.

2.7: RNA extraction and real-time RT-PCR

Material	Notes	Source
RNeasy micro kit	Cat. no.: 74004	Qiagen, UK
RNase zap wipes	Cat. no.: 9786	Ambion, UK
Chloroform	Cat. no.: C5312	Sigma-Aldrich, UK
Linear acrylamide	Cat. no.: 9520	Ambion, UK
MMLV Reverse transcriptase	Cat. no.: M1701 Buffer included	Promega, UK
Random primers (Pdn6)	Cat. no.: 48190-011	Invitrogen, UK
BSA	Cat. no.: 27-89-14	Amersham, UK
Real-time RT-PCR 2x mastermix	Cat. no.: AB1142	ABgene, UK
18s primers/probe	Cat. no.: 4310893E	Applied Biosystems, UK

Table 2.7: Materials and equipment used in methods detailed in section 2.7, *Cat. no. = Catalogue number.*

2.7.1: RNA extraction from whole tissues

For whole tissues, a frozen tissue homogenisation step was performed followed by a phenol/chloroform step, then isolation of pure RNA using Qiagen RNeasy Mini kit columns. For dissected luminal epithelium and stroma, the freezing and crushing steps were omitted. The protocol began with the phenol/chloroform step and was followed by isolation of pure RNA using Qiagen RNeasy Micro kit columns. The bench area and pipettes used were treated with RNase Zap wipes before extraction commenced. All tips and tubes used were certified DNase and RNase free.

Crushing step

The samples contained in 1.5 ml Eppendorf tubes were taken out of the -80 °C freezer and transported on dry ice to prevent thawing. Care was taken to avoid thawing at all steps up to the addition of Trizol. The mortar was pre-cooled by addition of a little liquid nitrogen. An insulating glove was worn on the hand holding the mortar to prevent freeze-burn. The sample was removed from its tube without

thawing and placed in the mortar. The sample was quickly covered with a piece of tinfoil and a little liquid nitrogen poured on to the tinfoil to cool it. The sample was then ground underneath the tin foil using the pestle. More liquid nitrogen was added if the mortar appeared to be warming above freezing. The powdered tissue was washed from the mortar and tinfoil using more liquid nitrogen into a pre-weighed tube that had been cooled on dry ice. The lid was held down but not shut tight to allow excess gaseous nitrogen to escape whilst preventing the tissue from popping out of the tube. The lid was then sealed and the tube weighed quickly to determine tissue yield. 500 µl of Trizol were added to the tube, which was kept on dry ice until all samples had been ground.

Trizol step

Samples were taken through this section of the extraction process in groups of 6 or 8. An extra 400 µl Trizol was added if the tube contained dissected LE and stroma in 100µl Trizol. The samples were thawed, vortexed well, dispersed with a Gilson tip and left for 5 minutes at 4 °C before vortexing/dispersing again. The samples were spun for 10 minutes, at 16,000 x g at 4 °C for whole tissues or 2 minutes at 16,000 x g for dissected LE or stroma, and the supernatants taken to fresh pre-labelled 1.5 ml Eppendorf tubes, leaving the pellet of remaining non-soluble extracted tissue behind.

In a fume hood, 100 µl of chloroform were added to the tube, which was then shaken vigorously by hand for 15 seconds then left at room temperature for 2 minutes. The tube was then spun at 12,000 x g at 4°C for 15 minutes. The upper aqueous layer (approx 300 µl) was then taken to a fresh, pre-labelled 1.5 ml Eppendorf tube. 2.4 µl of 5 mg/ml linear acrylamide (a co-precipitant that does not interfere with spectrophotometer readings) and 300 µl of 70% ethanol were added to the tube, which was then vortexed well and kept on ice prior to the next step.

Qiagen column step

This step is performed outside the fume hood. The ethanol/RNA mix was applied to either a Qiagen RNeasy mini column (whole tissues) or a micro column (dissected LE or stroma), which was then spun for 1 minute at 8,000 x g. The eluate was reapplied to the same column and spun again. The eluate was then discarded. 350µl of buffer RW1 (a buffer to bind RNA to the membrane of the spin column, supplied with the Qiagen kit) were applied to the column, which was then spun for 15 seconds at 8,000 x g. The eluate was discarded. 10 µl of DNase 1 stock solution were added to 70 µl of RDD buffer (a buffer to dilute the DNase and supply the enzyme with cofactors and optimum pH conditions, supplied with the Qiagen kit) and mixed by gently inverting a few times. The DNase mix was then applied to the column, and the column left at room temperature for 15 minutes, 350 µl of buffer RW1 (a buffer to wash the RNA bound to the column membrane, supplied with the Qiagen kit) were applied to the column, which was then spun for 15 seconds at 8,000 x g. The eluate was then discarded. The column was transferred to a fresh collecting tube, 500 µl of buffer RPE were applied and the column spun at 8,000 x g for 15 seconds. The eluate was then discarded. 500 µl of 80% ethanol were applied to the column, which was then spun for 2 minutes at 8,000 x g. The eluate was then discarded. The column was transferred to a fresh collecting tube then loaded into the centrifuge with its cap open and spun for 5 minutes at maximum speed to remove all residual ethanol and dry the membrane. The collecting tube was discarded and the column transferred to a fresh 1.5 ml collecting tube. 14 µl of RNase-free water were pipetted onto the column membrane and the tube spun at maximum speed for 1 minute to elute the RNA.

The yield was assessed using a Nanodrop spectrophotometer and either taken straight to the reverse transcription step, or frozen at -80 °C.

2.7.2: Precipitation of nucleic acids

0.1 volumes of 3 M sodium acetate (pH 5.2), 2.5 volumes of 100% ethanol and Linear Acrylamide to a final concentration of 10 µg/ml were added to the sample. The tube was vortexed to mix and precipitated for a minimum of 24 hours at -20 °C. The tubes were then spun at 12,000 x g for 15 minutes at 4 °C. The supernatant was removed with progressively finer pipette tips to avoid removing the pellet, then washed with 750 µl of 75% ethanol, before being spun at 13,000 x g for 5 minutes. The supernatant was then removed again and the pellet allowed to air dry in the dark, before being resuspended in an appropriate volume of nuclease-free water.

2.7.3: Reverse transcription of RNA for use in real-time RT-PCR

4 µl of Promega 5 X first strand buffer, 2 µl of 10 mM dNTPs, 2 µl of random primers and 2 µl of Pharmacia 1 mg/ml BSA were made up in a master mix for the appropriate number of tubes being reverse transcribed, then 10 µl aliquotted into individual tubes. 400 ng of RNA was made up to 9 µl using RNase-free water, then added to the appropriate tube.

The tubes were then placed on a PCR block pre-warmed to 65 °C for 1 minute (to remove RNA secondary structure and allow binding of random primers), placed on ice for 3 minutes (to avoid reforming secondary structure) then pulse spun down. 1 µl Promega MMLV reverse transcriptase (RT) was added to each tube, (1 µl of sterile water for a -MMLV control reaction) and the tube placed in the PCR machine at 37 °C for 1 hour, then 95 °C for 10 minutes (to destroy the enzyme and the RNA). The resulting samples were diluted 1 in 5 with 80 µl of sterile double distilled water and aliquotted into 6.5 µl samples.

The 'standard curve' method in real-time RT-PCR relies on relative rather than absolute quantification, using a dilution series of DNA containing the sequence of the gene or transcript of interest. Popular standard curve materials include genomic DNA, a total cDNA population from the tissue of interest or a

cloned copy of the gene of interest. The only criterion is that the expression level of the gene in the real-time RT-PCR samples to be measured must fall within the range of the standard curve. Standard stocks in these experiments were made from a pool of RNA comprising an equal amount from each of the unknown samples. The pool was made up to the same concentration as the unknowns using nuclease-free water, then a master mix made up as above. The RNA pool was aliquotted into individual tubes with master mix for reverse transcription, then the cDNA products combined, mixed and re-aliquotted into 15 µl aliquots.

2.7.4: Taqman® assay design

Assay design for real-time RT-PCR involves careful consideration of different technologies and techniques, which are discussed in section 1.3.1. It was decided that Taqman® was the most appropriate technique to use for these assays as collaborators had been using this technology previously and assays were running smoothly. Although the reactions are difficult to optimise, once working the assays are reliable and accurate (Bustin and Nolan, 2004). The use of *18s* rRNA (a small RNA component of the eukaryotic ribosome) as a housekeeping gene is considered more reliable than other popular housekeeping genes such as GAPDH (glyceraldehyde 3-phosphate dehydrogenase, a metabolic enzyme) and beta-actin (Bustin, 2000), a cytoskeletal protein. Absolute quantification in real-time PCR is very difficult because reaction efficiencies are not always constant, although it is possible to obtain an absolute standard curve by using plasmid DNA. Unless it is essential that an absolute quantification of gene expression needs to be achieved, then relative quantification is an adequate substitute. Relative quantification was used in this work for this reason (Dorak, 2006).

2.7.5: Designing, ordering and storing of primers and probes for Taqman®

Primers and probes were designed using Beacon Designer Software or Primer Express Software using gene information downloaded from Ensembl (http://www.ensembl.org/Mus_musculus/). Where possible, probes were designed to span exon-exon boundaries to avoid amplification of any contaminating genomic DNA. Primers and probes were blasted against the mouse genome to ensure specific binding (nucleotide-nucleotide blast at http://www.ncbi.nlm.nih.gov/BLAST/).

Primers/probes were ordered online from Sigma Genosys, the probe was modified with a 5' conjugated 5-carboxyfluorescein (FAM) as a fluorophore and a 3' conjugated 5-carboxytetramethylrhodamine (TAMRA) as a quencher. Primers and probes were stored lyophilised at -20 °C until needed. Then they were resuspended in their original tubes to 100µM and kept at -20 °C as a stock solution. Working solutions were made by diluting the stock to 10 µM for primers and 5 µM for probes. All dilutions were made using sterile double-distilled nuclease-free water. Probes are light sensitive so all tubes containing aliquots of probe were wrapped in aluminium foil. All aliquots of primers and probes were stored in an opaque black box at -20°C.

Figure legend for Tables 2.8 and 2.9

The tables summarise the sequence of each primer/probe set used in these studies, if they are positioned across an exon/exon boundary in the gene of interest, the RefSeq database accession number of the gene and the Ensembl transcript number of the gene (used to acquire the gene sequences to design the primers and probe), and whether the oligonucleotides were designed in house or acquired from a collaborator.

Table 2.8: Taqman primers/probe sets for Circadian genes

Primer name	Sequence 5' to 3'	Over exon boundary?	RefSeq accession	Ensembl transcript number	Designed in/by
Clock 5'	GCTCACGAAAGTCATCTCACAC	probe	NM_007715	ENSMUST00031148	Beacon
3'	GCTGTGTCATCTTTTCATGAGCT				Designer
Probe	TCAGACCCTTCCTCCACACCGACAA				
Bmal 5'	CCCACAGCATGGACAGCAT	probe	NM_007489	ENSMUST00000047321	Beacon
3'	CTGGAATGCCTGGGACAGTG				Designer
Probe	CTGCCCTCTGGAGAAGGTGGCCA				
Per2 5'	TGTTTCAGGATCCCACGAA	no	NM_011066	ENSMUST00000069620	Beacon
3'	TTCCCATTGTCGTCGCAGTC				Designer
Probe	CTGCCCTGAGAGTCCCGTCCCGTG				
Cry1 5'	AAGGAACGAGATGCAGCTATCAA	primer	NM_007771	ENSMUST00000020227	Beacon
3'	GATCTTGTCCAGGTCATACAGTGT				Designer
Probe	CGCACGATGACTTCCACGCCAGCC				
Per1 5'	TGGTTCAGGATCCCACGAA	probe	NM_011065	ENSMUST00000021217	Primer
3'	TGCTTGTATGGCTGCTCTGACT				Express
Probe	CCTCAGCCAGCATCACCCGCA				

Table 2.9: Taqman primers/probe sets for uterine marker genes

Primer name	Sequence 5' to 3'	Over exon boundary?	RefSeq accession	Ensembl transcript number	Designed in/by
Tn-c 5'	AAGCTCTCCTTGGGCATTTG	amplicon	NM_011607	ENSMUST00000030056	Dr Andrew Sharkey Department of Pathology University of Cambridge
3'	GCCTACATCAGTGCCTCAGTGA				
Probe	TGGGCGTCCAAGCAGACCACAC				
LIF 5'	CCCCTGTAAATGCCACCTGT	no	NM_008501	ENSMUST00000066283	Dr Andrew Sharkey Department of Pathology University of Cambridge
3'	CTTCTCTGTCCCGTTGCCAT				
Probe	CATACGCCACCCATGCCACGG				
EP_2 5'	CCATCACCTTCGCCATATGC	probe	NM_008964	ENSMUST00000046891	Primer express
3'	TAGGGAAGAGGTTTCATCCATGTAG				
Probe	CCTTTCACAATCTTTGC				
EP_3 5'	ACGGCCATCCAGCTCATG	probe	NM_011196	ENSMUST00000071906	Primer express
3'	GCTCAACCGACATCTGATTGAA				
Probe	TATCAATAGCGGCGACCAA				
Osf-2 5'	GCAAAGAAGATACCAGCCAACA	probe	?	ENSMUST00000081564	Dr Andrew Sharkey Department of Pathology University of Cambridge
3'	AGAAGGCCGTTCTCAGTGAAA				
Probe	AAGGGTTCAAGGGCCTAGAAGAC GATCA				

2.7.6: Running real-time RT-PCR

Plate set up

All cDNA samples to be run with *18s* primer/probes were diluted 1 in 100 before adding to the master mix: 5 µl of RNA were added to 495 µl of nuclease-free Millipore water. To make a standard curve, a 1 in 2 serial dilution series was made starting with a 6.5 µl aliquot of standard to which 6.5 µl nuclease-free Millipore water were added. The tube was vortexed gently to mix and with a fresh pipette tip, 6.5 µl of this mix were removed and taken to a fresh Eppendorf tube and the dilution series continued thus until the dilution reached 1 in 128.

For *18s* primers/probe, a master mix of 6 µl ABI *18s* mix, 60 µl Abgene buffer and 48 µl nuclease-free Millipore water was made up, 6 µl of the diluted RNA or relevant standard curve dilution were added to it. For other primers, a master mix of 60 µl ABI mix, 300 nM of primers and 200 nM of probes was made up to 114 µl with nuclease-free Millipore water, then 6 µl of the diluted RNA or relevant standard curve dilution were added to it. The final mix tubes were vortexed and spun down. 36 µl of each mix were pipetted into each of 3 wells on a 96 well plate (reaction triplication). The plate was sealed with optical lid strips and spun briefly in a centrifuge. The plate was either run immediately or stored wrapped in aluminium foil at 4 °C for up to 24 hours. The plate was run on either an MJ DNA engine Opticon 2 or an ABI Prism 7700 for 2 minutes at 50 °C, 15 minutes at 95 °C, then 40 cycles of 15 sec at 95 °C and 1 minute at 60 °C, with fluorescence acquisition at the end of each cycle.

2.7.7: Taqman® data analysis protocol

After running each plate with a primer probe set to generate fluorescence data, the machine software (*ABI SDS* for the ABI Prism 7700 and *Opticon Monitor* for the MJ Opticon) was used to generate a C_T value for each well (defined as the cycle at which the fluorescence intensity reaches a threshold level). This is illustrated in Figure 2.1.

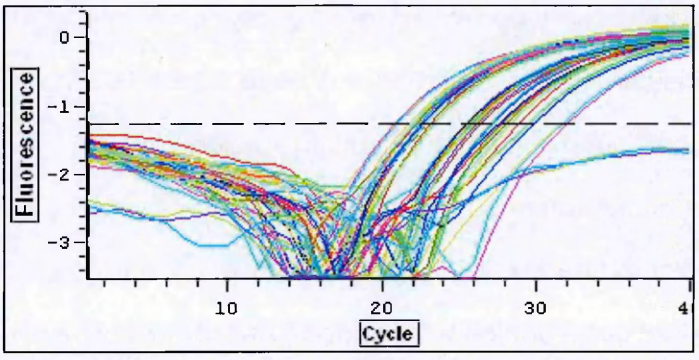

Figure 2.1: Example of a fluorescence plot generated by MJ Opticon 2 Monitor software. *The plot shows the number of cycles on the x axis and the log of the fluorescence level recorded by the detector on the y axis. Several samples are represented on this plot, each by a different colour. The first 10 cycles are background fluorescence; the fluorescence levels in the highest concentration samples begin to increase exponentially around cycle 18, where the gradient of the line becomes constant. Lower concentration samples begin to increase around cycle 21. The threshold level is the black dashed line intersecting the y axis at around -1.2. It is user-defined and must be within the exponential phase of DNA replication. The point at which each sample's curve crosses the threshold level is called the* C_T

The fluorescence plots were scanned and the well numbers of any unusual plots noted. The C_T data were transferred into Microsoft Excel™. A standard curve was created by plotting the 3 replicate C_Ts of each of the 1-in-2 standard dilution series

samples against their relative dilution level. A line of best fit through the points on the standard curve was generated with a correlation value r^2 >0.95, outlying examples were excluded at this point. The C_Ts of the 'unknown' samples were then converted to arbitrary values using the equation of line through the standard curve. An example is given below.

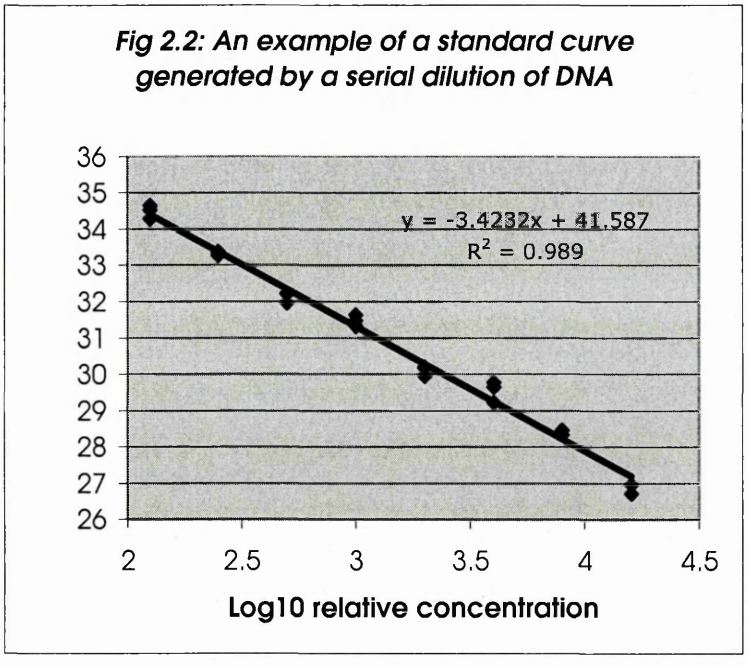

Figure 2.2: An example of a standard curve generated by a serial dilution of DNA, generated by Opticon Monitor 2 software from real-time RT-PCR results. *The Ct of the samples is plotted against the Log10 value of its relative concentration and a line of best fit drawn through the results. An efficient reaction should give a gradient of close to -3.3 (in this case the gradient is -3.4, which is acceptable. A correlation (R^2) value of 1 indicates that the three replicates for each concentration are reproducible (in this case the R^2 value is 0.989, which is acceptable.*

The three triplicates for each sample were then averaged. For single un-replicated conditions, the value was simply normalised to its corresponding *18s* value. If more than one replicate set was involved, values were first compared to the mean of

their set and a ratio calculated and then normalised to their *18s* value to control for variation between sets. The replicates for each value were then averaged and plotted on a graph with the standard error of the mean (SEM) for each time point (calculated as the standard deviation of the data set divided by the square root of the number of replicates).

Chapter 3: Tissue type markers for the pseudopregnant mouse uterus

Summary

3.1: Introduction

The aim of this part of the research was to validate and develop molecular markers for the luminal epithelium (LE) and stroma (S) of uterine endometrium in early pregnancy using real time RT-PCR on dissected tissue components, and to relate the molecular and histological data. The objective was ultimately to be able to identify confidently which tissue components were present in a dissected sample to be used for downstream application such as Taqman® and microarrays. The initial studies focussed on enzymically dissected stroma and luminal epithelial tissues. However, during this part of the study, it became clear from observing histological sections that the stroma contained glandular epithelial tissue and the luminal epithelium also sometimes had attached material that resembled glandular epithelium histologically. Therefore, in the second part of the study, markers were used to try to distinguish all three tissues, so that the extent of glandular contamination could be assessed. The approach used was to investigate the transcriptome of each tissue around the time of implantation. Because the presence of an embryo complicates the tissue architecture through both its presence and the decidual reaction it induces, markers were sought in uteri from pseudopregnant mice. The presence or absence of the markers was investigated with real-time RT-PCR using Taqman® fluorogenic probes on cDNA made from RNA extracted from samples of pseudopregnant mouse uterus.

3.2: Observations from preliminary histological studies

Preliminary studies were undertaken to characterise the material recovered by the dispase-dissection procedure by relating macroscopic observations on the dissected tissues to their histological structure.

Macroscopic

In preliminary studies on pseudopregnant uteri the dispase separation technique (section 2.2.4) seemed to yield luminal epithelium contaminated with stroma.

The luminal epithelium appeared as a sleeve (with an appearance like chiffon), attached to what appeared to be stroma (with a 'cotton wool' appearance). In the cases where the epithelium and stroma came out whole and attached to each other, the extract seemed to be 'inside out' with the stroma on the outside and the epithelium on the inside. The two tissues were separated by gently picking off the epithelium using forceps, or pulling the epithelium out from the inside of the stroma using a gentle tugging motion with the forceps. Sometimes this could be achieved by peeling it off like a sleeve and at other times it came off in strips. Occasionally the isolated LE appeared to be slightly woolly in appearance, which was speculated to be due to the presence of stromal contamination. Furthermore, epithelia from day 5 of pseudopregnancy appeared to have spiky projections from the LE pointing into the stroma and it was speculated that these were endometrial glands. The various macroscopic patterns of epithelium observed were recorded for comparison with microscopic images.

Microscopic

Histological studies were undertaken to investigate the macroscopic observations recorded above. 4 and 5 day pseudopregnant mice were obtained by mating female MF1 mice with vasectomised males (2.2.3). One example of each of the

following tissues from both days were removed to an Eppendorf tube containing 1 ml of a 50:50 mix of Bouin's fix and 70% ethanol for subsequent histological processing and analysis (see materials and methods): 1: Whole uterus incubated for 2 1/2 hours in HBSS (no dispase), then removed for fixing; 2: Whole uterus incubated in 0.5% dispase in HBSS for 2 1/2 hours, then removed for fixing; 2: Whole uterus incubated in 0.5% dispase in HBSS for 2 1/2 hours, then subjected to mechanical separation of stroma/luminal epithelium. Both (a) the stroma/epithelium and (b) the residual parts of the uterus were removed for fixing separately.

Representative photos

1. Untreated whole uterus

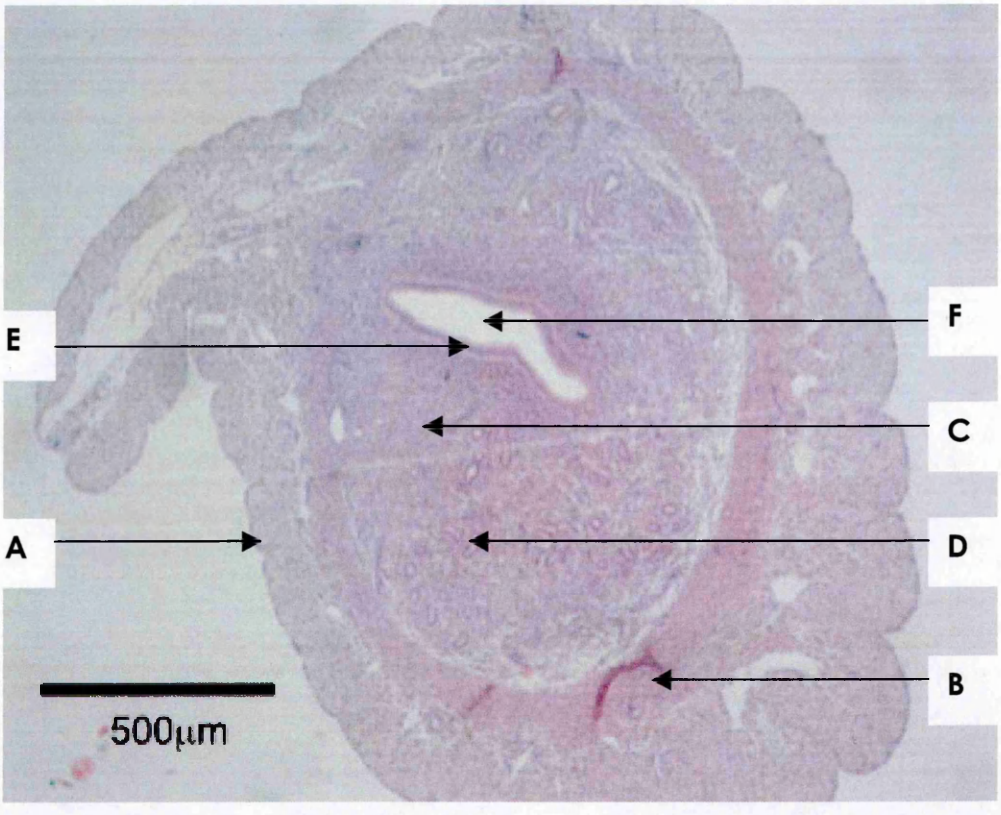

Figure 3.1: Transverse H&E stained section through untreated whole uterus (also shown as Figure 1.1). *The pale-staining outer mesenchymal layer (A) can be seen on the outside surrounding the strongly staining myometrium (B), composed first of a layer of longitudinal smooth muscle, then a layer of circular smooth muscle. The endometrium, which lies inside the musculature, consists of a diffuse stroma that is denser and stains darker in the area surrounding the luminal epithlium (C.) The stromq contains darkly staining circular patches of glandular epithelium (D) throughout. The central lumen (F) is surrounded by the columnar luminal epithelium (E), which is separated from the stroma by an epithelial basement membrane.*

2. Dispase-treated uterus

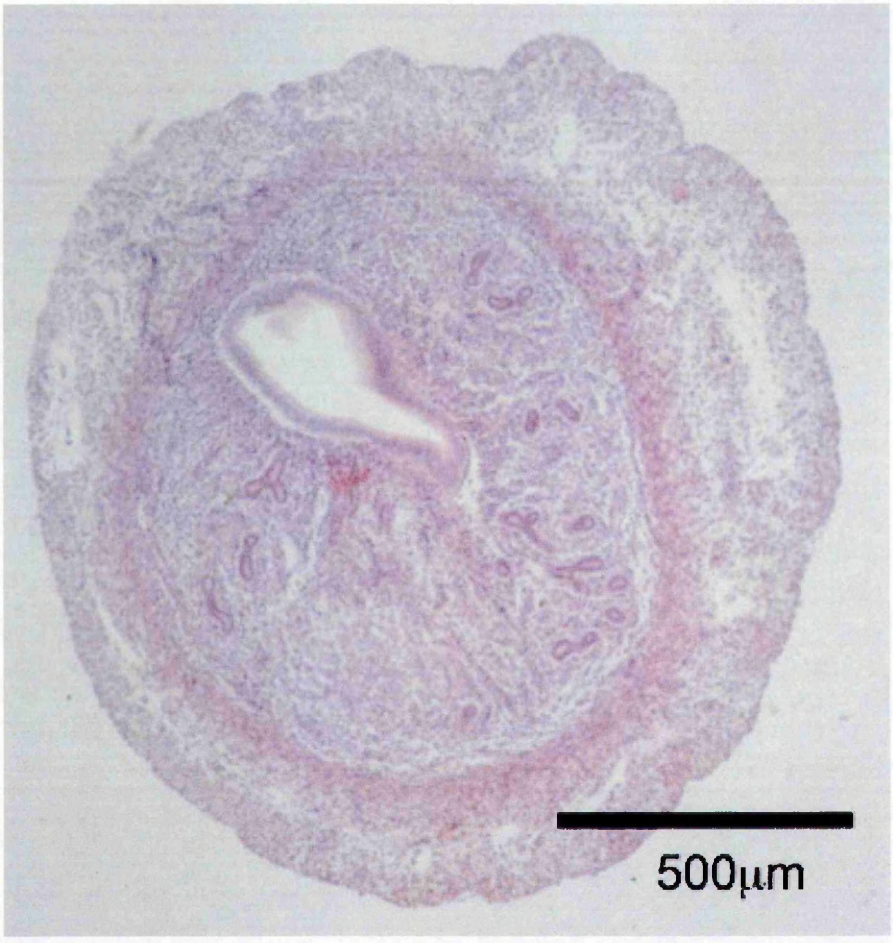

Figure 3.2: Transverse H&E stained section through dispase treated uterus: *the structure of the uterus is similar to the untreated uterine section shown in Figure 3.1, but in the treated uterus shown here in Figure 3,2 the luminal epithelium can be seen to have dissociated from the underlying stroma in most places. This is a result of the dispase treatment.*

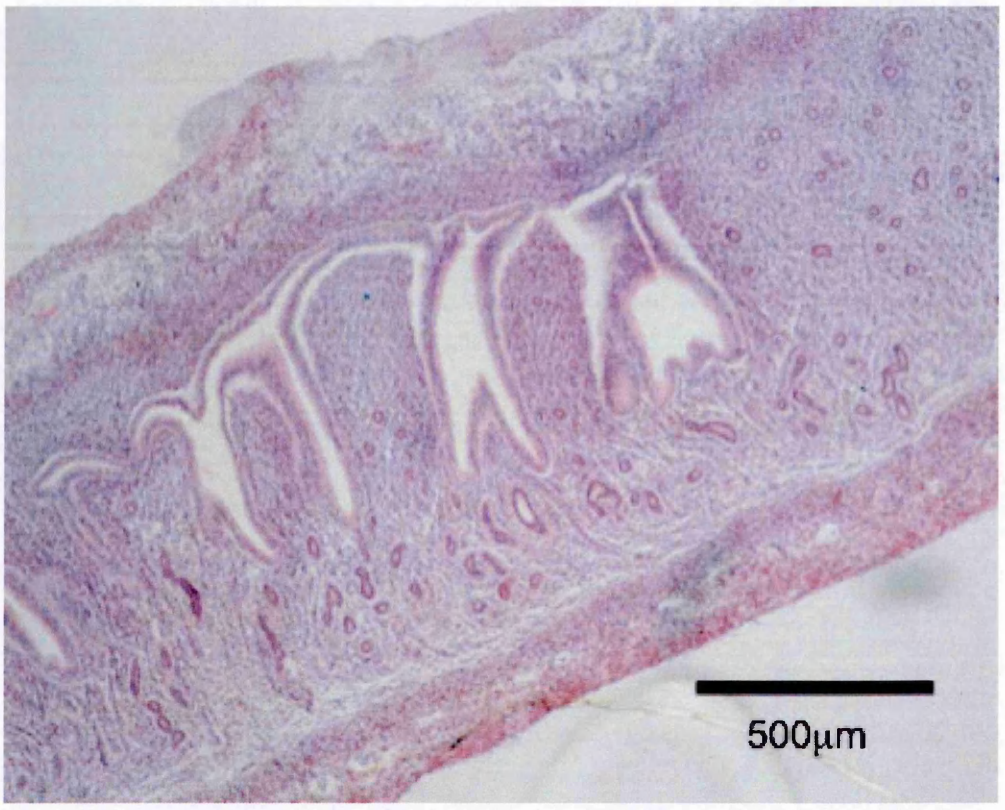

Figure 3.3. Longitudinal/oblique H&E stained section through dispase-treated uterus: *the dissociation from the underlying stroma can be seen more clearly in this oblique section. The zig-zag appearance of the lumen l is due to 'wrinkling' of the section before embedding.*

3. Epithelium and stroma extracted from dispase-treated uterus

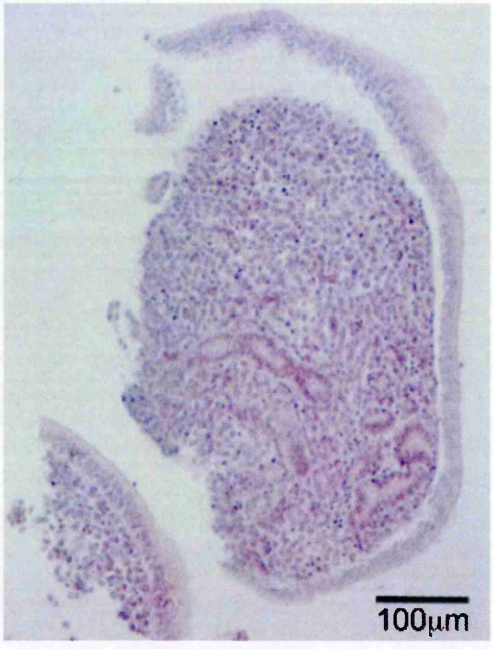

***Figure 3.4. H&E stained extracted epithelium/stroma showing epithelium partly dissociated from stroma and glands**: this is a result of dispase treatment and mechanical extraction on a pseudopregnant uterus, showing that the epithelium is still partially attached to the stroma, but it is possible for it to be picked off.*

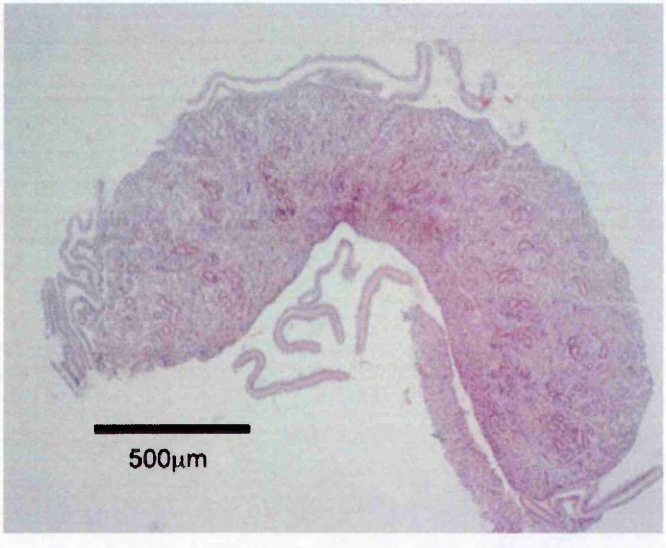

***Figure 3.5 . H&E stained extracted epithelium/stroma showing epithelium in several small pieces, some still attached to stroma**: the epithelium is very delicate, so often rips as it is being picked off the stroma after extraction.*

Conclusions from preliminary studies

Dispase treatment followed by mechanical extraction of epithelium on pseudopregnant uterine horns yields epithelium attached to underlying stroma. Picking off stroma does not guarantee that all stromal or glandular contamination is removed. This must be assessed in other ways. Glandular epithelium is embedded in the stroma. It would not be possible for it to be removed by mechanical means, so contamination must be assessed in other ways. The composition of extracted epithelial samples isolated from stroma was not assessed at this time, but later experiments to view mechanically extracted epithelia under the microscope in tandem with molecular biology results addressed this.

Histology is a useful way of looking qualitatively at the composition of samples extracted using the dispase technique, but it has its limitations (as discussed above.) Also, once a uterine horn is embedded and sectioned for histological analysis, the tissue is essentially destroyed and molecular techniques such as real-time RT-PCR cannot be performed on it. The solution to this (and the problem of minor stromal contamination that may not be readily detected by histological analysis), is to research genes expressed discretely in each of the three tissue types to use as 'molecular markers' for tissue composition.

3.3: Collection of experimental material

After observing that the dispase treatment technique could work on pseudopregnant uteri, it was decided that the constitution of 4 and 5 day pseudopregnant samples would be assessed in two ways: one histological (H and E stained thin sections viewed under a light microscope) and one molecular (real-time PCR using dual-labelled fluorogenic Taqman® probes). The histological findings, as well as confirming the macroscopic observations, would then be backed up by the outcome from experiments using PCR-based markers for tissue type. The uterus was separated into two horns before the dispase treatment, so the epithelium and stroma from one horn could be used for histological analysis and the other for real-time PCR.

It was decided to focus on days 4 and 5 post-implantation: this being the peri-implantation period, and the most important (and therefore most studied) time in early pregnancy. Because of this, preliminary PubMed searching showed a large number of differentially expressed markers that had been characterised for this time by *in-situ* hybridisation and/or immunocytochemistry. It was decided to use pseudopregnant rather than pregnant mice. There were two reasons for this: so no embryos were present to complicate the collecting of uterine tissues, and so the gene expression of the uterus was not complicated by signalling between the implanting embryo and the endometrium leading to massive stromal decidualisation. Because this complication was removed, the only effects observed will be the maternal responses to the hormonal changes set in train by mating rather than the presence of the embryo itself.

Four females in day 5 of pseudopregnancy and 3 females in day 4 of pseudopregnancy (section 2.2.3) were sacrificed. Their uteri were removed and incubated in 0.5% dispase in HBSS at room temperature for 2.5 hours, before being subjected to mechanical extraction of the epithelium and attached stroma

(section 2.2.4). Notes were made on the appearance of the uteri at removal and the ease of extraction. The extracted products from each of the uterine horns were separated as much as possible into epithelium and stroma/glands and removed to either an Eppendorf tube containing 1 ml of 50:50 Bouin's fix: 70% ethanol (for histological analysis) or an Eppendorf containing 100µl Trizol (for RNA extraction). The Trizol tubes were then frozen and stored at -80°C.

Results

Three mice were sacrificed on day four of pseudopregnancy, four mice were sacrificed on day five. Observations from the dissection of the uterus and and separation of stroma and glands are recorded in Table 3.1.

Day	Mouse number	Histological analysis	RNA analysis	Observations
4	1	Yes	Yes	Easy and clean extractions
4	2	Yes	Yes	Easy and clean extractions
4	3	Yes	No	Difficult extraction, quite 'sticky' epithelia
5	1	Yes	Yes	Difficult extractions, appears to be glands contaminating LE
5	2	Yes	No	Difficult extractions
5	3	Yes	Yes	Easy extractions
5	4	Yes	Yes	Easy extraction but potential GE contamination of LE

Table 3.1: Observations from epithelial extractions of day 4 and 5 pseudopregnant mice, *showing the day of pseudopregnancy, the number of mice used for each day, whether samples could be obtained for both histological analysis and RNA analysis and notes on the ease of extraction of the epithelium. Two dissections were difficult and only yielded enough epithelium for histological analysis; they were fixed for histology in preference to being taken for RNA extraction as it was*

thought that more relevant data could be obtained that way. Two further dissections may have produced cross-contaminated samples, and three were scored as clean. Comparison of visual scoring macroscopically with both histology and molecular markers could thus be performed informatively on these variable samples. GE = glandular epithelium, LE = luminal epithelium.

3.4: Histological analysis of samples

The samples taken for histology as described above were fixed, embedded in paraffin wax (section 2.3.1) and microtomed as 7µm sections (section 2.3.2) before being mounted on slides and H&E stained (section 2.3.3). The slides were viewed with the x4, x10 and x20 objectives and notes made on the appearance of the sections.

Figure 3.6: A sample of H&E stained "pure" luminal epithelium (x20 objective). *"Purity" is characterised by the absence of any clear stromal cells; ribbons of epithelium can be seen with the basal lamina still intact.*

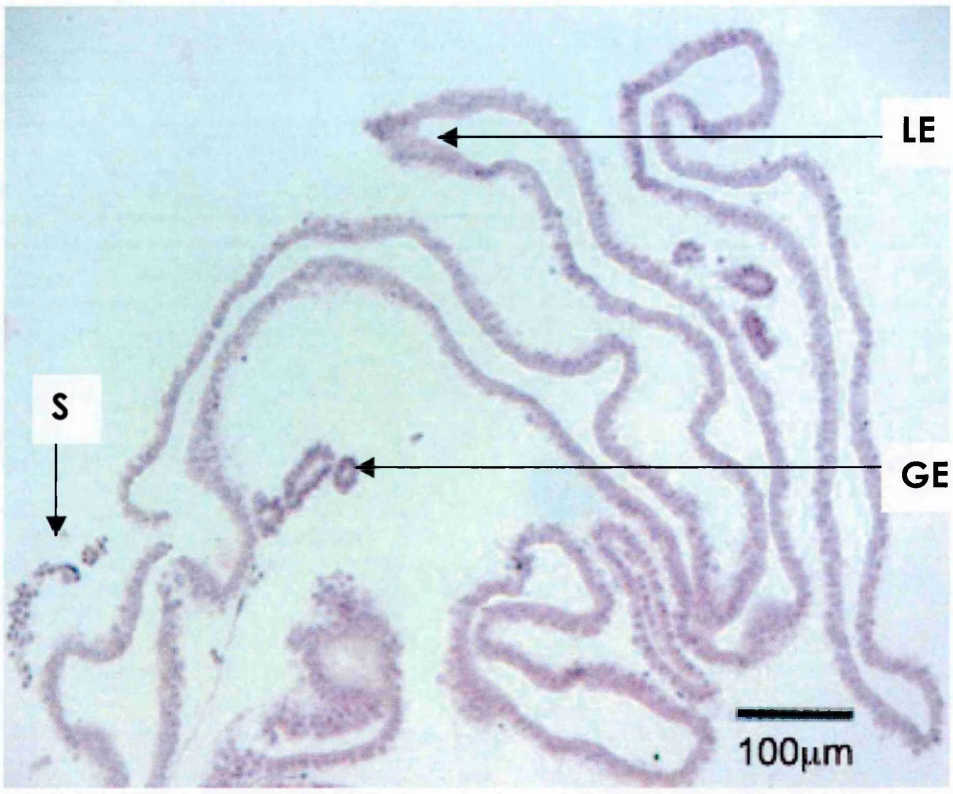

Figure 3.7: Luminal epithelium (LE) contaminated with glandular epithelium (G) and stroma (S). *Glandular tissue can be seen as dark circular patches attached to the epithelium in some samples. Stromal tissue can also be seen in some samples as diffuse darkly staining nuclei.*

To assess contamination of the embedded samples a systematic scoring method was employed, as shown in Table 3.2. The embedded sections were cut using a microtome into long ribbons, then the ribbons cut into smaller ribbons of 6 sections each. Alternate ribbons were systematically mounted onto slides so one ribbon was at the top and one at the bottom to give ten slides in total, each bearing two ribbons. If there were too many ribbons to mount on ten slides then every second ribbon was discarded and the remainder were mounted. If the sample was particularly small, all sections were mounted, even if the number came to less than ten slides. To score for glandular and stromal contamination, each ribbon of six was scanned through and the number of glands counted. Because each 6 were

consecutive samples, glands were often present in the same place on all of the sections in a ribbon.

Day and Sample	Row	*Number of glands in slide number...*										Average number of Glands
		1	2	3	4	5	6	7	8	9	10	
4.1	Top	0	0	0	0	0	0	0	0	0	0	0
	bottom	0	0	0	0	0	0	0	0	0	0	
	Stroma?											
4.2	top	0	2	0	2	0	0	0	0	1	1	0.7
	bottom	2	0	1	2	0	0	0	0	2	1	
	Stroma?		Y	Y								
5.1	top	9	13	9	7	16	5	4	3	2		6.45
	bottom	6	9	11	3	16	8	4	2	2		
	Stroma?	Y	Y	Y								
5.3	top	3	3	1	0	0	2	4	4	3	4	2.1
	bottom	5	3	1	0	0	3	0	3	2	1	
	Stroma?											
5.4	top	3	2	0	0	1	0	1	2	1	1	1.15
	bottom	3	2	1	0	1	2	2	1	0	0	
	Stroma?											

Table 3.2: Histological assessment of epithelial samples for glandular and stromal contamination. *Numbers refer to numbers of glands. Stroma?= stromal contamination present on slide? Y = yes.*

The number of glands in each set of six was counted, rather than the number of glands in each individual section. Stromal contamination was noted if present. The average number of glands per ribbon of 6 sections was calculated. The results were recorded in Table 3.2.

The histological analysis after dispase treatment and mechanical extraction indicates that day 5 epithelial samples appear to contain more glands than day 4

samples. Although the epithelium up-regulates expression of adhesion molecules as the window of implantation progresses, they have been found to be present in the apical membrane (to promote trophoblast attachment), rather than the basal membrane (which would promote epithelial attachment to stroma and result in the 'stickiness' described above) (Aplin, 1997) (Kimber and Spanswick, 2000). Despite this, the stroma and glandular epithelium also express integrins (Bowen and Hunt, 2000) although the type and temporal expression has not been fully characterised in mice. The stroma also contains extra-cellular matrix proteins that act as ligands for integrins on the trophoblast as it invades the stroma and promotes decidualisation. The complex patterns of adhesion molecule expression in the uterus mean that it is likely that the layers of the uterus adhere to each other as well as to the trophoblast around the window of implantation, making the layers of the uterus more difficult to remove from each other. This is discussed further in section 5.2.

3.5: Identification and establishment of molecular markers

The histological observations were then tested by finding markers for each tissue type, and their expression investigated using PCR.

Search for peri-implantation molecular markers

The identification of molecular markers for pregnant uterus tissue subtypes was initially based on a PubMed (http://www.pubmed.net) search of previously published literature. The aim was to pull out some possible markers. These included markers described as only being expressed over this period and markers that were described as being localised immunohistochemically (IHC) or by *in situ* hybridisation (ISH) in restricted anatomical locations. Markers concerned with implantation were of particular interest. The PubMed search string used was 'mouse uterus implantation'. The abstracts of papers found were read to see if they contained information of relevance, then the paper downloaded if it was thought to be useful.

Discussion of papers containing evidence for potential markers

The markers were narrowed down to those that displayed single-tissue expression. Literature databases were searched for papers containing these markers. The evidence found in these papers is discussed below.

In the discussion of all these papers the notation used is day 1 as day of plug. This has been converted from any different notation used by the authors of the paper under discussion.

Epithelial markers

1. Osf2

Osf-2 (Osteoblast stimulating factor 2) was discovered by a microarray analysis to be strongly downregulated by a progesterone inhibitor in the peri-implantation pregnant uterus, implying it is progesterone-regulated (Cheon et al., 2002). Northern blot analysis of whole uterus extract showed *Osf-2* was undetectable on days 1-3 of pregnancy then highly expressed on day 4, and expressed at a slightly lower level on day 5. *In situ* hybridisation revealed that *Osf-2* was localised specifically to the luminal epithelium between days 3 and 5 of pregnancy, with a peak of intensity on day 4.

2. ***EP2***

EP2 is a subtype of prostaglandin E_2 receptor (prostaglandin E_2 receptor subtype EP_2). Northern blots using whole uterus extract show that the level of expression of the *EP2* transcript is barely detectable on day 1 of pseudopregnancy, low levels are found on days 2-4 and a sudden increase causes a peak on day 5 and a subsequent fall to pre-day 5 levels. This pattern is the same in both pregnant (Lim and Dey, 1997) and pseudopregnant mouse uteri (Katsuyama et al., 1996).

In situ hybridizations on pregnant uteri (Lim and Dey, 1997) revealed distinct temporal and cell-specific localization of the *EP2* mRNA during the peri-implantation period. On days 1 and 2, no specific signals for *EP2* mRNA were detected in any uterine cell type. In contrast, weak signals were first detected exclusively in the luminal epithelium on day 3 followed by augmentation of these signals on days 4 and 5 of pregnancy. Pseudopregnant uteri (Katsuyama et al., 1996) were found not to express *EP2* on day 0 of pregnancy (pro-oestrus), but strong expression exclusive to the luminal epithelium was found on day 5. No accumulation was noted in the glandular epithelium in pregnant mice (Lim and Dey, 1997). The same

paper also suggested that luminal epithelial expression of *EP2* mRNA is regulated primarily by circulating steroid hormones, but not by resident blastocysts, implying that the situation would be similar in pseudopregnant mice. *EP2* has previously been used as a successful marker for luminal epithelium (Cheng et al., 2001).

Stromal markers

1. ***Tn-c***

Tn-c (Tenascin-C) is an extracellular matrix glycoprotein, localised along the basement membrane between the luminal epithelium and stroma during early pregnancy. *In situ* hybridisation shows that subluminal stromal cells express *Tn-c* on days 1-3 of pregnancy or pseudopregnancy, expression is reduced on day 4 but reappears on day 5 (Noda et al., 2000). Expression of *Tn-c* is not observed in non-pregnant mice at either the protein or the mRNA level.

2. ***EP3***

EP3, like *EP2*, is a subtype of Prostaglandin receptor E_2 (prostaglandin E_2 receptor subtype EP_3). Northern blots on whole pseudopregnant mouse uterus extract indicate a similar pattern of temporal expression to *EP2* (Katsuyama et al., 1996). *EP3* mRNA was hardly detected on day 0 (pro-oestrus). Beginning on day 1, the transcript progressively increased in abundance to reach the maximum on day 5, which was about 13-fold the level observed on day 1. On days 7 and 9, expression decreased to lower levels than those on day 1. Northern blots on whole pregnant mouse uterus indicate high levels of *EP3* present on days 3 and 4 of pregnancy. Lower levels are present on days 1-2 and day 5 (Yang et al., 1997). *In situ* hybridisation indicates that *EP3* mRNA accumulates in the circular muscle of the myometrium and in the stroma at the mesometrial pole on day 4 of pregnancy, with expression declining on day 5. Expression is similar on day 4 of

pseudopregnancy (Yang et al., 1997). However, another study showed EP_3 to be exclusively in the myometrium of pseudopregnant mice on day 4 of pseudopregnancy (Katsuyama et al., 1996).

Glandular marker

LIF

LIF (leukaemia inhibitory factor) is a cytokine expressed at low levels in a variety of organs, and at a particularly high level in day 4 pregnant uteri, as well as at lower levels on days 1-3 and day 5 onwards (Bhatt et al., 1991). *In situ* hybridisation showed that *LIF* was localised specifically in the endometrial glands on day 4 of pregnancy. Low signals were present throughout the endometrium on days 1-3. As the endometrial glands degenerated from day 5 onwards, their *LIF* expression declined. Day 4 pseudopregnant females also exhibited strong LIF expression, implying that expression is maternally controlled. *LIF* is expressed by the glandular epithelium and binds to *LIF* receptors in the luminal epithelium, where it initiates a transcription cascade to prepare the epithelium for implantation. LIF has previously been used as a successful marker for glandular epithelium (Cheng et al., 2001).

Prostaglandin receptor expression

Based on the evidence presented above, it was decided initially to undertake preliminary studies on the two prostaglandin receptors EP_2 and EP_3 as markers for luminal epithelium and stroma respectively. It was decided to test them using conventional RT-PCR (see figure 3.8) at first, then move on to real-time RT-PCR if this gave grounds for doing so.

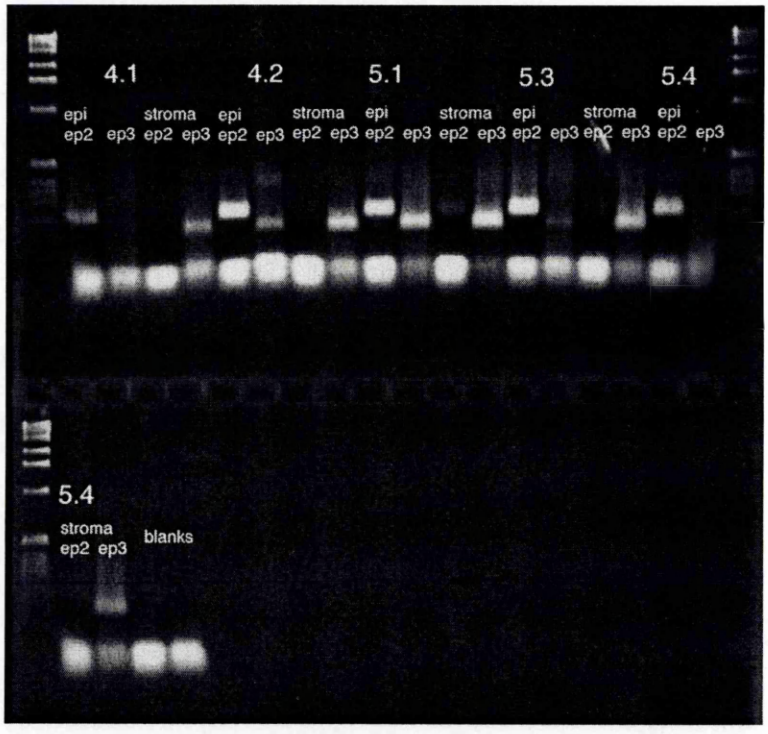

Figure 3.8: Gel electrophoresis of EP_2 and EP_3 PCR products. *Primers were optimised using a stock of day 4 pseudopregnant whole-uterus cDNA. They were then used in PCR reactions with the sample sets from day 4 and 5 pseudopregnant uteri (section 2.6.1). Lanes at the extreme edges of the gel are NEB 1kb molecular mass markers. Details of primers and PCR product size expected are detailed in section 2.6.2. Key: epi = epithelium, stroma = stromal tissue, Numbers indicate the day of pseudopregnancy and the sample number.*

The results from Figure 3.8 show that sample 4.1 has EP_2 present in epithelium but not stroma and EP_3 present in stroma but not epithelium. Sample 4.2 has EP_2 present in epithelium but not stroma and EP_3 present strongly in stroma, weaker in epithelium. Sample 5.1 has EP_2 present strongly in epithelium, weakly in stroma and EP_3 present strongly in epithelium and stroma. Sample 5.3 has EP_2 present in epithelium but not stroma and EP_3 present strongly in stroma, weakly in epithelium. Sample 5.4 has EP_2 present in epithelium but not stroma and EP_3 present in stroma but not epithelium. For verification that these results were real and not a result of the PCR failing, the PCR was repeated, with the same outcome.

EP_2 appeared to be a good marker for luminal epithelium, because it clearly distinguished between luminal epithelium and stroma. In the case of sample 5.1 (where it appears to be present in the stroma), some luminal epithelium contaminating the stromal preparation could be seen (data not shown). *EP_3* was present in all of the stromal samples, but also in 3 out of 5 of the epithelial samples. There are several interpretations of this finding. If it is assumed that the paper indicating *EP_3* as a stromal marker is reliable, then the result might represent the presence of stromal contamination in the epithelial preparations. Alternatively, *EP_3* may be expressed in glandular tissue (or some other uterine component), or the luminal epithelium may express *EP_3* at a low level. The gross observations recorded when the epithelia were extracted (see earlier) do not help resolve which of these explanations is correct: there was no correlation between the presence of *EP_3* in epithelial preparations and the difficulty of the extraction. The validity of *EP_3* as a stromal marker needed to be confirmed by real-time RT-PCR with a range of samples, and other markers tested as well. Although EP_2 appeared to be a good marker of luminal epithelium, it was considered a good idea to look at other potential markers also. In addition, standard RT-PCR is not quantitative, as the PCR product is visualised on a gel at the plateau phase of amplification. The presence or absence of gene expression is evident, but it is not possible to quantify it.

Therefore, sets of Taqman® primers and probes for both *EP*$_2$ and *EP*$_3$ were designed (Table 2.8) and samples of Taqman® primer/probe sets for the potential markers *Tn-C* (stroma), *Osf-2* (luminal epithelium) and *LIF* (glandular epithelium) were obtained from collaborators (Table 2.9) with the aim of defining suitable markers for each tissue type.

3.6: Real-Time PCR analysis using Taqman®

Following RNA extraction and reverse transcription, real-time RT-PCR analysis was performed with primer/probe sets for the genes *EP2, EP3, Tn-c, LIF* and *18s* (section 2.7.5) using an ABI Prism 7700 Real-Time PCR machine (section 2.7.6) and the data obtained were analysed using Opticon Monitor Software and Microsoft Excel™ (section 2.7.7). The technology behind Taqman®, the relative merits of different protocols for real-time PCR and how a decision was arrived at on which of them to use is discussed in sections 2.7.4 and 2.7.5.

Using 18s rRNA as a normaliser gene

The samples were run using the 18s rRNA gene as a normaliser in two technical replicates, which are shown in Figure 3.9. An average of the two technical replicates was used when obtaining the normalised ratio of the gene of interest.

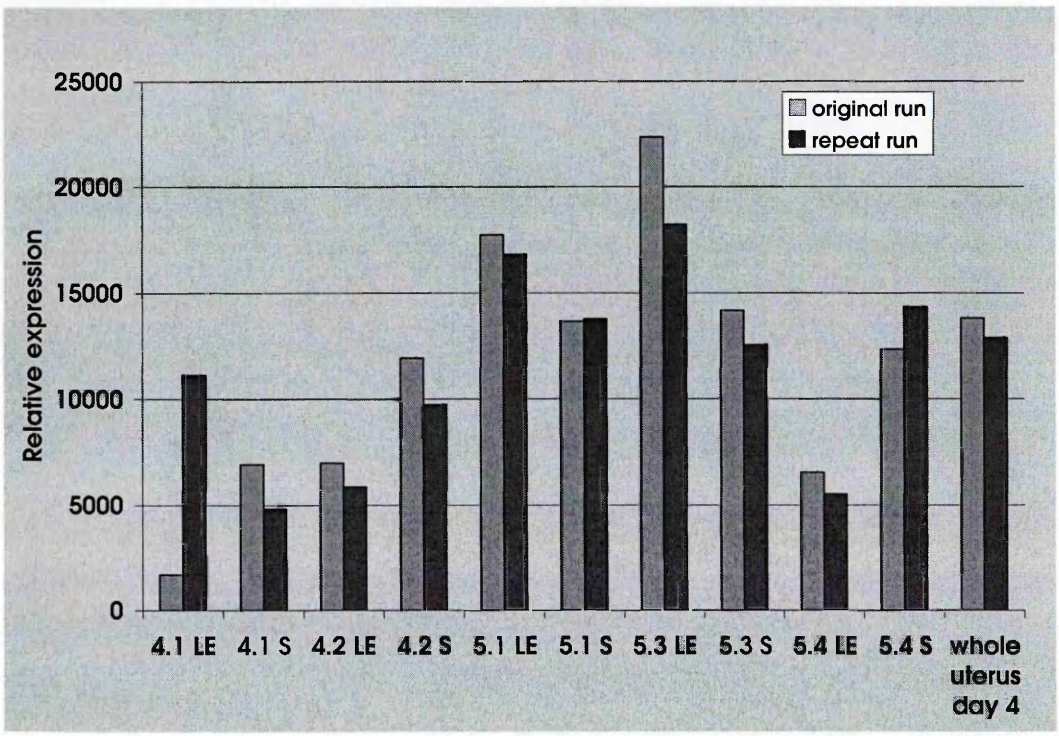

Figure 3.9: Results obtained by Real-time RT-PCR using Taqman®, comparing two replicate experiments quantifying 18s rRNA gene expression in manually dissected samples of luminal epithelium (LE), stroma/glands (S) and whole uterus from days 4 and 5 of pseudopregnancy. *An average of the two technical replicates was used when obtaining the normalised ratio of the gene of interest.*

Quantification of specific marker genes

As discussed in section 3.5, two of the tissue types have more than one gene identified to test as a potential marker. The results obtained by testing each of the Taqman® sets on the pseudopregnant uterine tissues and the results of the histological examination of the corresponding uterine horns were compared to decide which of the potential markers was the most appropriate to use as an indicator of the composition of uterine tissue samples. The results are discussed in section 3.8.

Luminal epithelium markers

Two potential luminal epithelium markers were available for analysis, Osf-2 and EP_2. Their patterns of expression are shown in Figures 3.10 and 3.11.

Osf-2

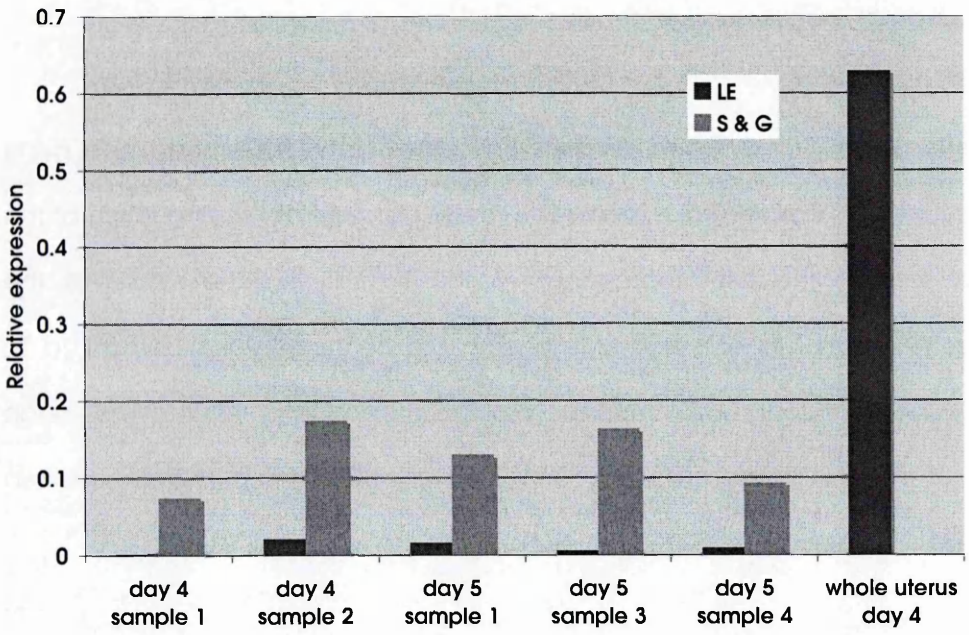

Figure 3.10: Results obtained by Real-time RT-PCR using Taqman®, showing the ratio of Osf-2 expression to 18s expression in manually dissected samples of luminal epithelium (LE), stroma/glands (S&G) and whole uterus from days 4 and 5 of pseudopregnancy.

Despite evidence indicating that *Osf-2* is expressed specifically in the luminal epithelium (Cheon et al., 2002), it is present at higher levels in the S&G samples than it is in the LE samples. It is also present at a very high level in the whole uterus sample. There does not appear to be any correlation between the day the samples were taken and the levels of Osf-2 present. It is present in the whole uterus sample at a much higher level than individual S&G or LE samples.

EP2

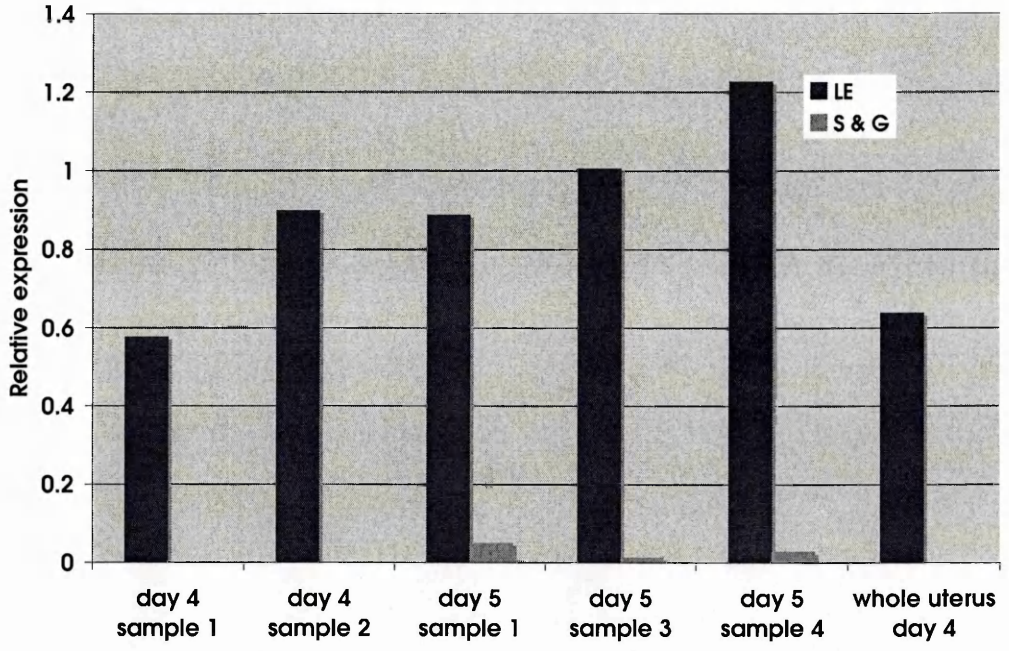

Figure 3.11: Results obtained by Real-time RT-PCR using Taqman®, showing the ratio of EP_2 expression to 18s expression in manually dissected samples of luminal epithelium (LE), stroma/glands (S&G) and whole uterus from days 4 and 5 of pseudopregnancy.

Figure 3.11 shows that *EP_2* is present at high levels in the LE samples, and at low levels (if at all) in S&G samples. The day 5 S&G samples contain a higher level of *EP_2* than the day 4 S&G samples. There does not appear to be any correlation between the day of sample and level of EP_2 present in the LE samples. EP_2 is present at a higher level in LE samples than it is in the whole uterus sample in all LE samples apart from 4.1.

Stromal markers

Two potential stromal markers were available for analysis: *Tn-c* and *EP3*. Their expression patterns are shown in Figures 3.12 and 3.13.

Tn-c

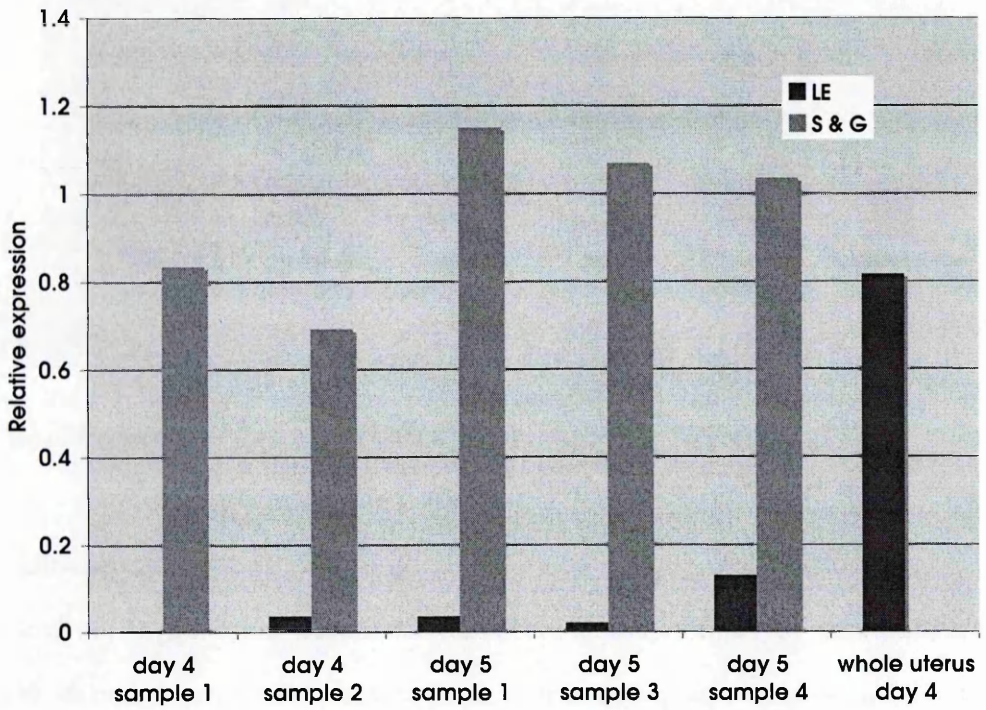

Figure 3.12: Results obtained by Real-time RT-PCR using Taqman®, showing the ratio of Tn-C expression to 18s expression in manually dissected samples of luminal epithelium (LE), stroma/glands (S&G) and whole uterus from days 4 and 5 of pseudopregnancy.

Figure 3.12 shows that Tn-c is present in the S&G samples at a much higher level than in the LE samples. There appears to be a slightly higher level of Tn-c in day 5 S&G samples compared to day 4. Some Tn-c is present in all LE samples, but the level does not seem to correlate with day. Tn-c is present at higher levels in the day 5 S&G samples than in the whole uterus sample. For day 4 S&G samples it is at the same level or slightly lower than the whole uterus sample.

EP3

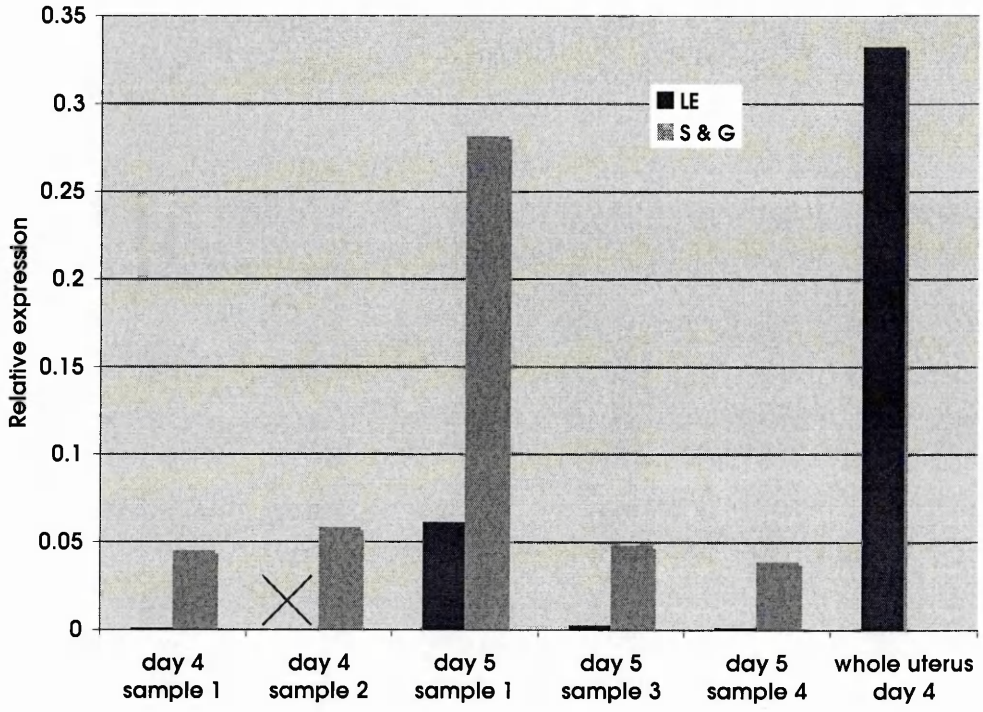

Figure 3.13: Results obtained by Real-time RT-PCR using Taqman®, showing the ratio of EP_3 expression to 18s expression in manually dissected samples of luminal epithelium (LE), stroma/glands (S&G) and whole uterus from days 4 and 5 of pseudopregnancy.

Figure 3.13 shows that EP_3 is present in the S&G samples at a higher level than the LE samples. There does not seem to be much of a difference in level of expression between day 4 and day 5 samples. Some EP_3 is present in all LE samples but the level of expression does not seem to correlate with day. EP_3 is present at a higher level in the whole uterus sample than it is in the S&G samples. NB: There was not enough cDNA left from the day 4 sample 2 LE to run using this primer set. The sample has been included in the graph above so that the paired format is kept, but a red cross has been placed through its column to indicate that the sample was not run with EP_3.

Glandular epithelium marker- *LIF*

Only one gene was identified as a potential marker of glandular epithelium: LIF. *Figure 3.14 shows its expression pattern.*

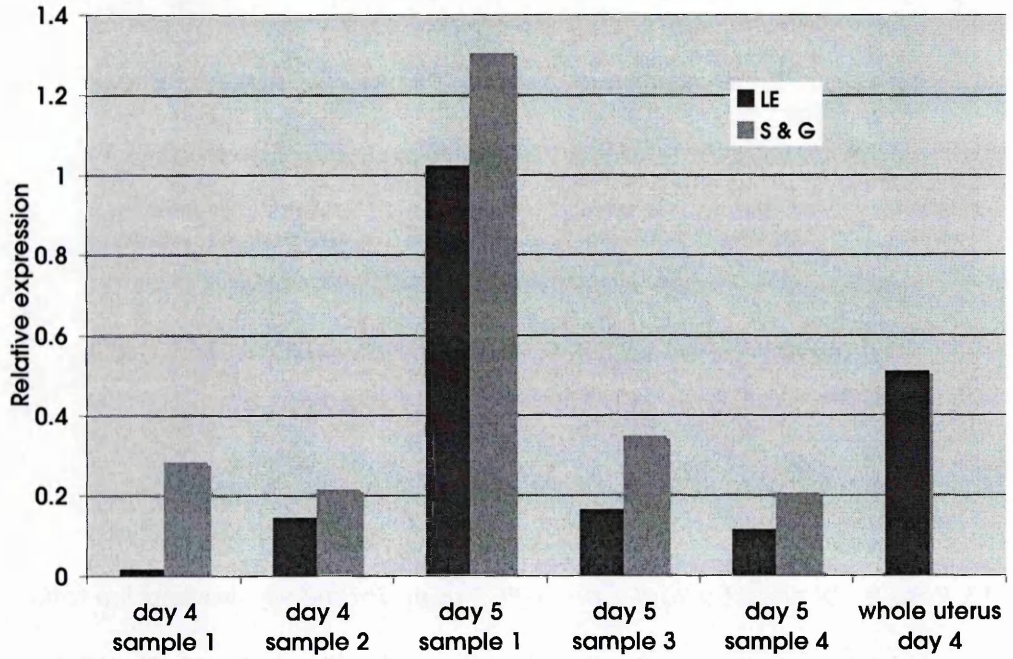

Figure 3.14: Results obtained by Real-time RT-PCR using Taqman®, showing the ratio of LIF expression to 18s expression in manually dissected samples of luminal epithelium (LE), stroma/glands (S&G) and whole uterus from days 4 and 5 of pseudopregnancy.

Figure 3.14 shows that LIF appears to be present at slightly higher levels in the S&G samples of each pair. It is present at very high levels in both the LE and S&G of sample 5.1. It is present at a slightly higher level in the whole uterus sample than in individual S&G or LE samples (except sample 5.1).

3.7: Testing markers on a panel of samples for use in a microarray

To test their usefulness in a practical situation, the uterine tissue type Taqman® primer/probe sets discussed in section 3.6 (with the exception of the set for *Osf-2*) were used to assess the composition of 12 luminal epithelium and stroma/glands samples taken from across the peri-implantation period (two from Day 3 21:00, three from day 4 09:00, two from day 4 21:00, two from day 5 09:00 and three from day 5 21:00) for use in a microarray study (Campbell et al., 2006). The results are shown in Figure 3.15.

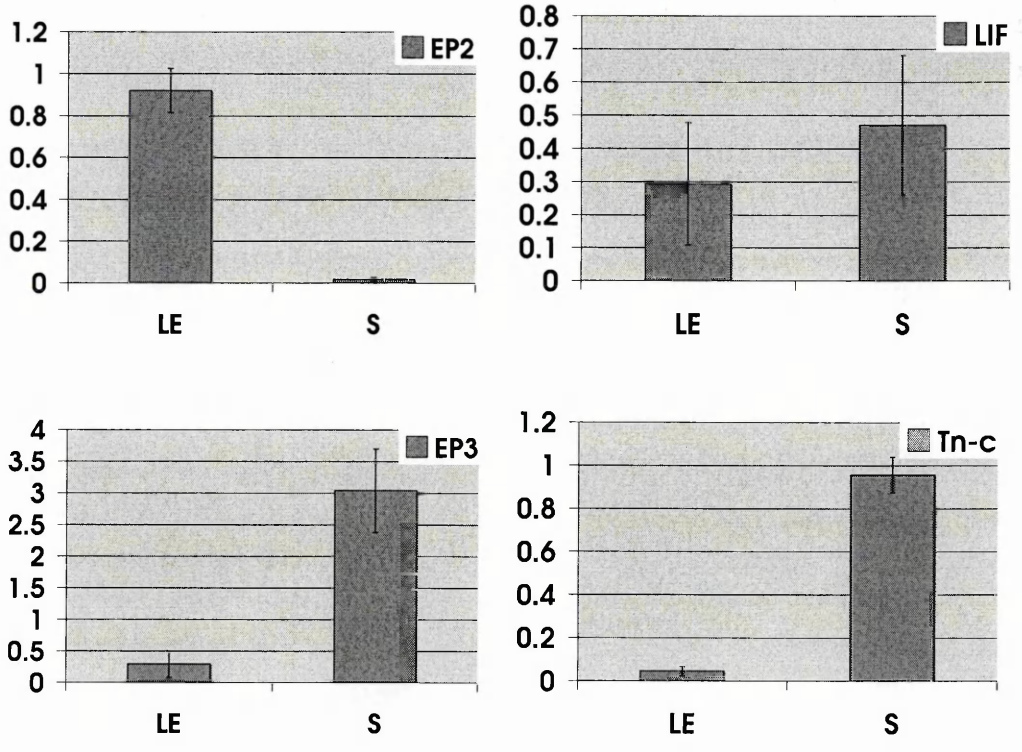

Figure 3.15: Results obtained by Real-time RT-PCR using Taqman®, showing the mean and SEM of EP_2, LIF, EP_3 and Tn-c expression in relation to 18s expression in manually dissected samples of luminal epithelium (LE) and stroma/glands (S&G) from days 3, 4 and 5 of pseudopregnancy.

The means and SEMs shown in Figure 3.15 were calculated for the 12 samples. The results are similar to those obtained in section 3.6. EP_2 was strongly expressed in LE samples, S&G samples were enriched for EP_3 and Tn-c and LIF was found to be present in both LE and S&G samples, although at a slightly higher level in the S&G samples.

The tissues tested above were used successfully in a subsequent microarray study (Campbell et al., 2006). This is discussed in Chapter 5.

3.8: Discussion of Chapter 3

The aim of this part of the research was to validate and develop molecular markers for the luminal epithelium (LE) and stroma (S) of uterine endometrium in early pregnancy using real-time RT-PCR on dissected tissue components, and to relate the molecular and histological data. The initial studies focussed on enzymically dissected stroma and luminal epithelial tissues. This technique (Bigsby et al., 1986) had been used before in non-pregnant, pregnant and pseudopregnant mice RNA extracted from these tissues has been used successfully in many of the techniques described in section 1.3.1, including northern blotting (Cheng et al., 2001; Kurita et al., 2001; Kurita et al., 2000; Sidhu and Kimber, 1999), conventional RT-PCR (Illingworth et al., 2000; Tong et al., 1996), real-time RT-PCR (Catalano et al., 2005), ribonuclease protection assays (Cheng et al., 2001) and microarrays on both pseudopregnant (Campbell et al., 2006) and neonatal (Hu et al., 2004) tissue.

Preliminary studies were undertaken to look at the complications of using this technique in pseudopregnant animals. During this part of the study, it was observed that in pseudopregnant animals the extraction procedure resulted in LE remaining attached to the stroma, and it was separated by picking off using forceps. Day 5 pseudopregnant epithelia were also observed to contain glandular epithelium. The stroma also contained glandular epithelium. Therefore, in the second part of the study, markers that distinguished all three tissues were identified by a PubMed search. Markers were picked for further study if they appeared to be exclusive to one tissue type. Taqman® primer and probe sets were designed or obtained for these marker genes, and used to look at samples of stroma and epithelium from day 4 and 5 pseudopregnant mice. These results were validated by histological studies confirming the relative purity of the samples, as shown in Table 3.3.

Sample number	Tissue	EP2	Tn-c	EP3	LIF	Histology observations
4.1	LE	√	X	X	X	No glandular or stromal contamination in
	S&G	X	√√	√	√	LE samples
4.2	LE	√√	X	n/a	√	Slight glandular and stromal
	S&G	x	√√	√	√	contamination in LE samples
5.1	LE	√√	X	√	√√	Relatively high glandular contamination
	S&G	X	√√	√√	√√	and slight stromal contamination in LE samples
5.3	LE	√√	X	x	√	Slight glandular contamination in LE
	S&G	x	√√	√	√	samples, no stromal contamination
5.4	LE	√√	√	X	√	Slight glandular contamination in LE
	S&G	X	√√	√	√	samples, no stromal contamination
Whole uterus	Whole uterus	√√	√√	√√	√	

Table 3.3: A comparison of Taqman® results for the genes EP_2, Tn-c, EP_3 and LIF with histological observations from day 4 and 5 LE and stroma/glands samples used in Chapter 3. *The Taqman® results were scored as follows; √√: the normalised value for the appropriate sample was between the highest value recorded for that primer set and half the highest value recorded for that primer set (excluding the whole uterus value), √: the normalised value for the appropriate sample was between half the highest value recorded for that primer set and 1/10th of the highest value recorded for that primer set (excluding whole uterus), X: the normalised value for the appropriate sample was below 1/10th of the highest value recorded for that primer set (excluding the whole uterus value). N/a = data not available.*

Epithelial markers

When comparing the real-time RT-PCR results as represented by Figure 3.10 and Figure 3.11, the immediate conclusion is that *EP_2* is a more appropriate marker for epithelium than *Osf-2*. High levels of *EP_2* are present in LE samples on both day 4

and day 5, backing up previous results from other papers (Lim and Dey, 1997) (Katsuyama et al., 1996). It is assumed on the basis of the histology results that the LE samples are composed mainly of luminal epithelium (Table 3.2), so this implies that the luminal epithelium expresses *EP2* at a much higher level than the stroma. This result contrasts with *Osf-2*, which was found to be present at a higher level in S&G samples than it was in LE samples.

A possible reason why these experiments indicate a very different expression pattern of *Osf-2*, is that the original experiments used pregnant animals and the ones in these studies used pseudopregnant animals (Cheon et al., 2002). The expression of *Osf-2* may be induced by or affected by the presence of an embryo, which could explain the difference in results. A further explanation is that *Osf-2* may be expressed in glandular epithelium or stroma in pseudopregnant animals, as this would concur with the pattern of expression shown by the real-time RT-PCR. Another point to note is the distinctly higher expression of *Osf-2* in the whole uterus sample compared to individual S&G and LE samples. This may be due to expression in another uterine tissue such as myometrium. This could be investigated by performing RNA extraction and real-time RT-PCR on the residual uterine tissue left after dispase treatment and mechanical extraction of the luminal epithelium and stroma, or by laser capture microdissection, as described in Chapter 4.

The explanation for the presence of traces of *EP2* in S&G samples from day 5 could be explained in one of two ways. Either the stroma or glands expressed *EP2* only on day 5, or the day 5 samples were more likely to have contaminating luminal epithelium in the stroma samples. Since previous papers (Lim and Dey, 1997) (Katsuyama et al., 1996) indicate exclusive expression in the luminal epithelium it is most likely to be due to small amounts of contamination of luminal epithelium in my S&G samples.

Stromal markers

Tn-c is a convincing marker for stroma. Its gene product is present at much higher levels in S&G samples than in luminal epithelium samples, implying that the stroma expresses it at a higher level than the LE. The presence of low levels of *Tn-c* in all the epithelium samples could have three explanations. Either the luminal epithelium expresses *Tn-c* at a very low level, the glandular epithelium also expresses *Tn-c* (and GE is present in the LE samples), or the luminal epithelium preps are contaminated with low levels of stroma. Looking at the histological assessment of epithelial samples (Table 3.2), stroma is noted in only 2 of them. Stromal contamination is difficult to score unless it is present in large fragments, so it is possible that smaller fragments were present in the sections that were unable to be scored accurately. Also, two separate uterine horns from the same uterus are used for RNA extraction and histology and it is possible that each had different levels of stromal contamination, as no two extractions are the same. The possibility that the glandular epithelium expresses low levels of *Tn-c*, is investigated further in Chapter 4 using laser microdissection.

EP3 is a less certain stromal marker. Although it is present at higher levels in stroma samples than it is in epithelial samples, it is present at quite a low level even in these stroma samples compared to the whole uterus. The only stroma sample that seems to contain *EP3* at a high level is day 5 sample 1.

EP3 is expressed in the myometrium as well as the stroma (Yang et al., 1997), although there is some disagreement about whether the expression is in the myometrium only (Katsuyama et al., 1996). Myometrial expression would explain why the whole uterus sample has a higher level of EP_3 than the individual LE or S&G samples. It is unlikely that the level of EP_3 in the S&G or LE samples shown here is due to myometrial contamination because the dispase treatment and mechanical dissection is unlikely to affect the myometrial layers of the uterus, but this cannot be ruled out. Laser microdissection is used in Chapter 4 to investigate this further.

Glandular epithelium marker

Levels of *LIF* mRNA are particularly high in both sample 5 LE and S&G. Histological analysis shows that LE sample 5.1 seems to be enriched for glandular epithelium (Table 3.2), which implies that glandular epithelium is expressing *LIF*. Previous studies (Bhatt et al., 1991) on pregnant mice show *LIF* as being expressed strongly only on day 4, with day 5 levels declining. This is because in pregnant animals the endometrial glands are starting to disintegrate on day 5 and *LIF* signal is being lost. Since day 5 pseudopregnant mice still have intact glandular epithelium they should still be expressing *LIF*. It cannot be concluded that *LIF* is a good marker for glandular epithelium without further study. Unlike the luminal epithelium and stroma samples, it is difficult to obtain glandular epithelium in relatively pure amounts using mechanical extraction alone. This problem will be further addressed in Chapter 4.

Investigating localisation of potential marker genes in this part of the study resulted in promising data to verify their exclusive expression for use as markers for each tissue type. Despite this, the experiments did not confirm for certain that *LIF* is exclusively expressed in glandular epithelium. Previous studies show exclusive expression in the glandular epithelium (Bhatt et al., 1991) and in this study higher levels of *LIF* were observed in samples containing more glandular epithelium. But in order to confirm these results, it is desirable to obtain a pure sample of glandular epithelium. In Chapter 4 this problem is addressed using laser microdissection.

Chapter 4: Markers specific for uterine sub-component tissues

Summary

4.1: Introduction

The epithelial and stromal samples obtained using enzymatic separation and manual dissection cannot be assumed to be pure samples of one cell type. Glandular epithelium is clearly embedded in the uterine stroma and impossible to remove by manual dissection, as seen in the dissected tissues discussed in Chapter 3. In addition, some epithelial samples, especially those obtained on day 5 of pseudopregnancy have some dilations that look as though some glandular tissue may have been isolated as a contaminant. On current evidence, the tissues can only be described as 'enriched' rather than pure. In order to test whether the markers used on these luminal epithelial and stroma samples are tissue specific, tissue samples of more certain composition were obtained. The technique chosen to obtain pure samples was laser microdissection, the value of which is discussed in section 2.4.3.

Using laser microdissection, putatively pure samples of luminal epithelium, glands and stroma were obtained from day 5 pseudopregnant uteri. Real-time RT-PCR was run on these samples to confirm that the markers identified in Chapter 3 were indeed tissue specific, followed by a microarray experiment aiming to find more markers specific for each tissue type.

4.2: Laser microdissection of uterine tissues

4.2.1: Obtaining samples

The original aim of this experiment was to confirm that the previously identified markers were specific and to run a microarray experiment to find new markers, and also to look at the expression of circadian genes in each individual tissue over a 24 hour period. This method was used to obtain duplicate sets of three uterine tissues (LE, stroma and glands) from seven time points spaced every 4 hours around day 5 of pseudo-pregnancy. This aim was modified during the experiment after only low amounts of RNA were obtained from the tissues.

Duplicate sets of tissues were obtained from pseudopregnant mice sacrificed at 7 time points from days 5 and 6, giving a total of 14 samples (sections 2.2.3, 2.2.4). The first time-point taken was ZT0 (ZT= 'zeitgeber time', ZT0 is defined as the 'lights on' in a laboratory 12 hour light: 12 hour dark lighting schedule) on day 5, then samples were taken at 4 hour time points until 6am on day 6: designated ZT24. After removing the uterine horns, half of one horn was placed into a sterile 1.5ml Eppendorf tube, flash-frozen in liquid nitrogen then stored at -80°C. These half horns were taken for laser microdissection preparation. The epithelium and stroma from the remaining 1.5 horns were removed after dispase treatment and mechanical extraction as before, then placed in a 1.5ml Eppendorf tube containing 100µl Trizol and frozen at -80°C. These samples were taken for RNA extraction (see Chapter 5).

The half-horns destined for laser microdissection were embedded in OCT embedding medium and sectioned using a cryostat to a thickness of 12µm (section 2.4.2). The sections were mounted on membrane slides and stained with cresyl violet (section 2.4.4) before being taken immediately for laser microdissection on a Leica LMD6000 microscope (section 2.4.5). Luminal epithelium, glandular epithelium and sub-luminal stroma were microdissected for each sample. Each

tissue type from each sample was dissected for approximately half an hour to obtain similar amounts, and the areas dissected were recorded in Table 4.1

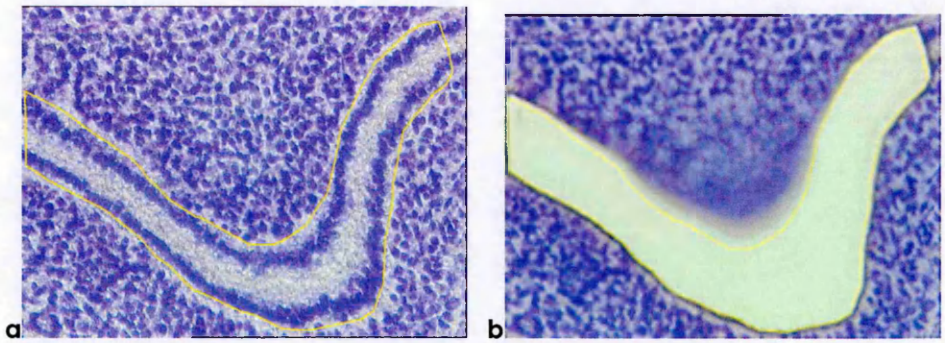

Figure 4.1: Representative photos before (a) and after (b) laser microdissection of luminal epithelium from frozen sections of whole uterus stained with cresyl violet.

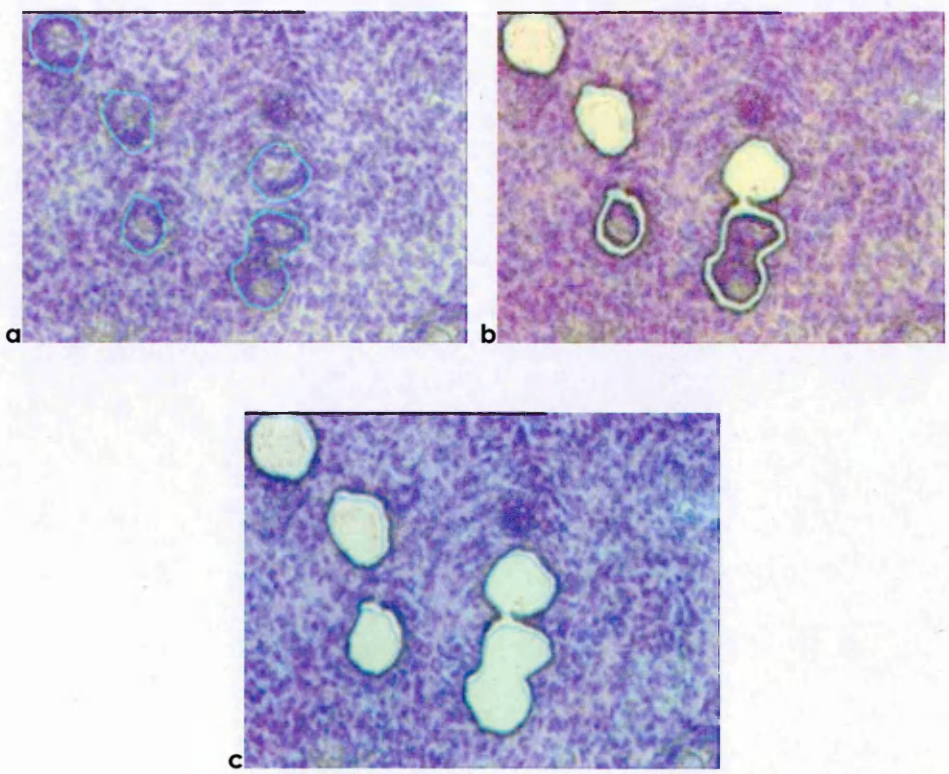

Figure 4.2: Representative photos before (a), during (b) and after (c) laser microdissection of glandular epithelium from frozen sections of whole uterus stained with cresyl violet.

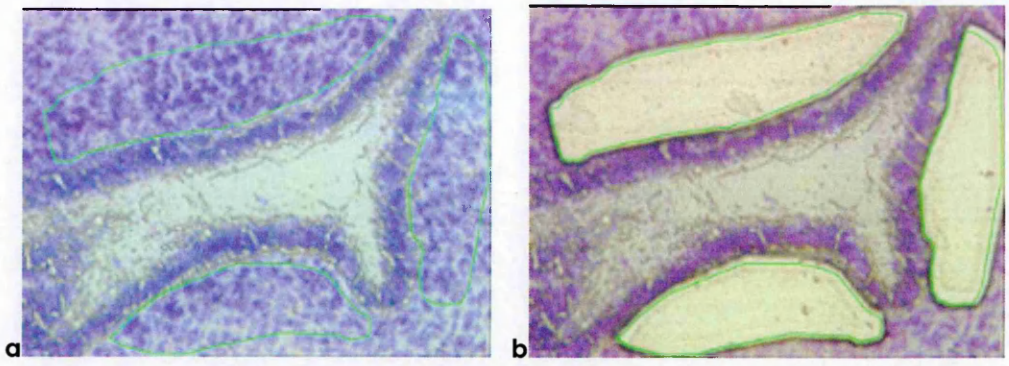

Figure 4.3: Representative photos of the sub-luminal stroma before (a) and after (b) laser microdissection from frozen sections of whole uterus stained with cresyl violet.

Sample	ZT (hrs)	LE (mm^2)	Stroma (mm^2)	Glands (mm^2)
1	4	0.051	0.06	0.037
2	4	0.113	0.083	0.026
3	16	0.062	0.070	0.030
4	16	0.113	0.109	0.047
5	20	0	0	0
6	20	0.110	0.071	0.044
7	24	0.205	0.148	0.082
8	24	0.071	0.071	0.055
9	0	0.220	0.227	0.110
10	0	0.182	0.106	0.036
11	8	0.160	0.101	0.052
12	8	0.281	0.170	0.070
13	12	0.168	0.116	0.048
14	12	0.070	0.036	0.041
Average		0.139	0.106	0.052
SEM		±0.019	±0.014	±0.006
Total (mm^2)		1.804	1.371	0.678

Table 4.1: Summary of the area of laser microdissected samples obtained from each of the 14 tissue samples, *The average and standard error of the mean obtained for each tissue type (LE, stroma and glands) and the total area (in mm^2) obtained from each tissue type is also given. Sections from sample 5 (CT 20) could not be obtained on the cryostat, leaving 13 samples with no duplicate for the 20-hour time point. ZT= zeitgeber time, LE= luminal epithelium.*

All tissue types were easily identifiable using the cresyl violet staining method. The boundaries between each tissue type were clear, allowing defined areas to be selected for microdissection. Luminal epithelium and subluminal stroma were easy to obtain, since large areas could be cut. However there were fewer areas present to take, since if luminal epithelium was cut from one particular area, the surrounding subluminal stroma was not used for the stoma sample to ensure no remaining luminal epithelium was removed with it. Areas of luminal epithelium also contained the lumen of the uterus, seen on the photographs as the gap between two layers of epithelium. This meant that although the area of luminal epithelium obtained was the largest of the three tissues (see Table 4.1), the amount of RNA obtained per unit area was the smallest. Since stromal tissue is not dense compared to epithelial tissue, the yield of RNA per unit area was also relatively low. It would have been possible to cut thin strips of epithelium to avoid taking the lumen space, but smaller areas of tissue do not detach as easily from the slide as larger areas.

Glandular epithelium was more difficult to obtain. Since the glands are relatively small, less tissue is obtained from the same length of cutting time (as can be seen in Table 4.1). But because the glandular tissue is dense, it yields proportionately more RNA per unit area. At several points during the cutting of each sample, the cut sections were visualised in the tube cap underneath the slide. This verified that the sections were detaching from the slide and collecting in the cap.

4.2.2: Obtaining RNA

After obtaining microdissected tissues, RNA was extracted from the samples using the Arcturus PicoPure RNA extraction kit (section 2.4.6). 1µl RNA was quantified using a NanoDrop spectrophotometer, leaving 10µl RNA remaining in each sample. Yields are shown in Table 4.2.

Sample	ZT (hrs)	LE total RNA (ng)	S total RNA (ng)	G total RNA (ng)
1	4	20	None	17
2	4	13.5	25	21.7
3	16	19.8	32.7	20.3
4	16	58.1	48.2	31.9
6	20	26.1	13.7	22
7	24	73.7	50.9	37.5
8	24	48.3	114.3	57.2
9	0	71.3	43	46.3
10	0	20.2	22.3	45.3
11	8	51.3	50.3	47.8
12	8	42.8	52	26.7
13	12	46.8	44.3	56.9
14	12	51 & 54	30	27
		42.6	43.9	35.2
Average ± SEM		± 5.25	± 7.38	± 3.93
Total		596.9	526.7	457.6
Yield per unit area (ng/mm²)		330.7	384.0	674.5

Table 4.2: Amount of RNA obtained from laser microdissection samples using the Arcturus PicoPure RNA extraction kit. *Units are given in nanograms (ng). Amount of RNA per area of tissue obtained from laser microdissection is also shown, given in nanograms per millimetre squared (ng/mm²). Sample 1 stroma tube shattered in the centrifuge during RNA extraction, so no RNA was obtained. Two samples of tissue were taken for sample 14 LE. LE= luminal epithelium, S= subluminal stroma, G= glandular epithelium.*

As detailed in section 4.2.1, the original aim of taking duplicate samples of each tissue at four-hourly time points was to investigate whether each tissue had a separate peripheral circadian rhythm, as well as confirming tissue-specific marker expression and running a microarray. A 500ng RNA sample is required for the pre-

microarray reverse transcription reaction. 1st strand product can be subsequently sampled from this pool after reverse transcription and taken for Taqman®; 100ng at a time is then labelled for use for a microarray. As shown in Table 4.2, there was insufficient material in each individual sample to perform duplicate microarray and Taqman® analysis on each tissue for each time point. This left four options:

1. Combine all time points but not replicates, giving 2 replicates of each of the three tissues containing samples from all 7 time-points.

	LE (ng)	S (ng)	G (ng)
Set 1 (samples 1,3,6,7,9,11,13)	309	234.9	247.8
Set 2 (samples 2,4,8,10,12,14)	287.9	291.8	209.8

Table 4.3: Amount of RNA that would be obtained from making two pools of the RNA from samples obtained by laser microdissection of day 5 pseudopregnant uterus, each pool containing one of the replicates from each time point. *Values are for luminal epithelium (LE), stroma (S) and glands (G) samples in nanograms of RNA (ng).*

2. Combine the duplicate biological replicates, giving 7 time points with 2 replicates in each for each of the three tissues.

ZT	Samples	L (ng)	S (ng)	G (ng)
0	9, 10	91.5	65.3	91.6
4	1,2	33.5	25	38.7
8	11,12	94.1	50.3	74.5
12	13,14	151.8	74.3	83.9
16	3,4	77.9	80.9	52.2
20	6	26.1	13.7	22
24	7,8	122	165.2	94.7

Table 4.4

Table 4.4: Amount of RNA that would be obtained from pooling both of the replicates of the RNA from samples obtained by laser microdissection of day 5 pseudopregnant uterus sections from each time point sample. *Values are for luminal epithelium (LE), stroma (S) and glands (G) samples in nanograms of RNA (ng).*

3. Combine replicates for the early time point samples (ct 0, 4, 8, 12) and late time point samples (16, 20, 24) giving two pools for each tissue type.

	LE (ng)	S (ng)	G (ng)
ZT 0-12 (samples 9, 10, 1, 2, 11, 12, 13, 14)	370.9	266.9	288.7
ZT 16- 24 (samples 3,4,6,7,8)	226	259.8	168.9

Table 4.5: Amount of RNA that would be obtained from making two pools of RNA, one containing all samples with a ZT of between 0-12 and the other containing all samples with a ZT of between 16-24, *Values are for luminal epithelium (LE), stroma (S) and glands (G) samples in nanograms of RNA (ng).*

4. Combine all samples of each tissue type

Sample	Total amount of RNA (ng)
Luminal epithelium	596.9
Stroma	526.7
Glands	457.6

Table 4.6: Amount of RNA that would be obtained from combining all samples from each tissue.

Option 4 was chosen, as it was the only one to yield the 500ng necessary for the 1st strand RT reaction. Although this meant that the option of quantifying canonical circadian genes in separate uterine tissues over the course of the peri-implantation period was now not possible, the primary objective of confirming existing potential markers of tissues using Taqman® and searching for new ones using microarrays was still possible.

Since the samples were now in a total volume of 120 to 140 µl and needed to be in a total volume of 3µl for the first strand reaction, all samples for each tissue were pooled as discussed above, the RNA precipitated using sodium acetate and ethanol (section 2.7.2) and resuspended in 3.5µl nuclease-free water. 0.5µl RNA was made into a 1 in 4 dilution (with 1.5µl nuclease-free water) and quantified using a NanoDrop spectrophotometer. The concentrations after precipitation are shown in Table 4.7

	RNA Concentration of 1 in 4 dilution (ng/µl)	Total amount of RNA (ng)
LE	34.47	413.64
S	20.06	360.96
G	30.08	240.72

Table 4.7: Total RNA available for first strand synthesis, *Values are given in nanograms per microlitre (ng/µl) or nanograms (ng) and are calculated using the NanoDrop spectrophotometer readings and multiplying by a dilution factor of 4, then by the total volume of the remaining sample. LE= luminal epithelium, S= subluminal stroma, G= glandular epithelium.*

Microarray 1st strand synthesis (section 2.5.1) was performed on the remaining 3µl of undiluted RNA. Despite none of the samples containing more than 500ng after precipitation the first strand reaction was run with the full amount of RNA for each, as the concentration would be assessed again after the microarray amplification

reaction to ensure equal amounts were used for the microarray. After 1st strand synthesis, the RNA was in a volume of 10µl. 2µl were taken for cDNA amplification for microarray analysis (section 4.4), the other 8µl were used for real-time PCR using Taqman® (section 4.3).

4.3: Confirming specificity of uterine tissue markers using Taqman®

Following RNA extraction and reverse transcription, real-time RT-PCR analysis was performed with primer/probe sets for the genes *EP2, EP3, Tn-c, LIF* and *18s* (section 2.7.6) using an MJ DNA Opticon 2 Real-Time PCR machine, and the data obtained were analysed using Opticon Monitor Software and Microsoft Excel™ (section 2.7.7). Results are shown below. The technology behind Taqman®, the relative merits of different protocols for real-time PCR and how a decision was arrived at on which of these to use is discussed in sections 2.7.4 and 2.7.5. The results of the Real-Time PCR are discussed in section 4.5.

4.3.1: Luminal epithelium marker- *EP2*

In Chapter 3, two potential luminal epithelium markers were tested: *Osf-2* and *EP2*. Real-time PCR results showed more *Osf-2* in the stroma/glands samples than in the epithelium samples, so it was removed from consideration as a luminal epithelium marker. Thus, only *EP2* was tested on the laser microdissection samples. Results are shown in Figure 4.4.

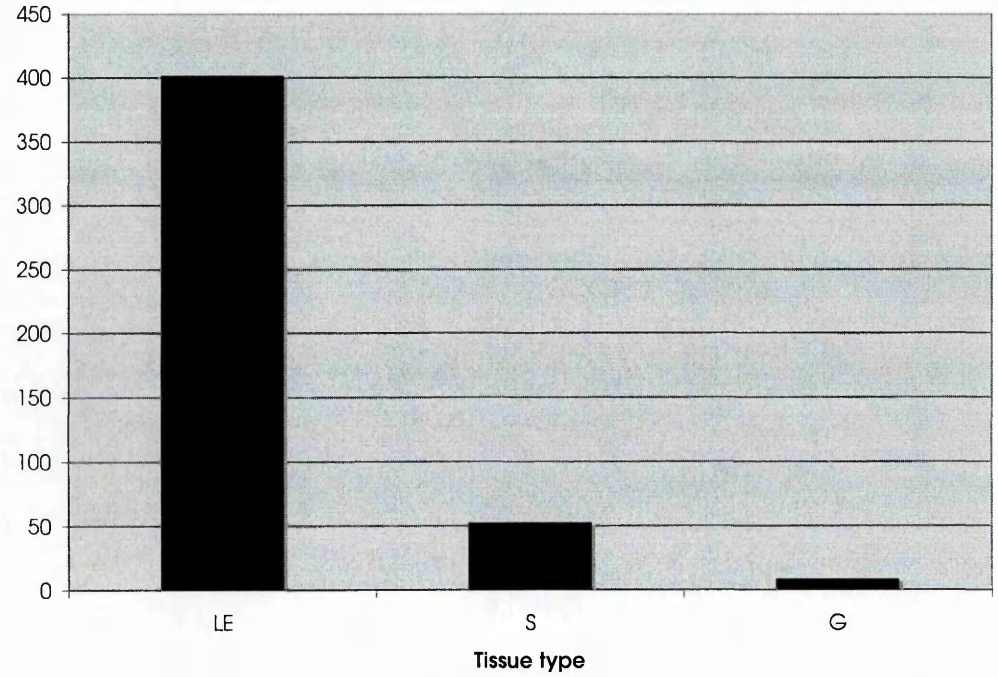

Figure 4.4: Results obtained by Real-time RT-PCR using Taqman®, showing the ratio of EP_2 expression to 18s expression in samples consisting of luminal epithelium (LE), sub-luminal stroma (S) and glands (G) laser microdissected from frozen sections of uterus on day 5 of pseudopregnancy.

In Chapter 3, it was shown that LE samples obtained by manual dissection (and therefore potentially containing glands and/or stroma) expressed EP_2 at a high level. Stroma and glands samples had comparatively very low levels of EP_2 (less than one tenth the value of the epithelium samples). In Figure 4.4, a high level of EP_2 was shown to be present in the luminal epithelium (LE) sample. Some EP_2 was present in the stroma sample (S: $1/8^{th}$ of the LE sample) and a negligible amount in the glandular epithelium (G) sample.

4.3.2: Stromal markers: *Tn-c* and *EP3*

In Chapter 3, two potential stromal markers were tested: *Tn-c* and *EP3*. Real-time PCR results showed both *Tn-c* and *EP3* were present at higher levels in the stroma/glands samples than in the LE samples, so both were tested on the laser microdissection samples. The aim was to ascertain whether the markers were exclusive to the stroma or were also expressed in the glands. Results are shown in Figures 4.5 and 4.6.

Tn-c

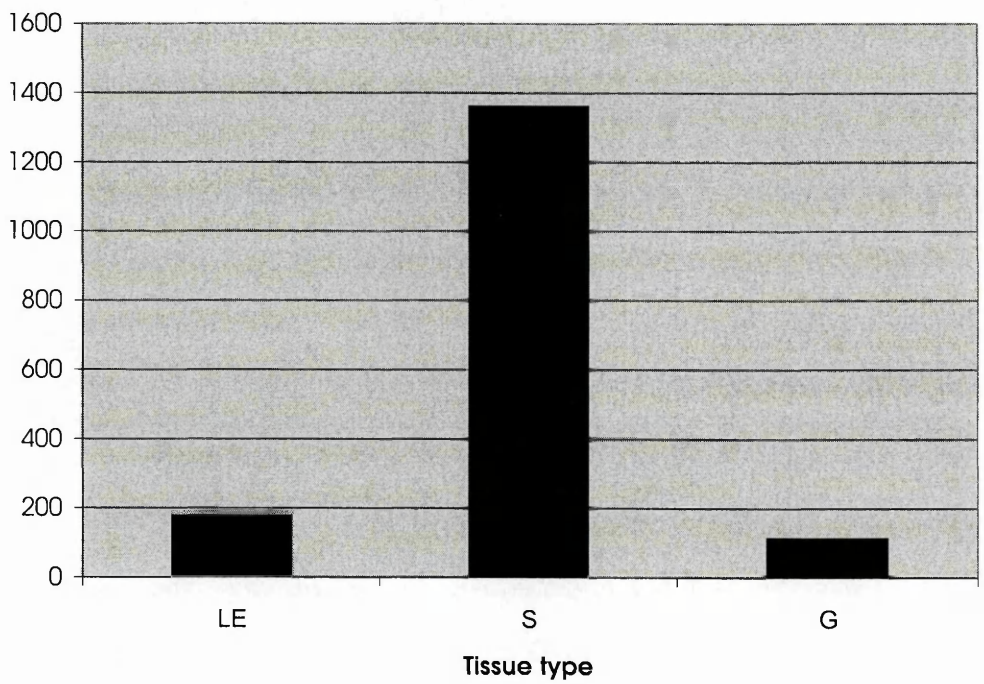

Figure 4.5: Results obtained by Real-time RT-PCR using Taqman®, showing the ratio of Tn-c expression to 18s expression in samples of luminal epithelium (LE), sub-luminal stroma (S) and glands (G) laser microdissected from frozen sections of uterus on day 5 of pseudopregnancy.

In Chapter 3, it was shown that stroma/glands samples expressed Tn-c at a high level. LE samples had comparatively very low levels of Tn-c. From these results it could not be determined whether the expression of EP_3 was in the stroma, the glands or both. In Figure 4.5, a high level of Tn-c was present in the stroma sample (S). Some Tn-c was present in the glands (G) and LE samples (around $1/8^{th}$ of the level in the stroma sample).

EP_3

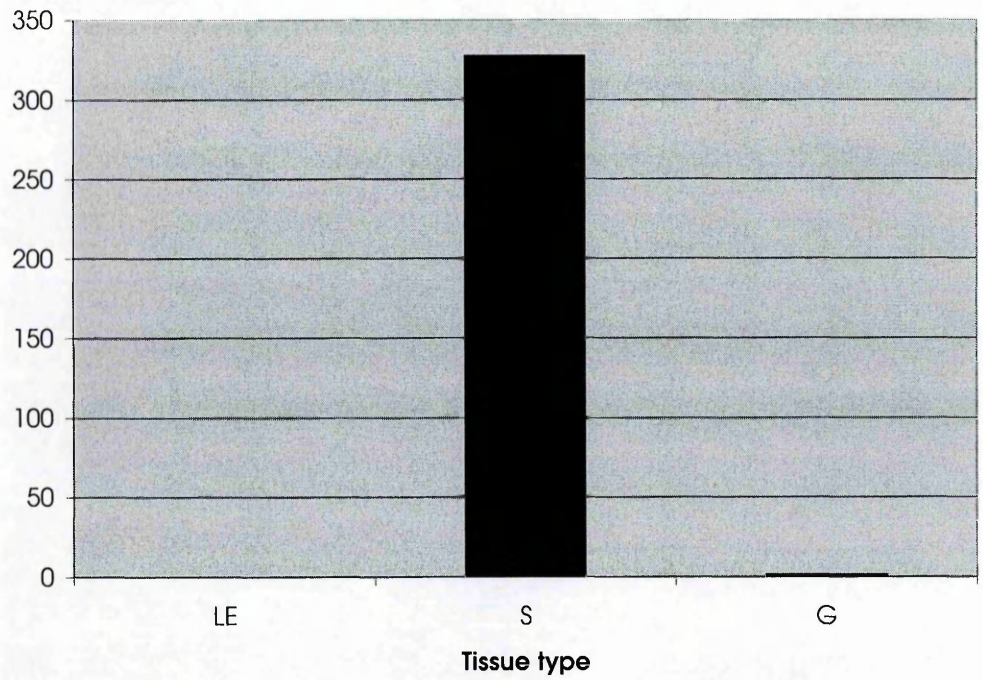

Figure 4.6: Results obtained by Real-time RT-PCR using Taqman®, showing the ratio of EP_3 expression to 18s expression in samples of luminal epithelium (LE), sub-luminal stroma (S) and glands (G) laser microdissected from frozen sections of uterus on day 5 of pseudopregnancy

In Chapter 3, it was shown that stroma/glands samples expressed EP_3 at a higher level than their corresponding paired LE samples, but from these results it could not be established whether the expression of EP_3 was in the stroma, the glands or both. In Figure 4.6, a high level of EP_3 was present in the stroma sample. No EP_3 was present in the LE and a negligible amount was present in the glandular epithelium sample.

4.3.3: Glandular epithelium marker- *LIF*

In Chapter 3, *LIF* was tested as a potential glandular epithelium marker. Real-time PCR results showed more *LIF* in stroma/glands samples than luminal epithelium samples. It could not be ascertained whether *LIF* was exclusively expressed in the glandular epithelium, as pure samples could not be obtained from mechanical dissection. Laser microdissection gave pure samples to be tested for specificity of *LIF* using Taqman®. The results are shown in Figure 4.7.

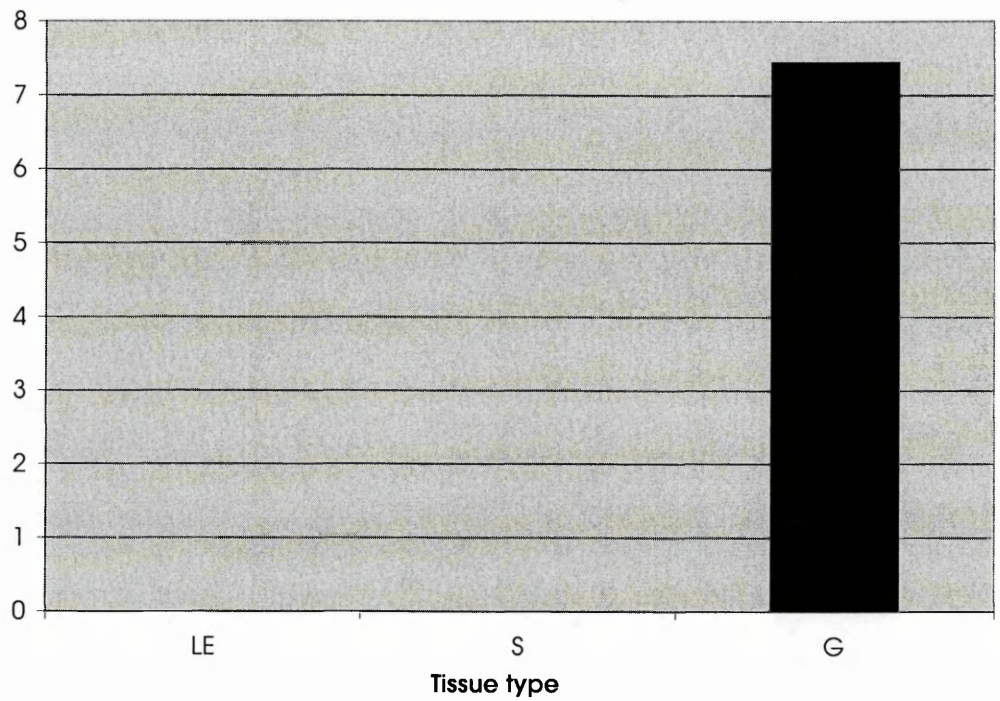

Figure 4.7: Results obtained by Real-time RT-PCR using Taqman®, showing the ratio of LIF expression to 18s expression in samples of luminal epithelium (LE), sub-luminal stroma (S) and glands (G) laser microdissected from frozen sections of uterus on day 5 of pseudopregnancy.

In Chapter 3, it was shown that stroma/glands samples expressed LIF at a slightly higher level than LE samples. LE levels of LIF were around half to three-quarters of

the level expressed in the corresponding paired stroma/glands samples. From these results it could not be determined whether the expression of LIF was specifically in the glands, or in more than one uterine tissue. In Figure 4.7, a comparatively high level of LIF was present in the glands sample. No LIF was present in the LE or stroma samples.

4.4: Searching for new uterine tissue markers using microarrays

4.4.1: Running the microarray

2µl of the 1st strand reaction volume was amplified for 15 cycles using the SMART™ PCR cDNA Synthesis kit. 21µl of the final volume of 100µl was then labelled by incorporation of cy3-dCTP and purified (section 2.5.1). 21µl of RNA from pooled luminal epithelium (PLE, a pool of manually dissected luminal epithelium taken from five mice at each of the following time points: day 3 21:00, day 4 9:00, day 4 21:00, day 5 9:00 and day 5 21:00) was labelled with cy5-dCTP and used as the reference. Incorporation of the dyes was checked using a NanoDrop spectrophotometer to measure absorbance at 550nm for cy3 and 649nm for cy5.

The concentration of cDNA in each pool was too low to hybridise to more than one array for each condition, so 63µl of the remaining amplified cDNA were amplified and labelled. This gave enough labelled cDNA to hybridise to three array experiments for each of the conditions: one from the first labelling attempt and two from the second, as summarised in Table 4.8. The cy3 and cy5 labelled products were combined, precipitated and hybridised (section 2.5.1) to RFCGR_HGMP_Mouse_Mm_SGC_Av2 array chips (section 2.1.2). Slides were scanned on a Genepix Axon scanner and imported into Bluefuse for analysis. A summary of the microarray analyses undertaken is shown in Table 4.8.

Sample	First attempt cDNA (ng/µl)	Chips hybridised	Second attempt cDNA (ng/µl)	Chips hybridised
Reference	138.8	3	726.67	6
LE	26.53	1	773.9	2
G	352.08	1	759.8	2
S	317.22	1	767.89	2

Table 4.8: A summary of the amount of labelled cDNA generated for hybridising to the microarray chips, and the number of chips that were hybridised using each pool of cDNA. *LE= luminal epithelium S= stroma, G= glandular epithelium.*

4.4.2: Analysing the microarray

The data generated by Bluefuse were analysed and filtered as detailed in section 2.5.2. Condition Tree analysis was performed. This showed that the tissue specific gene expression profiles from the three arrays obtained from the first set of labelling were very different from the profiles generated by the two arrays run from the second set of labelling. It was decided that analysis would concentrate on the six chips obtained from the second set of labelling experiments, as the duplicated runs allowed data obtained to be verified.

Lists of genes apparently upregulated ('Up' gene lists) from both of the arrays performed on each tissue were combined in Microsoft Excel™ and a pivot table created to show how many of the four possible addresses for each gene were classed as up-regulated. The 'Down' gene lists (genes apparently down-regulated) were also amalgamated in this way, giving six pivot tables in all. Data for all of the six chips were then merged and a further pivot table generated. This allowed the genes that were specifically up or down-regulated in one tissue but not in other tissues to be selected. Since each gene is represented by two addresses and each tissue by two chips, there were a total of four sets of data for

each gene in each tissue. Genes that were present in 4 or 3 out of the 4 addresses of one or two tissues but in one or none of the addresses of the other tissues were considered specifically up/down-regulated.

Information on each gene was sought from a variety of sources, including Pubmed (www.pubmed.net), the Jackson Laboratory website (www.jax.org), and Embl Bioinformatics Harvester (http://harvester.embl.de/). If the gene itself, its gene family or a process it is involved in had previously been investigated in the uterus it was designated 'previously investigated'. The literature referring to the genes in these lists will be discussed further in section 4.2.2. Genes identified in this way are listed in Tables 4.9 to 4.19 and their functions classified in Table 4.20.

Gene name	Accession number	Description	Previously reported?
DNMT1 associated protein-1 (*Dmap1*)	AF265229	Transcription factors & DNA/chromatin modifiers	No
Claudin 4 (*Cldn4*)	NM_009903	Associated with cell adhesion & junctions	Yes
Cleavage and polyadenylation specificity factor 1 (*Cpsf1*)	NM_008484	RNA processing	No
Formin binding protein 4 (*Fnbp4*)	NM_018785	Cytoskeletal	No
Laminin, beta 3 (*Lamb3*)	NM_008484	Associated with cell adhesion & junctions	Yes
Per-hexamer repeat gene 5 (*Phxr5*)	NM_008836	Other	No
Transcription factor 2 (*Tcf2*)	NM_009330	Transcription factors and DNA/chromatin modifiers	Yes

Table 4.9: Genes up-regulated in the LE samples, *showing gene name (and acronym if used), GenBank Accession number, a brief description of its function and whether it has been previously reported in literature or gene databases as being involved in implantation.*

Gene name	Accession number	Description	Previously reported?
BALB/c elongation factor 2	U89415	Translation related	No
1-acyl-sn-glycerol-3-phosphate acyltransferase (*Agapt1*)	NM_018862	Other metabolism/catabolism	Yes
TNF receptor-associated factor 1 (*Traf1*)	NM_009421	Apoptosis	Yes
Regulated secretory protein-23	U64446	Endomembrane pathway	No
Solute carrier family 1, member 7 (*Slc1a7*)	NM_009201	Ion transport and binding	Yes
Transcytosis associated protein p115	AF096868	Endomembrane pathway	No

Table 4.10: Genes up-regulated in the glandular samples, *showing gene name (and acronym if used), GenBank Accession number, a brief description of its function and whether it has been previously reported in literature or gene databases as being involved in implantation.*

Gene name	Accession number	Description	Previously reported?
Microtubule-actin crosslinking factor (*Macf*)	AF150755	Cytoskeletal	No

Table 4.11: Genes up-regulated in the stromal samples, *showing gene name (and acronym if used), GenBank Accession number, a brief description of its function and whether it has been previously reported in literature or gene databases as being involved in implantation.*

Gene name	Accession number	Description	Previously reported?
Poly(A) binding protein, nuclear 1 (*Pabpn1*)	NM_019402	RNA processing	No
Bright and dead ringer gene product homologous protein *Bdp* (LOC56380)	NM_019689	Transcription factors and DNA/chromatin modifiers	No
GTP binding protein 2 (*Gtpbp2*)	NM_019581	Translation related	No
Hypermethylated in cancer 1 (*Hic1*)	NM_010430	Cell cycle and oncogene	No

Table 4.12: Genes up-regulated in the LE and glandular samples, *showing gene name (and acronym if used), GenBank Accession number, a brief description of its function and whether it has been previously reported in literature or gene databases as being involved in implantation.*

Gene name	Accession number	Description	Previously reported?
Beta-galactoside alpha2,6-sialyltransferase (*St6gal1*)	AF153680	Endomembrane pathway	Yes
Alpha-2 type IV collagen	J04695	Extracellular matrix	Yes

Table 4.13: Genes up-regulated in the glandular and stromal samples, *showing gene name (and acronym if used), GenBank Accession number, a brief description of its function and whether it has been previously reported in literature or gene databases as being involved in implantation.*

Gene name	Accession number	Description	Previously reported?
Ribosomal protein L10A (*Rpl10a*)	NM_011287	RNA processing	Yes

Table 4.14: Genes up-regulated in the LE and stromal samples, *showing gene name (and acronym if used), GenBank Accession number, a brief description of its function and whether it has been previously reported in literature or gene databases as being involved in implantation.*

Tables of genes specifically down-regulated in one or two of the three tissues of interest

Gene name	Accession number	Description	Previously reported?
Proteasome (prosome, macropain) subunit, alpha type 6 (*Psma6*)	NM_008946	Protein metabolism/catabolism	No
Zinc finger protein 162 (*Zfp162*)	NM_011750	RNA processing	No
Mouse 1400 base pair ubiquitin	M81747	Protein metabolism/catabolism	Yes

Table 4.15: Genes down-regulated in the LE samples, *showing gene name (and acronym if used), GenBank Accession number, a brief description of its function and whether it has been previously reported in literature or gene databases as being involved in implantation.*

Gene name	Accession number	Description	Previously reported?
Ubiquitin C (*Ubc*)	NM_019639	Protein metabolism/catabolism	Yes

Table 4.16: Genes down-regulated in the glandular samples, *showing gene name (and acronym if used), GenBank Accession number, a brief description of its function and whether it has been previously reported in literature or gene databases as being involved in implantation.*

Gene name	Accession number	Description	Previously reported?
Hypothetical protein, clone:2-31 (LOC57423)	NM_020582	Ion transport and binding	No
Claudin 4 (*Cldn4*)	NM_009903	Associated with cell adhesion & junctions	Yes
Complement component 1 inhibitor (*C1nh*)	NM_009776	Immune function	Yes
Cytochrome c oxidase, subunit IV (*Cox4*)	NM_009941	Mitochondrial and oxidation/reduction	Yes
Tumor protein D52 (*Tpd52*)	NM_009412	Cell cycle and oncogene	No

Table 4.17: Genes down-regulated in the stromal samples, *showing gene name (and acronym if used), GenBank Accession number, a brief description of its function and whether it has been previously reported in literature or gene databases as being involved in implantation.*

Gene name	Accession number	Description	Previously reported?
Cd63 antigen (*Cd63*)	NM_007653	Endomembrane pathway	Yes
Transketolase (*Tkf*)	NM_009388	Other metabolism/catabolism	No

Table 4.18: Genes down-regulated in the glandular and stromal samples, *showing gene name (and acronym if used), GenBank Accession number, a brief description of its function and whether it has been previously reported in literature or gene databases as being involved in implantation.*

Gene name	Accession number	Description	Previously reported?
Calpain 4 (*Capn4*)	NM_009795	Protein metabolism/catabolism	Yes

Table 4.19: Genes down-regulated in the LE and stromal samples, *showing gene name (and acronym if used), GenBank Accession number, a brief description of its function and whether it has been previously reported in literature or gene databases as being involved in implantation.*

The results of this system of filtering did not contain *EP2, EP3, Tn-c* and *LIF*: the markers that had earlier been verified for each tissue. Ribosomal proteins were also present in the lists, even though their expression levels are known to be constant in changing conditions. These results raised the prospect of the chip data being unreliable and the genes being identified by chance. The data were therefore investigated further to test this possibility.

Firstly, the paired chip data files were searched for the tissue markers *EP2, EP3, Tn-c* and *LIF*. Since each gene is represented by two addresses and each tissue is represented by two chips, there were a total of four sets of data for each gene in each tissue. Although all of the data from the marker gene addresses would be filtered out because they were designated confidence levels of less than 0.5, most of the data would have been filtered out before that because the fluorescence levels in the cy3 or cy5 channels were below the 150 used as a cut off point for valid data (data not shown). Despite all values being under 150, the fluorescence levels found for *EP2* in the cy5 channel (the labelled reference) were at least twice as high as the other fluorescence values. This is probably because the reference is pooled luminal epithelium and would be expressing *EP2* strongly. But the levels of cy3 for *EP2* in the luminal epithelium chips (where it is expected to be high) is much lower than the reference, This implies that the laser microdissected tissue is not expressing *EP2* sufficiently. The implications of this are discussed in section 4.5. Because of these results the markers cannot be used to validate the microarray data.

Each chip contains 14 genes that are repeated 48 times. These genes are housekeeping genes that should theoretically be consistently expressed in all tissues and conditions. The percentage of the 288 addresses over 6 chips for each control gene that have confidence levels above 0.5, and the average and standard deviation of the log cy3/cy5 ratios for these addresses were collated (data not

shown). The results are varied; some genes have a relatively high percentage of addresses above 0.5, an average log cy3/cy5 close to 0 and a small range of values (as would be expected for a control gene), such as *L3* and *Rps4.x*. Other genes have very few addresses registering a confidence level above 0.5. Since the control genes are supposed to be consistently expressed across all tissues and conditions this may mean that the data are not reliable.

4.5: Discussion of Chapter 4

4.5.1: Discussion of real-time PCR data

Although relative, rather than absolute differences in the expression level of markers are seen with the quantitative real-time RT-PCR on the laser microdissection samples, they are more likely to reflect genuine differences in expression level than contamination, but elimination of contamination cannot formally be shown from this work.

Since *Osf-2* was eliminated early in the work, as reported in Chapter 3, as a potential marker for the luminal epithelium, the only epithelial marker tested on laser microdissected samples was *EP2*. In Chapter 3, it was shown that LE samples obtained by manual dissection (and therefore potentially containing glands and/or stroma) expressed *EP2* at a high level. Stroma/glands samples had comparatively very low levels of *EP2* (less than one tenth the value of the epithelium samples). Figure 4.4 shows that a high level of *EP2* was present in the luminal epithelium sample. Some *EP2* was present in the stroma sample ($1/8^{th}$ of the LE sample) and a negligible amount in the glandular epithelium sample. Since the laser microdissection samples are pure samples of tissues, the low levels of *EP2* in the manually dissected samples of stroma/glands is likely to be from the stromal tissue in these samples. It is therefore a good marker to check that luminal epithelium tissue has been obtained from a manual dissection, but not to test stroma/glands samples for the presence of luminal epithelium tissue.

Two markers were tested in Chapter 3 as potential stromal markers. Stroma/glands samples were enriched for both *EP3* and *Tn-c* compared to luminal epithelium samples. From these results it could not be determined whether the expression of these markers was in the stroma, the glands or both. Since previously published results found *EP3* to be present in the myometrium of pseudopregnant mice and not in the stroma or glands at all (Katsuyama et al., 1996), there was also

the possibility of myometrial contamination. Figure 4.5 shows that a high level of *Tn-c* was present in the stroma sample. Some *Tn-c* was present in the glands and LE samples (around 1/8th of the level in the stroma sample. Figure 4.6 shows that a high level of *EP3* was present in the stroma sample. No *EP3* was present in the LE and a negligible amount was present in the glandular epithelium sample. This result confirms that *EP3* is expressed in the stroma, and not the glands or luminal epithelium. Since myometrial samples were not taken for Taqman® analysis, myometrial contamination in the manually dissected samples cannot be ruled out, but the laser microdissected samples are pure and express high levels of *EP3*. This result confirms that the stroma is an independent source of *EP3*, contradicting previously published results (Ichikawa, 2003). This may be because the previous study used *in situ* hybridisation, which is less sensitive than real-time PCR. Since both *EP3* and *Tn-c* are expressed predominantly in the stroma, they are both potential markers for contamination of luminal epithelium by stroma in mechanical dissections. However, *Tn-c* appears to have a low expression level in LE and GE, making *EP3* the better marker if the sample is required to be ultra-pure.

In Chapter 3, it was shown that stroma/glands samples expressed *LIF* at a slightly higher level than LE samples. LE levels of *LIF* were around half to three-quarters of the level expressed in the corresponding paired stroma/glands samples. From these results it could not be elucidated whether the expression of *LIF* was specifically in the glands, or in more than one uterine tissue. Figure 4.7 shows a comparatively high level of *LIF* was present in the glands sample. No *LIF* was present in the LE or stroma samples. This result confirms that *LIF* is expressed exclusively in the glandular epithelium, making it a good marker for relative composition of uterine tissue dissections. Chapter 3 results on late day 4 and late day 5 samples imply that there is glandular contamination in the majority of manually dissected luminal epithelium samples. However, since the epithelium becomes 'stickier' as pseudopregnancy advances, cleaner sample preparations

may be obtained by taking samples at slightly earlier times. These problems are discussed further in Chapter 6.

It would not be possible to identify an unknown tissue sample exclusively from testing the levels of these four markers on it because of the problem of relativ expression levels. The raw fluorescence levels (see section 2.7.7) for *EP2* and *Tn-c* were relatively high, as shown by the units on the y axis of Figures 4.4 and 4.5. The raw fluorescence levels for *EP3* were slightly lower, and those for *LIF* were very low. Although the *LIF* level for glands is high when compared with the levels for stroma or LE, the raw fluorescence level is much lower than the other markers, so a glands sample would have a lower C_t for *EP2*, *EP3* and *Tn-c* than for *LIF*. Raw fluorescence level is not necessarily an indicator of the expression levels of the gene of interest, although if the efficiency of the assay is close to 100% and the standard curve used is the same for each run, then it may be. But Taqman® runs vary from one run to the next, and it is not possible to compare two samples that were not run on the same plate, with the same reagents.

4.5.2: Discussion of microarray data

When looking to analyse the data generated by the microarray, the reference used must be taken into consideration. The reference used was taken from a pool of manually dissected luminal epithelium taken from five mice at each of the following time points: day 3 21:00, day 4 9:00, day 4 21:00, day 5 9:00 and day 5 21:00. A reference taken from a pool of whole uterus would have been preferable, as comparisons between the levels of expression in each tissue compared to the uterus as a whole would have been possible. But the results can still be interpreted when using luminal epithelium as a reference. The analysis is simple when looking at genes exclusively up or down regulated in glands, stroma or glands and stroma. Since the luminal epithelium is the reference used to judge whether they are up or

down regulated, a gene found to be exclusively up regulated in the glandular epithelium compared to the reference luminal epithelium can also be thought of as being down regulated in the reference luminal epithelium compared to the glands. When considering the gene lists where genes appear to be up or down regulated in the laser capture luminal epithelium compared to the reference luminal epithelium or luminal epithelium and stroma or glands, the analysis is slightly less clear-cut. The pooled luminal epithelium is taken from time points that are, on average, earlier in the luteal phase of pseudopregnancy (samples average is day 5, reference average is day 4 21:00), so the comparison is between the laser microdissected luminal epithelium taken around and just after the window of implantation, and the reference luminal epithelium with an average time of just before the window of implantation. So a gene that appears to be up-regulated in test laser microdissected LE is up-regulated in comparison to an earlier time point, or a gene that appears to be down-regulated in test laser microdissected LE is down-regulated in comparison to an earlier time point.

Filtering the microarray data as described in section 4.4.2 generated lists of genes up or down regulated in one or two uterine tissues. Information on each gene was sought from a variety of sources, including Pubmed (www.pubmed.net), the Jackson Laboratory website (www.jax.org), and Embl Bioinformatics Harvester (http://harvester.embl.de/). If the gene itself, its gene family or a process it is involved in had previously been investigated in the uterus it was designated 'previously investigated'. It was found that 14 out of 31 genes had previously been investigated in the uterus. Their expression patterns were then analysed in the context of the reference. The gene functions are summarised in Table 4.20 and further discussed below.

Class of gene function	Number of genes	Previously Investigated
Associated with cell adhesion & junctions	2	2
Cytoskeletal	2	0
Extracellular matrix	1	1
Ion transport and binding	2	1
Transcription factors and DNA/chromatin modifiers	3	1
Apoptosis	1	1
Cell cycle and oncogene	2	0
Protein metabolism/catabolism	3	2
Other metabolism/catabolism	2	1
Mitochondrial and oxidation/reduction related	1	1
RNA processing	4	1
Translation related	2	0
Immune function	1	1
Endomembrane pathway	4	2
Other	1	0
Total	**31**	**14**

Table 4.20: Classification of genes identified by microarray into categories describing their function, *showing the number of genes that are classified by each category, and, of these, the number that have been previously implicated in implantation.*

It is interesting to note that none of the genes were described by these three categories: Growth factors & hormones, Receptors and associated molecules and Second messengers and intra-cellular signalling. These categories contain genes such as the steroid hormone receptors for oestrogen and progesterone, the cytokine LIF and the growth factor HB-EGF that have previously been a focus of implantation research, yet are not present in these microarray results. These genes have very specific roles in implantation and when they are knocked out or mutated they often result in an infertile phenotype (see discussions on previous literature in Chapter 1). The genes identified by this microarray are mainly coding for proteins such as enzymes and transcription factors, which may have functional

redundancy: their lost activity is compensated for by the activity of a different gene or genetic pathway. If so, null mutations in these redundant genes are unlikely to give an infertile phenotype, as other genes will compensate for their activity, so it would have been unlikely that they were identified in functional studies.

Genes found in more than one of the microarray lists

Of these genes, only *claudin 4* has been previously associated with implantation. *Claudin 4 (Cldn4)* was present in both the 'up-regulated in LE' and the 'down-regulated in stroma' lists. Because of the reference used it is both up-regulated in day 5 pseudopregnant luminal epithelium with respect to luminal epithelium from an earlier time point, as well as being down-regulated in stroma with respect to luminal epithelium from an earlier time point. Claudin 4 is a protein found in the tight junctions mediating intercellular adhesion. Tight junctions have been found to be induced as a transitory permeability barrier created by decidual cells immediately surrounding the implanting embryo (Wang et al., 2003). *Cldn1* transcripts are found at low levels in the luminal epithelium on day 4 of pregnancy. After implantation on day 5, *Cldn1* is found in the luminal epithelium and stromal cells surrounding the blastocyst (Wang et al., 2003). *Cldn4* has been identified by microarray in two studies as up-regulated in receptive compared to prereceptive human endometrium (Riesewijk et al., 2003); (Carson et al., 2002). Its transcript has been verified as being expressed in luminal epithelium by immunohistochemistry (Carson et al., 2002).

Genes up-regulated in the LE samples (Table 4.9)

Among those previously identified in or associated with implantation are laminin beta 3 and transcription factor 2, and several that have not been involved in this

process: Dam nuclear methyltransferase, Cleavage and polyadenylation specificity factor 1, Formin binding protein 4 and Per-hexamer repeat gene 5.

Laminin, beta 3 (Lamb3) is part of the extracellular matrix in the uterus. It is a well-characterised adhesion molecule in implantation, binding to a variety of molecules including integrins *(Aplin, 1997)*. Previous microarray studies show that *Lamb3* is up-regulated in human receptive endometrium compared to late proliferative phase (Kao et al., 2002). *Lamb3* has also been identified in two previous microarray studies as being down-regulated by chronic progesterone treatment in the uterus (Jeong et al., 2005) and up-regulated after treatment with a progesterone inhibitor (Cheon et al., 2002), By comparing the microarray data to the reference, it can be concluded that *Lamb3* is up-regulated in the luminal epithelium compared to luminal epithelium from an earlier time point, which correlates with previous data.

Transcription factor 2 (Tcf2) is a transcription factor previously found to be regulated in the luminal epithelium of pseudopregnant mice, showing a gradual increase in expression from late day 3 to late day 5 (Campbell et al.)

Genes not previously identified in implantation but shown here to be upregulated are as follows: DNMT-associated protein: Dam nuclear methyltransferase is a histone methyltransferase. Although DNMT has not been specifically characterised in the uterus, another histone/protein methyltransferase is required for optimal estrogen response in female reproductive tissues (Carling et al., 2004). Cleavage and polyadenylation specificity factor 1 (Cpsf1) is involved in post-transcriptional processing of RNA (Murthy and Manley, 1995). Formin binding protein 4 (Fnbp4) is a protein that binds Formin, a regulator of actin assembly (Kovar, 2006). Per-hexamer repeat gene 5 (Phxr5) is a member of the Per hexamer repeat genes which are murine homologues of hexamer repeats associated with the *Drosophila* period gene, a component of the circadian clock (Shin et al., 1985).

Genes up-regulated in the glandular samples (Table 4.10)

Up-regulated genes previously identified in or associated with implantation include Agpat 1, TNF receptor-associated factor 1, and Solute carrier family 1, member 7. Those not previously implicated in implantation include BALB/c elongation factor 2, Regulated secretory protein-23, and Transcytosis associated protein p115.

Agpat1 (1-acyl-sn-glycerol-3-phosphate transferase) converts LPA (lysophosphatidic acid or 1-acyl-sn-glycerol-3-phosphate) into phosphatidic acid. It is an important enzyme in the generation of glycerolipids. Although Agpat1 itself has not been fully investigated in the uterus, LPA is known to be involved in downstream activation of implantation genes such as *Cox-2* and *HB-EGF* (Shah and Catt, 2005).

TNF receptor-associated factor 1 (Traf1): The TNF-alpha signalling pathway has been previously documented in implantation. It is thought to be involved in apoptosis of epithelial cells (Joswig et al., 2003). TRAFs are a family of proteins that associate with TNF-alpha receptors. TRAF1 has been shown to be a negative regulator of TNF-alpha signaling (Tsitskov et al., 2001). Although *Traf1* transcript has not been shown to be present in the uterus, *Traf5* is known to be regulated in the luminal epithelium over the peri-implantation period, with a gradual increase over the window of receptivity (Campbell et al.).

Solute carrier family 1, member 7 (Slc1a7) is a glutamate transporter with around 40% homology to other members of the solute carrier family 1 protein family. It has not previously been characterised in the uterus but has been characterised in the retina (Arriza et al., 1997). However, *Slc1a1* has been identified by microarray as being up-regulated during secretory phase of the human menstrual cycle (Riesewijk et al., 2003), and *Slc1a5* is down-regulated in response to progesterone treatment in the uterus (Jeong et al., 2005).

Other genes identified in this group have not been previously implicated in the process of implantation. BALB/c elongation factor 2 is a translation elongation

factor in protein synthesis (Chu and Paul, 1998). Regulated secretory protein-23 is also known as storage granule protein-23. It is involved in the endomembrane secretory pathway (Lang et al., 1996). Transcytosis associated protein p115 is a general fusion factor required for binding of vesicles to acceptor membranes . It is not surprising that both regulated secretory protein-23 and transcytosis associated protein p115 are up-regulated in secretory glandular epithelium as both are involved in the endomembrane secretory pathway, which is highly active in glandular epithelium.

Genes up-regulated in the stromal samples (Table 4.11)

Microtubule-actin crosslinking factor (Macf) is an actin/calcium binding protein, and has not previously been identified in implantation (Leung et al., 1999).

Genes up-regulated in the LE and glandular samples (Table 4.12)

Several genes are in this group that have not previously been identified in implantation. Poly(A) binding protein, nuclear 1 (Pabpn1) is involved in poly-A tail synthesis of mRNAs (Marie-Josee Sasseville et al., 2006). Bright and dead ringer gene product homologous protein Bdp (LOC56380) binds to AT rich sequences called ARIDs (Kortschak et al., 2000). GTP binding protein 2 (Gtpbp2) is a putative GTPase structurally related to peptidyl elongation factors (Kudo et al., 2000). Hypermethylated in cancer 1 (Hic1) is a tumour suppressor gene (Chen et al., 2003).

Genes up-regulated in the glandular and stromal samples (Table 4.13)

Two of these genes have previously been identified in or associated with implantation: Beta-galactoside alpha2,6-sialyltransferase and Alpha-2 type IV collagen.

Beta-galactoside alpha2,6-sialyltransferase (St6gall):Sialyltransferases add sialic acid residues to proteins. Glycoproteins play an important role in receptivity and implantation. A layer of glycoproteins known as the glycocalyx is present on the apical surface of the pre-receptive luminal epithelium to prevent premature attachment of the embryo to the luminal epithelium. As the implantation window begins the glycocalyx becomes thinner (Carson et al., 1998). Alpha 2-6 linked sialic acid residues are reduced in the luminal epithelium around the time of implantation, although stromal residues remain constantly high (Kimber et al., 2001). *St6gall* has also been shown to be expressed in the luminal epithelium over the implantation period, with an expression pattern that decreases from late day 3 to late day 5 (Campbell et al.). Since the reference used is luminal epithelium, *St6gall* can be said to be down-regulated in luminal epithelium with respect to glands and stroma, meaning fewer glycosylated proteins and a thinner glycocalyx. This correlates with previous research (Carson et al., 1998).

Alpha-2 type IV collagen encodes one of the six subunits of type IV collagen, a major structural component of epithelial basement membranes. Extracellular matrix proteins such as type IV collagen, laminin and fibronectin, are ligands for integrins. Integrins are expressed in both the basement membrane of epithelium and the trophoblast of the embryo and are important adhesion molecules of implantation (Kimber and Spanswick, 2000).

Genes up-regulated in the LE and stromal samples (Table 4.14)

Ribosomal protein L10a has been previously identified in or associated with implantation . It is identified by SAGE (Serial Analysis of Gene Expression) as being highly up-regulated at the implantation site in whole mouse uterus (Ma et al., 2006). Ribsomal proteins have previously been thought to be 'housekeeping' genes, ubiquitously expressed in all tissues (Eisenberg and Levanon, 2003).

Genes down-regulated in the LE samples (Table 4.15)

Mouse 1400 base pair ubiquitin has previously been identified in or associated with implantation. It appears to be the 5' end of Ubiquitin C, and is used uniquely in this microarray. The role of Ubiquitin in implantation is detailed below. Zinc finger protein 162 (Zfp162), also known as Zfm1 and Sf1 (splicing factor 1), has not previously been identified in implantation. It has been shown to be down-regulated in smooth muscle cells treated with Interleukin-1 beta and TNF alpha (Cattaruzza et al., 2002). Another gene not previously implicated in implantation is Proteasome (prosome, macropain) subunit, alpha type 6 (Psma6). This gene is a subumit of the ubiquitin-26s proteasome system, the essential cellular complex that digests proteins into short polypeptides and amino acids (Coux et al., 1996).

Genes down-regulated in the glandular samples (Table 4.16)

Expression of genes involved in the ubiquitin proteasome pathway have been reported in early pregnancy in several animals, but the system has not been fully elucidated. Down-regulation of ubiquitin C appears to inhibit embryo implantation by down-regulating matrix metalloproteinases involved in remodelling of the uterus during early pregnancy (Wang et al., 2004).

Genes down-regulated in the stromal samples (Table 4.17)

Two identified genes have previously been identified in or associated with implantation: Complement component 1 inhibitor and Cytochrome c oxidase, subunit IV. Complement component 1 inhibitor (C1nh): is a C1 inhibitor that regulates the first component of complement (C1) by inhibition of the proteolytic activity of its subcomponents C1r and C1s. This inhibits downstream activation of other complement components. C1 inhibitor also inhibits several other serine proteinases including kallikrein. *C1nh* has been found to be down-regulated by a progesterone inhibitor in a microarray study (Cheon et al., 2002) and kallikrein has

been found to be down-regulated by chronic progesterone treatment (Jeong et al., 2005). Cytochrome c oxidase, subunit IV (Cox4): Cytochrome c oxidase is part of the mitochrondrial electron transport chain of respiration. Another subunit of cytochrome c oxidase, subunit VIII has been found to be present in the luminal epithelium of early pseudopregnant mice, peaking at early day 4 (Campbell et al.).

Other genes identified here have not previously been identified in implantation. Hypothetical protein, clone:2-31 (LOC57423) is a synonym for ATP synthase, H+ transporting, mitochondrial F0 complex, subunit f, isoform 2 (Leyva et al., 2003). Tumor protein D52 (Tpd52) gene was initially identified as being overexpressed in human breast, lung, and prostate carcinomas. The function of its proteins is unclear (Byrne et al., 1998).

Genes down-regulated in the glandular and stromal samples (Table 4.18)

Cd63 antigen has been previously identified in or associated with implantation. It is a lysosomal membrane protein, and has been identified by a PCR differential-display method as being down-regulated by progesterone (but not oestrogen) in human endometrial stromal cells (Okada et al., 1999). *Cd63* has also been identified by SAGE as up-regulated at implantation sites (compared to inter-implantation sites) in mouse uterus, and subsequently localised to the subluminal stroma cells (Ma et al., 2006). These two results are apparently contradictory, but the later study uses pregnant uteri, whereas the earlier study is equivalent to human secretory phase (receptive) endometrium. The presence of an embryo changes gene expression in the uterus (as summarised in section 1.2.1). *Cd63* has also been found to have a gradual increase in luminal epithelium from day 3 to day 5 of pregnancy (Campbell et al.).

Transketolase (Tkt) has not previously been identified in implantation. It is an enzyme involved in both the Pentose Phosphate Pathway and the Calvin Cycle of photosynthesis (Alberts, 2002),

Genes down-regulated in the LE and stromal samples (Table 4.20)*Calpain 4* has not previously been found in the uterus, though two other calpains have: Calpain 6 (Jeong et al., 2005) and Calpain 7 (Yoon et al., 2004).

When interpreting microarray data the way the data are filtered can make a significant difference to the results generated. The filtering method used in this array has previously been employed (Campbell et al.). To make sure that real results are not being overlooked because of the filtering method used, four alternative ways of filtering the data were tested. One of the alternative filtering methods differed by the chip data entered into the analysis, two of the alternative filtering methods differed by the filtering of raw data and one differed by the subsequent analysis of filtered raw data using pivot tables.

Method 1 is to ***add the initial 3 chips to the analysis.*** As shown in Table 4.8, an initial chip was run with the cDNA obtained from each tissue type then subsequently another two chips were run for each tissue type. The data filtering in the analysis used for this array was performed using only the second pair of replicate chips for each tissue, because the data extracted from the first set of chips were shown to be very different from the paired replicates using a function of Genespring called Condition Trees.

Method 2 is to ***use results that have a 'C' flag or above rather than a '0.5' confidence level or above.*** Bluefuse ranks each address with a confidence level (expressed as a decimal) as well as a confidence grade (from A to E) based on the reliability of the raw fluorescence data at that address. Addresses with a confidence level of 0.5 or under were rejected in this study, although the

confidence grade 'C' ranges from 0.3 to 0.7. So filtering was repeated with rejection of any address with confidence level below C grade.

Method 3 is to ***remove the initial filtering steps.*** The initial filtering steps involve removing all data from the analysis that have raw fluorescence values lower than 250 arbitrary units and a confidence level lower than 0.5, then classing genes with log-2 ratios of cy3/cy5 greater than 1 or less than -1 as up or down regulated. The aim of filtering the data in this way was to remove false positives from the analysis, but it was also likely to be removing true positives from the analysis if their expression level was not strong enough to show a fluorescence level above 250 arbitrary units. In order to let these genes through, the confidence and fluorescence level filtering could have been removed.

Method 4 is to ***change the pivot table parameters.*** In order to categorise genes that are specific to each tissue, a pivot table method was applied to the resulting lists of up or down regulated genes for each chip. Each gene had a total of 4 addresses over two chips representing each tissue type. If a gene appeared in 3 or 4 of the addresses for one tissue and only 0 or 1 of the addresses for the other tissues, it was considered up/down regulated for that condition. The stringency of the filtering was relaxed so that genes found in 4, 3 or 2 of the addresses for that tissue and 0 or 1 of the addresses for other tissues were considered up/down regulated.

Although the methods detailed above allow genes through that may be significant but were scored as false by Bluefuse (so called 'false negatives'), they also allow more genuine negatives to be let through by the filter. Because of this, the subsequent pivot table filtering is compromised. The original method of filtering used in this array appeared to be the most reliable after some testing of the other options.

A problem encountered during this array analysis was that the tissue specific markers under investigation in the previous chapters did not appear in the

gene lists, and were in fact filtered out by both flag and raw fluorescence level in the initial data filtering steps. As discussed in section 4.4.2, most of the markers fail to survive the filtering because of both low raw fluorescence values and low confidence levels. The raw fluorescence value does have some impact on the confidence level. Low fluorescence levels in both the reference and the sample channels implies that the transcript is present at very low levels in the populations of cDNA hybridised to the chip. A reason for this could be that their expression levels in the uterus are very low. Quantitative real-time RT-PCR, as used earlier in this chapter and in Chapter 3, is a very sensitive technique that can pick up expression at very low levels. The microarray technology may not be sensitive enough to do this.

4.5.3: General conclusions and potential future directions

Although the lists generated did not return large numbers of potential genes up-regulated specifically in one uterine tissue, it gave a high proportion of genes that appeared to have already been investigated, and several candidates that have not. Although many of these genes have been previously investigated in implantation, their exact site of expression has not, so they cannot be used to validate the microarray data without further studies into their sites of expression. Unfortunately the luminal epithelium, the tissue that had already been investigated in the most depth, generated the largest number of potential markers. There were also six potential glandular markers, all worth investigating further using quantitative real-time RT-PCR on samples of luminal epithelium, glands and stroma produced by laser microdissection. The stroma yielded the fewest potential markers. This might have been because the stroma needs the presence of an implantation embryo to change its transcriptome, whereas the luminal epithelium changes its transcriptome rapidly through the oestrous cycle under hormonal stimulation.

The genes that would be worth investigating further consist of both genes that have already been identified in implantation, and potentially interesting genes that have not. *Lamb3* and *Claudin 4* appear to be LE-specific markers, but this cannot be definitely verified due to the nature of the reference used in the array. It would be interesting to see if *Lamb3* is specific to the luminal epithelium as well as being up-regulated in the luminal epithelium over the peri-implantation period. Glandular tissue gave a rich range of potential markers to investigate. *Traf, Agpat* and *Sc1a7* have already been linked with implantation so their site of expression would be worth investigating further. *Regulated secretory protein 23* and *Transcytosis associated factor p115,* although not previously linked to implantation, appear to be specific to glands because they are involved in the secretory pathway, which is very active in glandular tissue. *Microtubule actin cross-linking factor* is the only stromal-specific marker identified so it would definitely be worth investigating further, as well as the gland and stroma specific markers *Alpha type IV collagen* and *St6gall. Ribosomal protein L10a* is a mysterious candidate, as it has been identified in this study and also another transcriptional study (ref) as changing in the peri-implantation uterus, contrary to the previously accepted view that ribosomal proteins are 'housekeeping genes'.

The microarray would benefit from being repeated with a more appropriate reference representative of the whole uterus during the period of peri-implantation. The absence of the marker genes discussed in Chapter 3 from the results and the anomalous data for the housekeeping control genes (as discussed in section 4.4.2) suggest that the data obtained from these chips might not be reliable. However, the presence in the results lists of so many genes previously identified in implantation implies that the data may be useful after all. The best way to verify this would be to check some of the genes identified by the array using quantitative real-time RT-PCR.

Chapter 5: Investigation of expression of canonical circadian genes in uterine tissue

Summary

5.1: Introduction

A circadian rhythm is a biological rhythm that persists under constant environmental conditions with a period of approximately 24 hours. An interruption to these conditions can cause shifting of the cycle. The term 'circadian' is an amalgamation of the Latin words for 'about' (circa) and 'day' (dies). Circadian rhythms are found in animals, plants, fungi, single cell eukaryotes and cyanobacteria (Dunlap, 1999), allowing organisms to anticipate changing environments in ways that enhance their survival, for example, nocturnal mammals such as mice and diurnal mammals such as humans respond behaviourally and physiologically in opposite ways to changing levels of light. When kept in constant darkness, nocturnal rodents typically have a circadian period (τ) of less than 24

hours (Zheng et al., 2001). In laboratory conditions mice are entrained to a circadian period of exactly 24 hours by subjecting them to periods of 12 hours of light followed by 12 hours of dark. A strong entraining cue such as light is called a Zeitgeber (German for 'timekeeper'). The time of 'lights-on' is designated Zeitgeber time 0 (ZT0) and the time of 'lights-off' is designated ZT12 (Jud et al., 2005) . Circadian rhythms are very flexible because of their entrainability, demonstrated by the ability of humans to move through different time zones and adapt to working changing shift pattern. However, the human circadian rhythm cannot be reset immediately and sudden time shifts result in 'Jet lag'.

The molecular basis of the mammalian circadian clock is a negative feedback loop involving a small group of canonical clock-work gene products (Figure 5.1). The changes in expression of these genes in a group of neurons in the suprachiasmatic nucleus (SCN) of the anterior hypothalamus forms a central 'master clock' that coordinates the endogenous circadian rhythms in other peripheral organs. The entrainment cue to the SCN is provided by signals from the retina in response to light (Foster, 1998).

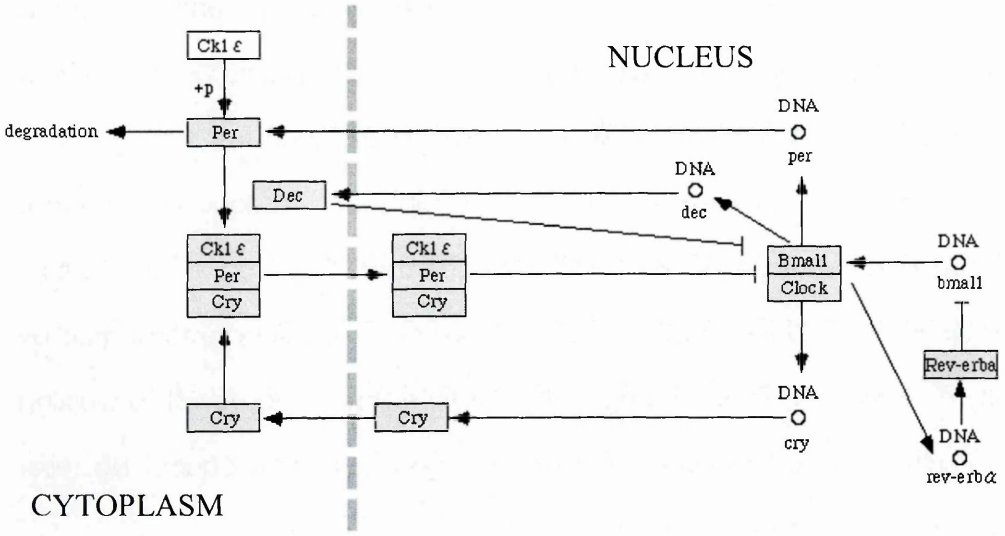

Figure 5.1: Diagram of the molecular clock adapted from http://www.genome.ad.jp. *Brain-muscle arnt-like (Bmal) and Circadian locomotor output cycles kaput (Clock) are transcribed and translated, form a heterodimer and activate transcription of Cryptochrome (Cry) and Period (Per) genes by binding to 'e-box' consensus sequences in their promoters. Per and Cry are transcribed and translated; phosphorylation of Per by casein kinase 1ε regulates dimerisation of Per-Cry heterodimers. The Per-Cry heterodimer enters the nucleus and binds to its own promoters to disrupt translational activation by the Bmal-Clock heterodimer. Per2 is thought to drive expression of Bmal through an unknown site, and a gene called Rev-erb alpha, itself activated by Bmal-Clock heterodimers, acts as a negative repressor of Bmal regulation.*

Canonical circadian genes have been found in many different peripheral organs and rhythmic circadian expression has been found in every tissue it has been investigated in, with the notable exception of the testes (Yamamoto et al., 2004). Other tissues have shown expression of canonical circadian genes but it is not yet known if the expression is rhythmic. The circadian rhythms of peripheral tissues have their own endogenous rhythms that can be entrained not only by the SCN but also by other cues, for example, feeding times provide a cue to entrain the circadian rhythm of the liver (Damiola et al., 2000). Circadian rhythms are

thought to influence the timing of most stages in the reproductive process (Kennaway, 2005). Canonical circadian genes are known to be expressed rhythmically in the non-pregnant rodent uterus (Dolatshad et al., 2006) and oviduct (Kennaway et al., 2003) and are known to be expressed (but have not yet been shown to be rhythmically cycling) in the pseudo-pregnant rodent uterus and pre-implantation embryo (Johnson et al., 2002). Circadian genes are expressed at certain stages of spermatogenesis, but are not rhythmic in the testes (Yamamoto et al., 2004) (Alvarez et al., 2003) (Morse et al., 2003) (Bittman et al., 2003). The non-pregnant uterus of a mouse in oestrus has an endogenous rhythm of circadian genes similar to that of other peripheral organs (Dolatshad et al., 2006). Real-time RT-PCR results show a sinusoidal pattern of expression with a 24-hour period. *Per2* and *Cry1* transcripts peak at ZT 14 and 18 respectively, with *Bmal* in antiphase peaking at ZT0. Because whole uterus cDNAs are used in these experiments, it is not clear from these results whether the rhythmic expression of these genes is present in just one of the uterine tissues or all of them, and if so whether each tissue has its own phase or the phase of each tissue is coordinated so the whole uterus is in synchronisation. If they are coordinated, is this by the SCN or is it by another cue such as hormonal effects? Chronic oestrogen treatment of ovariectomised mice causes a disturbed rhythm of *Per1* and *Per2* in the uterus (Nakamura et al., 2005). Instead of the normal sinusoidal pattern, the expression patterns have two peaks in 24 hours. This modification is not seen in the circadian rhythms of other organs in the oestrogen treated mouse, or in non-oestrogen treated uteri, implying that the circadian rhythms of the uterus are sensitive to oestrogen. It is not known whether this is a specific result of the action of oestrogen through the oestrogen receptor or a result of the rapid division of uterine epithelial cells when exposed to oestrogen.

It is not known whether the circadian rhythm present in the uterus has any downstream effects on the timing of embryo implantation. Mice with a loss-of-function deletion in the *Clock* gene that causes asynchrony in the expression of

Bmal, *Cry1* and *Per2* have decreased reproductive fitness, though this appears to be due to defects in oestrous cycle and parturition. There is no evidence for any defects in fertilisation, mating and implantation (Dolatshad et al., 2006).

The aim of this section of work was to find out whether rhythmic expression of canonical circadian genes exists in separate uterine layers. In addition, as well as being of interest in the timing of events in implantation and pregnancy, the expression of circadian rhythm genes in tissues is a good test of the quality of the RNA obtained from the dispase treatment/mechanical extraction technique, and a chance to test the markers identified in chapter 3 in a wider context.

5.2: Collection of experimental material

Two sets of tissues were obtained from pseudopregnant mice sacrificed in duplicate at 7 time points at 4-hour intervals over days 5 and 6 of pseudopregnancy (section 2.2.3). Because of the problem described in Chapter 4, where insufficient RNA was obtained from samples at each time point by laser capture, manually dissected epithelium and stroma/glands samples were collected.

For the first set, the first time-point taken was ZT0 (06:00) on day 5, then samples were taken at 4 hour time points until 06:00 on day 6: designated ZT24. After removing the uterine horns, half of one was placed into a sterile 1.5ml Eppendorf tube, flash frozen in liquid nitrogen then stored at -80°C. These half horns were taken for laser microdissection preparation (see chapter 4). The epithelium and stroma from the remaining 1.5 horns were removed after dispase treatment and mechanical extraction (section 2.2.4), then placed in a 1.5ml Eppendorf tube containing 100µl Trizol and frozen at -80°C. These samples were taken for RNA extraction. Details of the samples taken are logged in Table 5.1, along with qualitative assessments of the quantity and purity of tissue obtained.

For the second set of tissues, the time points ZT4, ZT8 and ZT12 were taken at 10:00, 14:00 and 18:00 respectively. The time points ZT16, ZT20, ZT24 and ZT0 were taken from mice that had been kept under reverse lighting conditions for the previous two weeks to reset their circadian rhythms, so were taken at 10:00, 14:00, 18:00 and again at 18:00 respectively (2.2.1). The epithelium and stroma from each horn was removed after dispase treatment and mechanical extraction (section 2.2.4), then placed in a 1.5ml Eppendorf tube containing 100µl Trizol and frozen at -80°C. These samples were taken for RNA extraction. Details of the samples taken are logged in Table 5.2 along with qualitative assessments of the quantity and purity of tissue obtained. During the dissection of the uterus it was noted whether

corpora lutea (CL) were pregnant on the ovary to confirm pseudopregnancy. A total of 14 samples were obtained for the first set and 14 for the second set.

Mouse number (and ZT)	1 (4)	2 (4)	3 (16)	4 (16)	5 (20)	6 (20)	7 (24)	8 (24)	9 (0)	10 (0)	11 (8)	12 (8)	13 (12)	14 (12)
Quantity of LE obtained	2	2	1	1	2	2	2	2	2	2	2	2	1	1
Quantity of stroma obtained	2	2	2	2	1	1	1	1	2	2	2	2	2	2
Difficulty of separation	0	0	1	0	0	1	1	1	0	0	0	1	0	0

Table 5.1: Notes on dissection and extraction of set 1 pseudopregant mice. Qualitative assessments of the quantity of tissue and difficulty of separation of the epithelial and stromal layers were made for each extraction. *Quantity of tissue was assessed on a scale of 0-2. 0= No material obtained from extraction, 1= Very little material obtained from extraction, 2= Reasonable amount of tissue obtained. Difficulty of separation was assessed on a scale of 0-1. 0= Easy separation, 1= Difficult separation. ZT= Zeitgeber time, LE= luminal epithelium.*

Mouse number (and ZT)	1 (4)	2 (8)	3 (20)	4 (24)	5 (12)	6 (16)	7 (12)	8 (20)	9 (8)	10 (16)	11 (4)	12 (24)	13 (0)	14 (0)
Quantity of LE obtained	2	1	2	1	2	2	2	2	2	2	2	1	2	1
Quantity of stroma obtained	2	2	2	2	2	1	2	2	2	2	2	1	2	1
Difficulty of separation	0	1	0	1	1	0	1	1	0	0	0	1	0	0

Table 5.2: Notes on dissection and extraction of set 2 pseudopregnant mice. Qualitative assessments of the quantity of tissue and difficulty of separation of the epithelial and stromal layers were made for each extraction. *Quantity of tissue was assessed on a scale of 0-2. 0= No material obtained from extraction, 1= Very little material obtained from extraction, 2= Reasonable amount of tissue obtained. Difficulty of separation was assessed on a scale of 0-1. 0= Easy separation, 1= Difficult separation. ZT= Zeitgeber time, LE= luminal epithelium.*

A sample obtained from a difficult separation of epithelium and stroma is more likely to have contamination from the other tissue layer because it is more difficult to pull the layers apart, so an easy separation is likely to be an indicator of the purity of a tissue, To investigate whether ease of separation (and therefore purity of tissue) is a property of the time of the time on day 5 that the sample was taken, average difficulty of separation over the 4 samples from each time point was calculated and is represented in Figure 5.2.

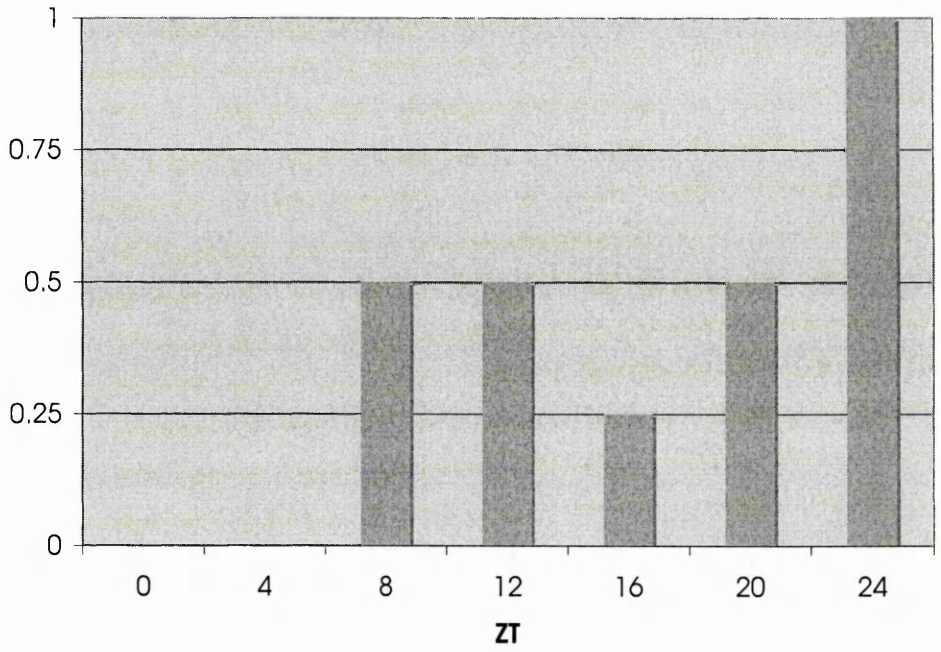

Figure 5.2: Average difficulty of separation for the four samples taken at each time point during day 5 of pseudopregnancy.

Figure 5.2 suggests that there is a correlation between the time of extraction (ZT) and the 'stickiness' of the sample. As discussed in section 3.4, the expression of adhesion molecules is up-regulated in the endometrium as the window of implantation progresses. This is likely to make mechanical separation of the uterine

layers more difficult and result in more glandular epithelium and stroma in the luminal epithelium samples.

Following collection of all samples in Trizol, RNA extraction was performed using a phenol/chloroform protocol followed by purification with a Qiagen kit (2.7.1) and reverse transcription (2.7.3).

5.3: Real-Time RT-PCR analysis using Taqman®

Following RNA extraction and reverse transcription, real-time RT-PCR analysis was performed using a DNA Opticon 2 Real-Time PCR machine (section 2.7.6). The technology behind Taqman®, the relative merits of different protocols for real-time PCR and how a decision on how which of these to use was arrived at, is discussed in section 2.7.4. The primers for *18s* were run on the samples first to assess the amount of cDNA in each. Samples with an *18s* value below 1/10th of the highest *18s* value, were excluded from the analysis, as shown in Tables 5.3 to 5.6 (excluded samples shown highlighted in grey). This was to prevent the inclusion of samples with very little cDNA that are more likely to give erroneous fluorescence readings for the other genes. To check the purity of each sample, the epithelium samples were run with the Tn-C primers/probe set and the stroma samples were run with the EP_2 primers/probe set. No significant EP_2 expression was found in any stromal sample. Cts greater than 35 were observed for *Tenascin-C* in some epithelial samples, implying mild stromal contamination. These samples are indicated in Tables 5.3 and 5.4.

Sample	1	2	4	5	6	7	8	9	10	11	12	13	14
ZT	4	4	16	20	20	24	24	0	0	8	8	12	12
18svalue	8356	1133	3562	10374	3911	39	5895	15476	16850	13556	8924	1249	4054
Tn-C?	Yes											Yes	

***Table 5.3: 18s and Ten-C results for Set 1 epithelium samples**, showing the sample number, the Zeitgeber time (ZT) at which the mouse was sacrificed, the 18s value in relative units and whether Tn-C was identified in the sample using real-time RT-PCR. Samples with an 18s value of less than 1/10th of the highest value in the set were not used in the analysis of canonical circadian gene products and are marked in grey.*

Sample	1	2	3	4	5	6	7	8	9	10	11	12	13	14
ZT	4	8	20	24	12	16	12	20	8	16	4	24	0	0
18svalue	17	5	155	78	58	224	38	157	200	5959	1439	2186	2762	2386
Tn-c?		Yes		Yes	Yes	Yes				Yes				Yes

Table 5.4: 18s and Ten-C results for Set 2 epithelium samples. *Showing the sample number, the Zeitgeber time (ZT) at which the mouse was killed, the 18s value in relative units and whether Tn-C was identified in the sample using real-time RT-PCR. Samples with an 18s value of less than 1/10th of the highest value in the set were not used in the analysis of canonical circadian gene products and are marked in grey.*

Sample	1	2	3	4	5	6	7	8	9	10	11	12	13	14
ZT	4	4	16	16	20	20	24	24	0	0	8	8	12	12
18svalue	5018	5474	5608	5043	4580	5608	5093	5961	6168	7099	5397	2686	4172	3739

Table 5.5: 18s results for Set 1 stroma samples. *Showing the sample number, the Zeitgeber time (ZT) at which the mouse was killed and the 18s value in relative units. All samples were used in the analysis of canonical circadian genes.*

Sample	1	2	3	4	5	6	7	8	9	10	11	12	14	15
ZT	4	8	20	24	12	16	12	20	8	16	4	24	0	0
18svalue	100	12095	91	7205	1684	47	169	40	165	226	84	249	352	1772

Table 5.6: 18s results for Set 2 stroma samples. *Showing the sample number, the Zeitgeber time (ZT) at which the mouse was killed and the 18s value in relative units. Samples with an 18s value of less than 1/10th of the highest value in the set were not used in the analysis of canonical circadian gene products and are marked in grey.*

Samples in set 1 had more consistent levels of cDNA than set 2. This is most likely to be due to low efficiency in the reverse transcription reaction for set 2, or

degradation of RNA during extraction. Because of this, the majority of the samples contributing to the analysis are from set 1.

The remaining samples were run with primer/probe sets for the genes *Bmal, Clock, Per1, Per2, Cry1* and *18s* (for sequence details see section 2.7.5). The mean value of each set (set 1 epithelium, set 1 stroma, set 2 epithelium and set 2 stroma) was calculated for each primer/probe set, including 18s. Each individual result was then divided by the mean of its own set, then circadian gene values were normalised by dividing by their own *18s* values, for example *Bmal* by *18s*. The two sets of results for each normalised circadian gene were then combined, and the average and standard error of the mean (SEM) were calculated for each time point, as described in section 2.7.7 and shown in Figures 5.2 to 5.11.

Figure legend for Figures 5.3 to 5.7

Average expression in the luminal epithelium of genes Bmal (Figure 5.3) Clock (Figure 5.4), Cry1 (Figure 5.5), Per1 (Figure 5.6) and Per2 (Figure 5.7) at four-hourly circadian time points, calculated from real-time RT-PCR results for the gene of interest normalised to the expression of 18s ribosomal RNA and plotted with the standard error of the mean as y-axis error bars for each time point.

Figure legend for Figures 5.8 to 5.12

Average expression in the stroma/glands of genes Bmal (Figure 5.8) Clock (Figure 5.9), Cry1 (Figure 5.10), Per1 (Figure 5.11) and Per2 (Figure 5.12) at four-hourly circadian time points, calculated from real-time RT-PCR results for the gene of interest normalised to the expression of 18s ribosomal RNA and plotted with the standard error of the mean as y-axis error bars for each time point.

5.3.2: Results from Taqman® on LE samples

Figure 5.3: Average expression of *Bmal* in LE over a 24 hour period on day 5 of pseudopregnancy, normalised to 18*s*

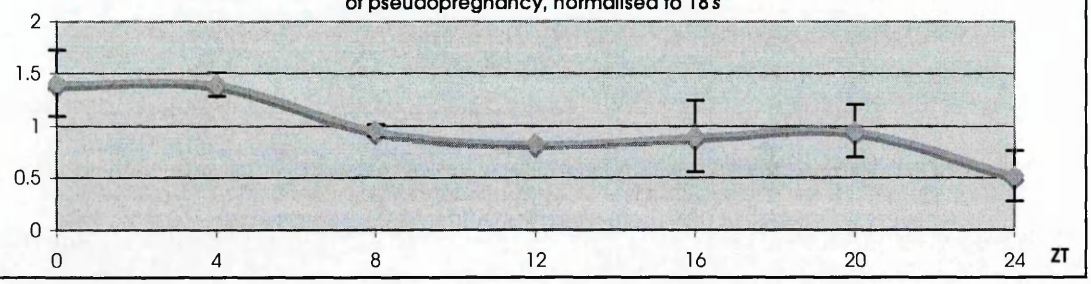

Figure 5.4: Average expression of *Clock* in LE over a 24 hour period on day 5 of pseudopregnancy, normalised to 18s

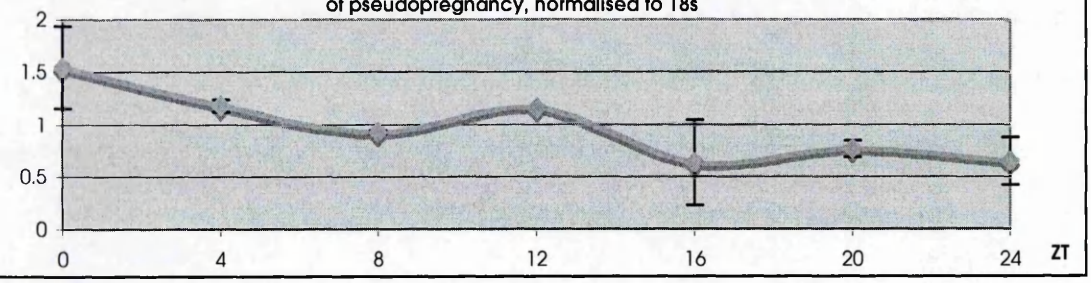

Figure 5.5: Average expression of *Cry1* in LE over a 24 hour period on day 5 of pseudopregnancy, normalised to 18s

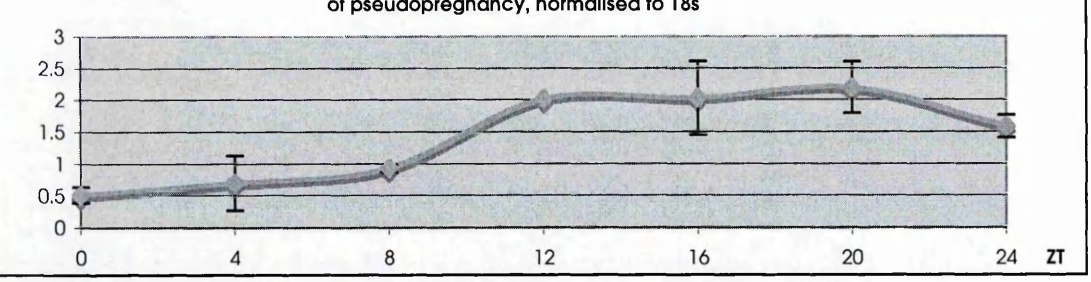

Figure 5.6: Average expression of *Per1* in LE over a 24 hour period on day 5 of pseudopregnancy, normalised to 18s

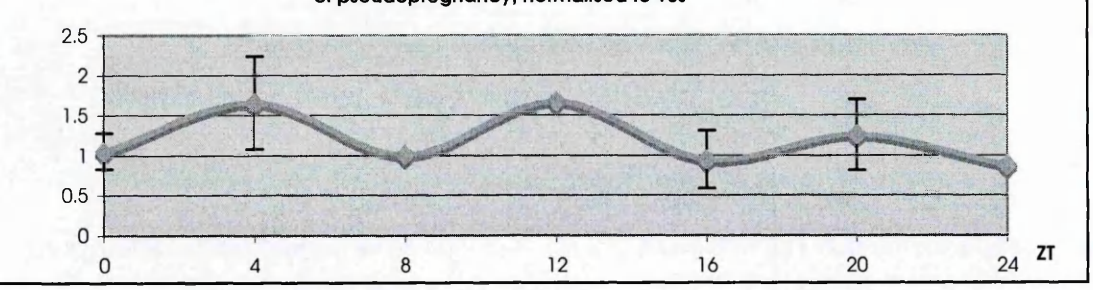

Figure 5.7: Average expression of *Per2* in LE over a 24 hour period on day 5 of pseudopregnancy, normalised to 18s

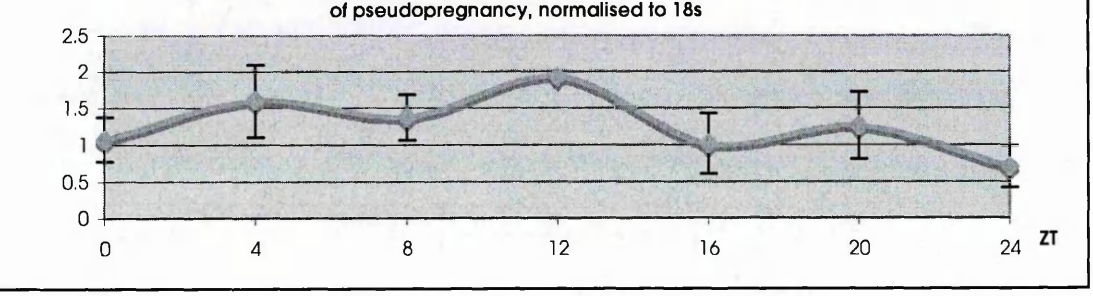

5.3.2: Results from Taqman® on S&G samples

Figure 5.8: Average expression of *Bmal* in stroma over a 24 hour period on day 5 of pseudopregnancy, normalised to 18s

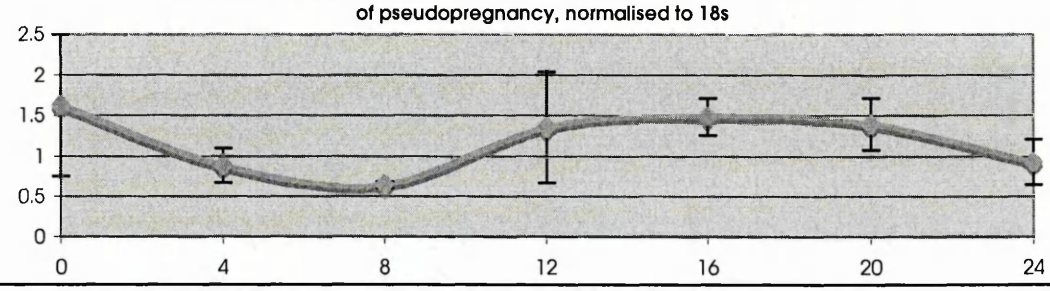

Figure 5.9: Average expression of *Clock* in stroma over a 24 hour period on day 5 of pseudopregnancy, normalised to 18s

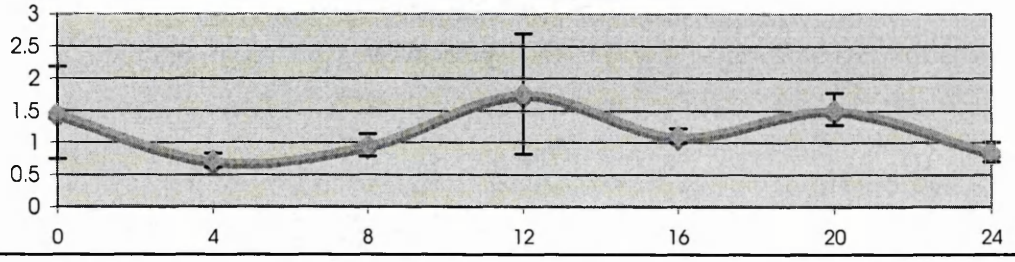

Figure 5.10: Average expression of *Cry1* in stroma over a 24 hour period on day 5 of pseudopregnancy, normalised to 18s

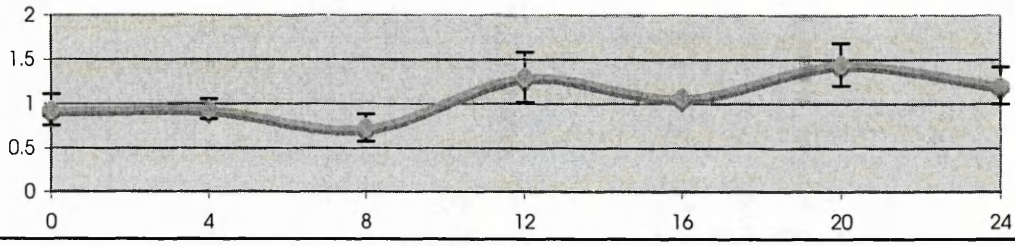

Figure 5.11: Average expression of *Per1* in stroma over a 24 hour period on day 5 of pseudopregnancy, normalised to 18s

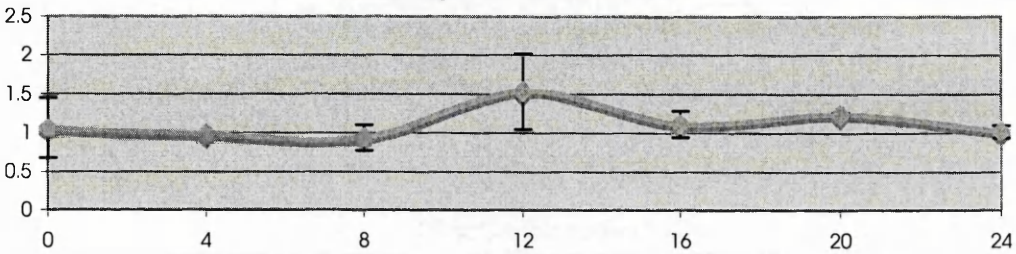

Figure 5.12: Average expression of *Per2* in stroma over a 24 hour period on day 5 of pseudopregnancy, normalised to 18s

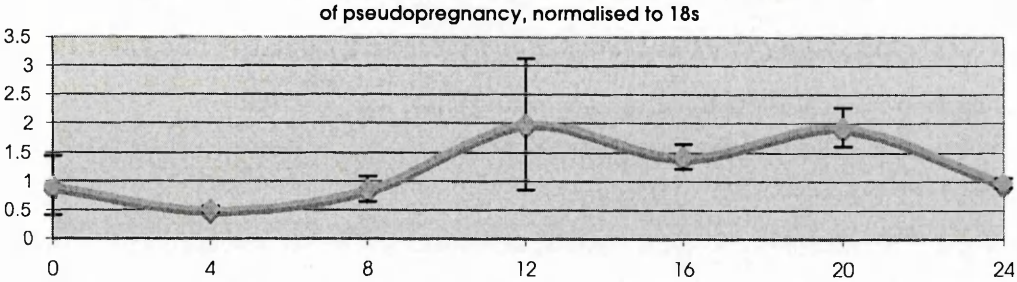

5.4: Discussion of Chapter 5

These results cannot be interpreted as evidence for canonical circadian gene rhythmic expression in the separate layers of the uterus, but cannot prove that the layers of the uterus are arrhythmic. In particular, two of the results, for *Cry1* and *Bmal* in the epithelium (Figure 5.3 and 5.5), are suggestive that there is a rhythm in this uterine layer but that more replicates and modification of the epithelium mechanical removal technique are needed. The characteristic pattern of expression of circadian genes is a sinusoidal curve with a 24-hour phase, as illustrated in Figure 5.13. The values for *Cry* and *Per* genes are generally in anti-phase with values for *Bmal* genes in both SCN and peripheral tissues (Oishi et al., 1998). By contrast, *Clock* gene expression is thought to be constant over the 24-hour period.

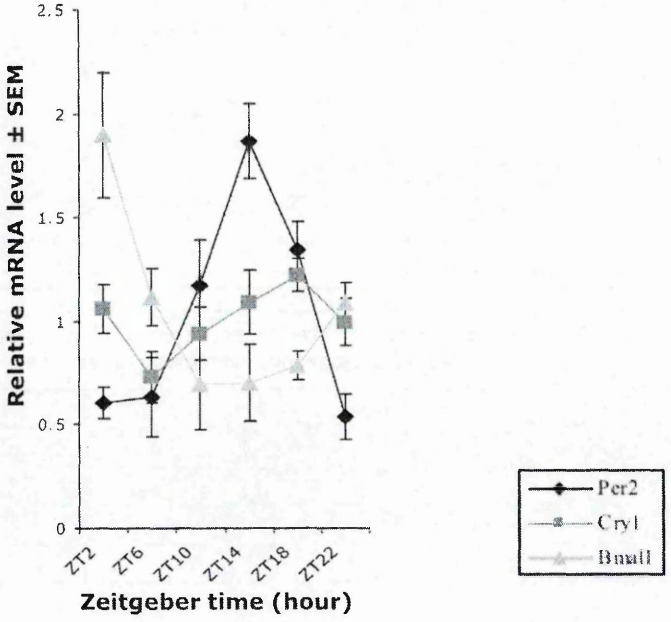

Figure 5.13: *(Taken from Dolatshad et al., 2006)* ***The mRNA expression profiles of Per2, Cry1 and Bmal genes in estrous uteri from wild type mice measured by real-time RT-PCR,*** *where ZT0 = lights on, and ZT12= lights off.*

Amongst the real-time RT-PCR results obtained in these experiments, the only sinusoidal curve characteristic of a 24-hour cycling circadian gene expression

pattern may be seen in *Bmal* expression in both LE (Figure 5.3) and stroma (Figure 5.8) and *Cry1* in LE (Figure 5.5, where it is in anti-phase to *Bmal*). *Per1* and *Per2* do not have obvious circadian patterns in either LE (Figures 5.6 and 5.7) or stroma (Figures 5.11 and 5.12) but their expression may be influenced by oestrogen, as discussed below. In order to conclude whether these results are biological or a result of the methodology, three possible points can be considered.

The first is that there is not a rhythm in the pseudo-pregnant uterus, despite the rhythmicity of the oestrous uterus (Dolatshad et al., 2006). The second possibility is that there is a rhythm in the individual layers but not enough replicates have been taken to show this. The third possibility is that there is a rhythm in the pseudopregnant uterus as a whole, but the mechanical separation and incubation for between two and three hours that is an integral part of the extraction protocol disturbs this rhythm in some way.

The first possibility is that there is no rhythm in the pseudopregnant uterus. To test this hypothesis, firstly real-time RT-PCR would have to be performed on whole uterus samples from the first 5 days of early pregnancy to confirm the presence of a circadian rhythm. A circadian rhythm in *Bmal, Cry1* and *Per2* has already been confirmed in uteri from mice in oestrous (Dolatshad et al., 2006). If the circadian rhythm is disrupted at some point, then the influence of ovarian steroid hormones could be investigated. It is possible that changes to the endogenous rhythm of the uterus take place during early pregnancy and that the 24-hour rhythm is modified by the combined action of progesterone and oestrogen. Chronic oestrogen treatment of ovariectomised mice has been shown to cause a disturbed rhythm of *Per1* and *Per2* in the uterus (Nakamura et al., 2005). Instead of the normal sinusoidal pattern, the expression patterns are biphasic, with a peak at ZT4 and a peak at ZT16. This modification is not seen in the circadian rhythms of other organs in the oestrogen treated mouse, or in non-oestrogen treated uteri, implying that the circadian rhythm of the uterus is specifically sensitive to oestrogen. It is not known

whether this is a specific result of the action of oestrogen through the oestrogen receptor or a result of the rapid division of uterine epithelial cells when exposed to oestrogen. None of the canonical circadian genes in this study (Figures 5.3- 5.12) show a strongly biphasic expression pattern, although this could be due to a lack of sufficient biological replicates (as discussed below) and the patterns of expression of *Per1* (Figure 5.6) and *Per2* (Figure 5.7) in luminal epithelium over a 24 hour period appear to be more biphasic when compared to the flatter patterns of *Bmal* (Figure 5.3) and *Cry1* (Figure 5.5) in luminal epithelium over the same period. More research is needed to determine whether the biphasic pattern of expression is a biological phenomenon during early pregnancy. Investigation of the action of nidatory oestrogen can be achieved through establishment of pseudopregnancy then ovariectomy before the nidatory oestrogen release on day 4 of pregnancy.

The second possibility is that there is a rhythm in the individual layers but not enough replicates have been taken to show this. Due to the poor quality of the cDNAs obtained from many of the samples in the second set, fewer biological replicates than the n=4 aimed for were taken for most time-points. Taking more biological replicates for each time point would help determine whether there are rhythms present but they are being overlooked. It may be that there is a rhythm in epithelium but not stroma, or vice versa. The expression of *Cry1* (Figure 5.5, peak at ZTs 12 to 20) is antiphase to Bmal (Figure 5.3, peak ZTs at 0 to 4) in the epithelium but not the stroma, although the pattern is not as strongly cyclic as that found in the whole uterus as shown in Figure 5.13. This is the most convincing observation that the results would benefit from further replicates and modifications of the technique.

The third possibility is that there is a rhythm in the pseudopregnant uterus as a whole, but the mechanical separation and incubation for between two and three hours that is an integral part of the extraction protocol disturbs this rhythm. The disturbance of rhythm could be either because the whole transcriptome is disturbed when cells are removed and incubated in HBSS with dispase, or because

the circadian genes specifically are disturbed when the tissue is incubated in this case.

The first explanation for disruption of the rhythm (that the whole RNA population is unrepresentative) is unlikely. Global changes in gene expression take place when a tissue is put under stress, such as heat shock protein expression or apoptosis. Degradation by RNases also influences the RNA population present in *in vitro* experiments. It is unlikely that the RNA population is unrepresentative in these experiments, as the dispase incubation and mechanical extraction technique has been previously used to produce tissues that have mainly been used for subsequent recombinant culturing, but have also been used for real-time RT-PCR analysis and microarray analysis in which RNA populations appear to be representative and give consistent results (discussed in section 2.2.5). RNase degradation is unlikely to happen when cells are not lysed and remain intact. It is more likely to be a problem in the downstream experiments that lyse the cells to extract RNA. RNase-free technique (section 2.4.1) was stringently observed throughout downstream experiments.

The second explanation for disruption of the rhythm that it is specifically the circadian genes that are disrupted is more likely. When tissues are removed and cultured they are separated from their master pacemaker, the SCN. In the past, it was thought that the SCN gave individual cells their rhythmicity, but two landmark papers (Nagoshi et al., 2004), (Welsh et al., 2004) re-evaluated this: individual cells in culture still have their own endogenous rhythms, but the SCN synchronises them so the organ they are a part of consists of perfectly synchronised cells. Removal of an organ from its SCN results in a slow de-synchronisation of the circadian rhythms of individual cells so that the organ as a whole becomes asynchronous even though individual cells are still cycling. However, the de-synchronisation of cells in culture occurs over a period of two to seven days (Yamazaki et al., 2000); too long a period for a disruption that would have to take effect over 2-3 hours in these

experiments. The lapse into asynchrony of cultured cell has been shown to be reversed within an hour with a 'serum shock', which resets cells by a rapid induction of *Per1* and *Per2* (Balsalobre et al., 1998). *In vitro* studies have tried to elucidate the nature of the substance in serum that acts as a mediator between a Zeitgeber such as light or feeding times and the synchronisation of cells. cAMP, protein kinase C, glucocorticoid hormones, calcium ions (Ca^{2+}) have been shown to be some of the components of serum that directly induce expression of *Per1 in vitro* (Balsalobre et al., 2000). These studies focus on identifying substances that can induce circadian gene expression *in vitro*, but it may be possible that a lack of these factors can disrupt the expression of *Per1* and other circadian genes. Sudden disruption of a circadian rhythm though tissue explanting has not been investigated, but tissue explants from mice with recently light-shifted circadian rhythms (a jet-lag style scenario) are asynchronous. It is also possible that the incubation medium may have had some effect on immediate gene expression: in this study, tissue explants were cultured in calcium- and magnesium-free Hank's Buffered Salt Solution (HBSS), whereas in other tissue explant experiments (Yamazaki et al., 2000) Dulbecco's Modified Eagle's Medium (containing calcium and magnesium) was used. As described above, calcium ions can induce *Per1* expression so a sudden change in the levels of calcium may be enough to disrupt its expression.

Since incubation with dispase after dissection is vital to prepare the epithelium and stroma for mechanical extraction, it is impossible to remove this step altogether, although experimenting with different incubation media may result in finding one that disrupts the tissue less. The only way to completely circumvent the problem of incubating the tissue with dispase before extraction is to extract tissues using laser microdissection, and this has its own problems associated with it, as discussed in Chapter 6.

Chapter 6: Discussion

Summary

6.1: Recap of aims of Thesis and problems encountered during the work

6.2: Comparisons with previous studies

6.3: Future directions

6.1: Recap of aims of Thesis and problems encountered during the work

The theme of these experiments was the investigation of changes in gene expression of tissues of the murine uterus around the time of implantation with a view to characterising molecular markers for each of the tissues. The work centred on a technique for separating the luminal epithelium from the rest of the uterine tissue using a mild enzymatic (dispase) digestion followed by mechanical extraction (Bigsby et al., 1986). This technique has been used successfully in several previous studies with down-stream techniques including co-culturing of the epithelium and stroma and RNA extraction followed by RT-PCR or northern hybridisation. Papers using this technique are discussed in Section 2.2.5.

In Chapter 3: *Tissue type markers for the pseudopregnant mouse uterus* luminal epithelium and stroma from day 4 and 5 pseudopregnant mice were obtained using the dispase method. These tissues were evaluated by histology. Through viewing histological sections of tissues isolated using the dispase technique, it was concluded that luminal epithelium samples obtained were predominantly luminal epithelium only, but with possible glandular and stromal contamination if taken from day 5 pseudopregnant mice. Stromal samples had patches of glandular epithelium throughout but little luminal epithelium

contamination. Neither luminal epithelium or stroma/glands samples appeared to contain any myometrium or residual tissue.

The initial aim of this work was to characterise molecular markers for the different tissues types in the uterine stroma, in order to verify the tissues present in manually dissected uterine samples. Realistically, manually dissected samples from the mouse uterus are not going to be pure tissues. If they are going to be used subsequently in applications such as microarrays then testing the tissues using real-time RT-PCR at least gives an idea of the levels of each tissue present in the samples. Markers for tissues in the peri-implantation uterus (days 4 and 5) were tabulated after a literature search. Possible markers that were specific for pseudopregnant uterine luminal epithelium (*EP2* and *Osf-2*), glands (*LIF*) and stroma (*Tn-c* and *EP3*) were identified. A set of paired luminal epithelium and stroma/glands tissues was obtained using the dispase technique and tested for the presence of these markers using real-time RT-PCR with Taqman® probes. *Osf-2* was present at higher levels in the stroma and glands samples than it was in the luminal epithelium samples, and it was concluded that *Osf-2* was not suitable as a luminal epithelium marker and was possibly expressed in either stroma, glands or myometrium due to the high expression in whole uterus extracts. *EP2* was present in luminal epithelium samples, but at very low levels in stroma/glands samples so was evaluated as a good marker for luminal epithelium tissues. *Tn-c* displayed the opposite pattern to *EP2* and was assessed as a good stromal marker. *EP3* was expressed at relatively low levels in luminal epithelium samples and relatively high levels in stroma/glands samples. Since it was not possible to obtain pure glandular epithelium tissues through manual dissection, *LIF* could not be verified as a glandular maker without the use of laser microdissection, as discussed in Chapter 4.

Searching for markers that are specifically expressed in LE, glands or stroma during the peri-implantation period revealed that the majority of genes that have been investigated during this time localise to more than one cell type, or change

their localisation influenced by progesterone, oestrogen and the presence of the implanting blastocyst, such as *Cox-2* (Chakraborty et al., 1996). The genes that have consistent expression are either ones such as *Tn-c* that are a structural component of the uterus, with very little change in expression during the oestrous cycle and early pregnancy (Noda et al., 2000), or those such as *LIF* that are induced in a narrow time window and switched off just as quickly (Bhatt et al., 1991). Although two markers were picked to test for both luminal epithelium and stromal specificity, it proved more difficult to find specific markers for glandular epithelium, and only *LIF* was identified as a possible marker. This is likely to be because the luminal and glandular epithelium are structurally very similar, originating from the anterior Müllerian duct during development (Mericskay et al., 2004), and many genes are up-regulated in both compared to the stroma.

Manually dissected epithelial and stromal samples were shown to contain both glandular epithelium and occasionally pieces of each other. These samples could not be used for a definitive verification of the expression of the putative markers. In Chapter 4: *Markers Specific For Uterine Sub- Component Tissues,* luminal epithelium, glandular and stromal tissues were taken from peri-implantation mice using laser microdissection, and the markers evaluated in Chapter 3 were confirmed as tissue specific using real-time RT-PCR. The tissues were also hybridised to microarray chips and analysed to compare the global expression of genes in each of the three tissue types and search for possible new markers. Laser microdissection confirmed the specificity of *EP_2*, *EP_3*, *Tn-c* and *LIF* as specific markers.

A microarray study comparing global gene expression patterns in each of the three tissues of interest yielded a list of genes that would benefit from further investigation. The initial aim was to gather samples from several time points on day 4 of pseudopregnancy so further experiments into canonical circadian rhythm gene expression could be performed. Unfortunately the low yield of laser

microdissection tissue meant that the time-point samples had to be combined to pool enough for the microarray, and the tissue for the circadian study was subsequently obtained by manual dissection. The experimental design of the microarray meant that analysing the results was difficult. The reference cDNA used consisted of a pool of luminal epithelium samples from several time points over the peri-implantation period. Although this meant that individual tissue samples could not be compared to whole uterine expression, useful data were obtained by comparing stromal or glandular tissue expression to LE, and LE expression at two different time points over the peri-implantation period.

Several verification methods were used to check that the data generated by the microarray was useable, but conflicting results were obtained. Control gene readings were highly variable, general fluorescence levels were low and none of the tissue-specific markers could be found in the relevant data sets. Despite this, many of the genes in the lists generated by the microarray had been confirmed as involved in implantation by previous studies. The implication of these conflicting results is that there is useful information in the microarray, but the experiment would benefit from being repeated and the gene lists generated tested using real-time RT-PCR. Unfortunately, the integrity of RNA obtained from laser microdissection may be affected by the freeze-thawing and chemical treatment necessary to obtain the samples, and this may in turn affect the results of downstream studies such as microarrays.

The low yield from the laser microdissection samples meant that the initial idea of testing pure samples of uterine tissues at specific time points on day 4 and 5 of pregnancy could not go ahead. Instead, In Chapter 5: *Investigation of expression of canonical circadian genes in uterine tissue,* luminal epithelium and stroma samples were taken at regular time points from day 5 pseudopregnant mice, then evaluated for cycling of canonical circadian gene transcripts using real-time RT-PCR. Epithelium samples were also tested with *Tn-c* to indicate any

samples that might have stromal contamination, but those that were found to have mild stromal contamination did not correlate with unusual real-time RT-PCR values for canonical circadian genes. The tissues could not be shown to possess rhythmic expression of canonical circadian genes. This may be a result representative of the layers of the uterus due to disruption of the circadian rhythm in early pregnancy, but could also be an artefact from disruption of the circadian rhythm during removal and dispase treatment of the tissues. More studies would be necessary to determine this and ideas are discussed further in Chapter 5.

These results may lead to questioning of the relevance of manual dissection of uterine tissues now that laser capture is becoming more widely available. Despite its obvious advantages, laser dissection is labour intensive and uses specialist equipment. Large-scale studies would be difficult to base around laser microdissection and collection of tissues. By contrast, manual dissection is quick, does not require any specialist equipment, and produces intact tissues for cell culture studies. If used in the right context, it is preferable to laser microdissection, for example. However laser dissection is preferable for many studies, such as the accurate quantifying of transcripts in very specific regions of the uterus.

6.2: Comparisons with previous studies

The peri-implantation uterus has been studied intensely, with the aim that elucidation of transcriptional changes during this time may be able to shed light on reproductive disorders in humans (Sharkey and Smith, 2003), or suggest starting points for research into novel forms of contraception (Catalano et al., 2005). Until the recent advent of microarray studies, progress has been slow due to a reliance on single-gene studies of null mutants with known reproductive defects. Microarrays have sped up the process of searching for new genes involved in implantation as they can generate lists of potentially interesting genes from one experiment. Despite this, they often produce contradictory results, but verification of generated data and repetition of studies is increasing confidence in these results. Many of these studies and their overlap with this work are discussed in Chapter 4.

The issue of the spatial complexity of the uterus during implantation has been ignored in array studies until the recent interest in the technology of laser microdissection. One study (Niklaus and Pollard, 2006), used laser microdissection to compare the transcriptomes of luminal and glandular epithelium from pregnant mice around the time of blastocyst implantation and luminal and glandular epithelium in a delayed model of implantation. The results showed that receptive and non-receptive glandular and luminal epithelium have very different transcriptomes, with 153 genes being significantly up-regulated in the receptive luminal epithelium and 118 in the receptive glandular epithelium. In the delayed implantation model, 130 genes were shown to be significantly up-regulated in the luminal epithelium and 152 in the glandular epithelium. The overlap between the receptive and non-receptive sets was just one gene: Srrm1 (Serine/arginine repetitive matrix 1). The study went on to verify the data using real-time RT-PCR and *in situ* hybridisation. Interestingly, this study also used previously characterised

markers as positive control genes for real-time RT-PCR. *Immune responsive gene 1 (Irg 1), Histamine decarboxylase (HDC)* and *Calbindin 28k (Clb1)* were used as positive controls for genes up-regulated in the LE, whereas *Interleukin-6 signal transducer (Il6st)* was used for the GE. Niklaus et al also note that there are more luminal epithelium-specific transcripts to investigate than gland-specific transcripts. There are differences in experimental design between this study and Niklaus et al., mainly that pseudopregnant mice are used in this study whereas pregnant mice are used in Niklaus et al. Using *Osf-2* as an example (Chapter 3), the expression pattern of a gene in a pregnant mouse is often very different to a pseudopregnant mouse at the same stage, due to the effects of communication between the luminal epithelium of the uterus and the implanting blastocyst. Consequently, there is not much overlap between the genes found to be up-regulated in LE and GE in this study, and those identified in the Niklaus et al. study. There are several instances of different genes from the same family being identified in both studies. *Claudin 7* in Niklaus et al. and *Claudin 4* in this study are both found to be up-regulated in luminal epithelium. Niklaus et al. also identifies several genes previously known to be involved in implantation as being up-regulated in the LE, such as *Histamine decarboxylase*. Like this microarray study, the Niklaus et al. list of genes up-regulated in LE and GE does not contain tissue-specific marker genes *EP_2* (LE) and *LIF* (GE). These genes regularly evade identification in microarray studies. The reason for this is unknown, but further studies may offer some insight.

The microarray studies discussed in section 1.3.2 use the mouse as a model organism. The mouse is a popular choice for microarray studies (as discussed in Chapter 1) because of the similarity of its uterus to the human uterus and the greater availability of tissue samples. For obvious reasons, implantation transcriptome changes are not studied in humans and microarray studies focus on the change from pre-receptive to receptive or receptive to post-receptive states of the menstrual cycle, which are comparable to the state of pseudopregnancy in

the mouse. Despite this, several microarray studies have been performed on human tissue samples (White and Salamonsen, 2005), including a laser microdissection study comparing the transcriptomes of proliferative phase luminal epithelium and stroma (Yanaihara et al., 2005). The overlap between human and mouse studies is similar to the overlap within the contingent of mouse studies (see Chapter 4 discussion for examples of genes identified in this microarray study that are also identified in human studies). A full review of human receptivity microarrays is beyond the scope of this discussion, but mouse microarray studies have a valuable part to play in the elucidation of the mammalian (and more specifically the human) implantation process, as there is much overlap between the genetic control of receptivity and implantation, and the scope for experimentation is much larger.

6.3: Future directions

The results of these studies are rich in springboards for potential future work. The characterisation of molecular markers for uterine tissue types is useful for verifying the composition of manually dissected uterine samples for subsequent work, and has already been used for that purpose in a microarray study (Campbell et al., 2006). A layer of the uterus neglected in this work is the myometrium. The myometrium is a relatively static tissue in early pregnancy but becomes more important as pregnancy progresses and the uterus expands to accommodate the growing foetuses, then aids the process of parturition. It is difficult to obtain myometrium thorough manual dissection, but laser capture would allow isolation of samples of pure myometrium.

The lists of genes generated by the microarray study can be tested on laser microdissected tissue samples to verify that their expression is tissue specific (Hong et al., 2004), or used as probes in *in situ* hybridisation studies. The question of whether canonical circadian gene expression in the uterus is arrhythmic can also be addressed by testing whole uterus samples from time points over early pregnancy, using laser microdissection to obtain samples of tissue and testing changes in the incubation medium for manually dissected samples.

The changes that take place in the transcriptomes of the mammalian uterus during receptivity and implantation are still not fully characterised, but a number of new techniques are contributing to the current knowledge with every new study published. The ultimate aim of elucidating the mechanisms of implantation is to be able to treat reproductive problems and develop new contraceptive technologies that could possibly be of use in the future.

Chapter 7: Bibliography

Alberts, B. (2002). Molecular Biology of the Cell, 4th edn: Garland Science).

Alvarez, J., Chen, D., Storer, E., and Sehgal, A. (2003). Non-cyclic and developmental stage-specific expression of circadian clock proteins during murine spermatogenesis. Biol Reprod *69*, 81-91.

Aplin, J. (1997). Adhesion molecules in implantation. Reviews of Reproduction *2*, 84-93.

Arcturus (2004). PixCell IIe LCM System- Take Advantage of the Benefits of LCM http://www.arctur.com/lab_portal/products/pixcell_take_advantage_lcm.htm As of 17th December 2006.

Arriza, J., Eliasof, S., Kavanaugh, M., and Amara, S. (1997). Exciatatory amino acid transporter 5, a retinal glutamate transporter coupled to a chloride conductance. PNAS *94*, 4155-4160.

Balsalobre, A., Damiola, F., and Schibler, U. (1998). A Serum Shock Induces Circadian Gene Expression in Mammalian Tissue Culture Cells. Cell *93*, 929-937.

Balsalobre, A., Marcacci, L., and Schibler, U. (2000). Multiple signaling pathways elicit circadian gene expression in cultured Rat-1 fibroblasts. Current Biology *10*, 1291-1294.

Benson, G., Lim, H., Paria, B., Satokata, I., Dey, S., and Maas, R. (1996). Mechanisms of reduced fertility in *Hoxa-10* mutant mice: uterine homeosis and loss of maternal *Hoxa-10* expression. Development *122*, 2687-2696.

Bhatt, H., Brunet, L. J., and Stewart, C. L. (1991). Uterine expression of leukemia inhibitory factor coincides with onset of blastocyst implantation. PNAS *88*, 11408-11412.

Bigsby, R., Cooke, P., and Cunha, G. (1986). A simple and efficient method for separating murine uterine epithelial and mesenchymal cells. Am J Physiol *251*, E630- E636.

Bittman, E., Doherty, L., Huang, L., and Paroskie, A. (2003). *Period* gene expression in mouse endocrine tissues. Am J Physiol Regul Integr Comp Physiol *285*, R561-569.

Bowen, J., and Hunt, J. (2000). The Role of Integrins in Reproduction. Proc Soc Exp Biol Med *223*, 331-343.

Buchanan, D., Kurita, T., Taylor, J., Lubahn, D., Cunha, G., and Cooke, P. (1998). Role of Stromal and Epithelial Estrogen Receptors in Vaginal Epithelial Proliferation, Stratification, and Cornification. Endocrinology, 4345-4352.

Buchanan, D., Setiawan, T., Lubahn, D., Taylor, J., Kurita, T., Cunha, G., and Cooke, P. (1999). Tissue compartment-specific estrogen receptor-alpha participation in the mouse uterine epithelial secretory response. Endocrinology *140*, 484-491.

Bustin, S. (2000). Absolute quantification of mRNA using real-time reverse transcription polymerase chain reaction assays. J Mol Endocrinol *25*, 169-193.

Bustin, S., and Nolan, T. (2004). Pitfalls of Quantitative Real-Time Reverse-Trasncription Polymerase Chain Reaction. J BioMol Techniques *15*, 155-166.

Byrne, J., Nourse, C., Basset, P., and Gunning, P. (1998). Identification of homo and heteromic interactions between members of the breast carcinoma-associated D52 protein family using the yeast two-hybrid system. Oncogene *16*, 873-881.

Campbell, L., O'Hara, L., Catalano, R. D., Sharkey, A. M., Freeman, T. C., and Johnson, M. H. (2006). Temporal expression profiling of the uterine luminal epithelium of the pseudo-pregnant mouse suggests receptivity to the fertilised egg is associated with complex transcriptional changes. Hum Reprod *21*, 68-79.

Carling, T., Kim, K.-C., Yang, X.-H., Gu, J., Zhang, X.-K., and Huang, S. (2004). A Histone Methyltransferase Is Required for Maximal Response to Female Sex Hormones. Mol Cell Biol *24*, 7032-7042.

Carson, D., Bagichi, I., Dey, S., Enders, A., Fazleabas, A., Lessey, B., and Yoshinaga, K. (2000). Embryo implantation. Dev Biol *223*, 217-237.

Carson, D., DeSouza, M., Kardon, R., Zhou, X., Lagow, E., and Julian, J. (1998). Mucin expression and function in the female reproductive tract. Hum Reprod Update *4*, 459-464.

Carson, D., Lagow, E., Thathiah, A., Al-Shami, R., Farach-Carson, M., Vernon, M., Yuan, L., Fritz, M., and Lessey, B. (2002). Changes in gene expression during the early to mid luteal (receptive phase) transition in human endometrium detected by high-density microarray screening. Mol Hum Reprod *8*, 871-879.

Catalano, R., Johnson, M., Campbell, E., Charnock-Jones, S., Smith, S., and Sharkey, A. (2005). Inhibition of Stat3 activation in the endometrium prevents implantation: a nonsteroidal approach to contraception. PNAS *102*, 8585-8590.

Cattaruzza, M., Schafer, K., and Hecker, M. (2002). Cytokine-induced Down-regulation of zfm1/Splicing Factor-1 Promotes Smooth Muscle Cell Proliferation. J Biol Chem *277*, 6582-6589.

Chakraborty, I., Das, S., and Dey, S. (1995). Differential expression of vascular endothelial growth factor and its receptor mRNAs in the mouse uterus around the time of implantation. J Endocrinol *147*, 339-352.

Chakraborty, I., Das, S., Wang, J., and Dey, S. (1996). Developmental expression of the cyclo-oxygenase-1 and cyclo-oxygenase-2 genes in the peri-implantation mouse uterus and their differential regulation by the blastocyst and ovarian steroids. J Mol Endocrinol *16*, 107-122.

Chen, J., Cheng, J.-G., Shatzer, T., Sewell, L., Hernandez, L., and Stewart, C. (2000). Leukemia inhibitory factor can substitute for nidatory estrogen and is essential to inducing a receptive uterus for implantation but is not essential for subsequent embryogenesis. Endocrinology *141*, 4365-4372.

Chen, W., Zeng, X., Carter, M., Morrell, C., Yen, R.-W., Esteller, M., Watkins, D., Herman, J., Mankowski, J., and Baylin, S. (2003). Heterozygous disruption of Hic1 predisposes mice to a gender-dependent spectrum of malignant tumors. Nature Genetics *33*, 197-202.

Cheng, J.-G., Chen, J., Hernandez, L., Alvord, W., and Stewart, C. L. (2001). Dual control of LIF expression and LIF receptor function regulate Stat3 activation at the onset of uterine receptivity and embryo implantatio. PNAS *98*, 8680-8685.

Cheon, Y.-P., Li, Q., Xu, X., Demayo, F., Bagchi, I., and Bagchi, M. (2002). A genomic approach to identify novel progesterone receptor regulated pathways in the uterus during implantation. Mol Endocrinol *16*, 2853-2871.

Chu, C., and Paul, W. (1998). Expressed genes in interleukin-4 treated B cells identified by cDNA representational difference analysis. Mol Immunol *35*, 487-502.

Cooke, P., Buchanan, D., Young, P., Setiawan, T., Brody, J., Korach, K., Taylor, J., Lubahn, D., and Cunha, G. (1997). Stromal estrogen receptors mediate mitogenic effects of estradiol on uterine epithelium. Proc Nat Acad Sci USA *94*, 6535-6540.

Coux, O., Tanaka, K., and Goldberg, A. (1996). Structure and functions of the 20S and 26S proteasomes. Ann Rev Biochem *65*, 801-847.

Daftary, G., Troy, P., Bagot, C., Young, S., and Taylor, H. (2005). Direct regulation of beta-3 integrin subunit gene expression by hoxa10 in endometrial cells. Mol Endocrinol *16*, 571-579.

Damiola, F., Minh, N., Preitner, N., Kornmann, B., Fleury-Olela, F., and Schibler, U. (2000). Restricted feeding uncouples circadian oscillators in peripheral tissues from the central pacemaker in the suprachiasmatic nucleus. Genes Dev *14*, 2950-2961.

Das, S., Lim, H., Paria, B., and Dey, S. (1999). Cyclin D3 in the mouse uterus is associated with the decidualization process during early pregnancy. J Mol Endocrinol *22*, 91-101.

Das, S., Tsukamura, H., Paria, B., Andrews, G., and Dey, S. (1994a). Differential expression of epidermal growth factor receptor (EGF-R) gene and regulation of EGF-R bioactivity by progesterone and estrogen in the adult mouse uterus. Endocrinology *134*, 971-981.

Das, S., Wang, X.-N., Paria, B., Damm, D., Abraham, J., Klagsbrun, M., Andrews, G., and Dey, S. (1994b). Heparin-binding EGF-like growth factor gene is induced in the mouse uterus temporally by the blastocyst solely at the site of its apposition: a possible ligand for interaction with blastocyst EGF-receptor in implantation. Development *120*, 1071-1083.

DeMayo, F., Zhao, B., Takamoto, N., and Tsai, S. (2002). Mechanisms of action of estrogen and progesterone. Ann NY Acad Sci *955*, 48-59.

Dey, S., Lim, H., Das, S., Reese, J., Paria, B., Daikoku, T., and Wang, H. (2004). Molecular cues to implantation. Endocrine reviews *25*, 341-373.

Dolatshad, H., Campbell, L., O'Hara, L., Maywood, E. S., Hastings, M. H., and Johnson, M. H. (2006). Developmental and reproductive performance in circadian mutant mice. Hum Reprod *21*, 68-79.

Dorak, M. (2006). Real-time PCR: Taylor and Francis).

Dunlap, J. (1999). Molecular Bases for Circadian Clocks. Cell *96*, 271-290.

Eisenberg, E., and Levanon, E. (2003). Human housekeeping genes are compact. Trends in Genetics *19*, 362-365.

Foster, R. (1998). Shedding Light on the Biological Clock. Neuron *20*, 829-832.

Fouladi-Nashta, A., Jones, C., Nijjar, N., Mohamet, L., Smith, A., Chambers, I., and Kimber, S. (2005). Characterization of the uterine phenotype during the peri-implantation period for LIF-null, MF1 strain mice. Dev Biol *281*, 1-21.

Hong, S., Nah, H., Lee, J., Lee, Y., Lee, J., Gye, M., Kim, C., Kang, B., and Kim, M. (2004). Estrogen Regulates the Expression of the Small Proline-rich 2 Gene Family in the Mouse Uterus. Mol Cells *17*, 477-484.

Horcajadas, J., Riesewijk, A., Dominguez, F., Cervero, A., Pellicer, A., and Simon, C. (2004). Determinants of Endometrial Receptivity. Ann NY Acad Sci *1034*, 166-175.

Hu, J., Gray, C., and Spencer, T. (2004). Gene expression profiling of neonatal mouse uterine development. Biol Reprod *70*, 1870-1876.

Ichikawa, A. (2003). Identification and characterization of a novel progesterone receptor-binding element in the mouse prostaglandin E receptor subtype EP2 gene. Genes to cells.

Illera, M., Cullinan, E., Gui, Y., Yuan, L., Beyler, S., and Lessey, B. (2000). Blockade of the alpha v beta 3 Integrin Adversely Affects Implantation in the Mouse. Biol Reprod *62*, 1285-1290.

Illingworth, I., Kiszka, I., Bagley, S., Ireland, G., Garrod, D., and Kimber, S. (2000). Desmosomes Are Reduced in the Mouse Uterine Luminal Epithelium During the

Preimplantation Period of Pregnancy: A Mechanism for Facilitation of Implantation. Biol Reprod *63*, 1764-1773.

Jeong, J.-W., Demayo, F., Lee, K., Kwak, I., White, L., Hilsenbeck, S., Lydon, J., and Demayo, F. (2005). Identification of murine uterine genes regulated in a ligand-dependent manner by the progesterone receptor. Endocrinology *146*, 3490-3505.

Johnson, M., Lim, A., Fernando, D., and Day, M. (2002). Circadian clockwork genes are expressed in the reproductive tract and conceptus of the early pregnant mouse. Reprod Biomed Online *4*, 140-145.

Johnson, M. H., and Everitt, B. (2000). Essential Reproduction, 5th edn: Blackwell Science (UK)).

Joswig, A., Gabriel, H.-D., Kibschull, M., and Winterhager, E. (2003). Apoptosis in uterine epithelium and decidua in response to implantation: evidence for two different pathways. Reproductive biology and endocrinology *1*, http://www.rbej.com/content/1/1/44.

Jud, C., Schmutz, I., Hampp, G., Oster, H., and Albrecht, U. (2005). A guideline for analyzing circadian wheel-running behavior in rodents under different light conditions. Biol Proced Online *7*, 101-116.

Kao, L., Tulac, S., Lobo, S., B, I., JP, Y., A, G., K, O., RN, T., BA, L., and LC, G. (2002). Global gene profiling in human endometrium during the window of implantation. Endocrinology *143*, 2119-2138.

Katsuyama, M., Sugimoto, Y., Morimoto, K., Hatsumoto, K.-Y., Fukumoto, M., Negishi, M., and Ichikawa, A. (1996). Distinct cellular localization of the messenger ribonucleic acid for prostaglandin E receptor subtypes in the mouse uterus during pseudopregnancy. Endocrinology *138*, 344-350.

Kennaway, D. (2005). The role of circadian rhythmicity in reproduction. Hum Reprod Update *11*, 91-101.

Kennaway, D., Varcoe, T., and Mau, V. (2003). Rhythmic expression of clock and clock-controlled genes in the rat oviduct. Mol Hum Reprod *9*, 503-507.

Kimber, S., Stones, R., and Sidhu, S. (2001). Glycosylation changes during differentiation of the murine uterine epithelium. Biochem Soc Transact *29*, 156-161.

Kimber, S. J., and Spanswick, C. (2000). Blastocyst implantation: The adhesion cascade. Stem Cell Dev Bio *11*, 77-92.

Kortschak, R., Tucker, P., and Saint, R. (2000). ARID proteins come in from the desert. Trends Biochem Sci *25*, 294-299.

Kovar, D. (2006). Cell polarity: formin on the move. Current Biology *25;16*, R535-538.

Kudo, H., Senju, S., Mitsuya, H., and Nishimura, Y. (2000). Mouse and human GTPBP2, newly identified members of the GP-1 family of GTPase. Biophys Res Commun *272*, 456-465.

Kurita, T., Lee, K., Saunders, P., Cooke, P., Taylor, J., Lubahn, D., Zhao, C., Makela, S., Gustafsson, J., Dahiya, R., and Cunha, G. (2001). Regulation of progesterone receptors and decidualization in the uterine stroma of the estrogen receptor-alpha knockout mouse. Biol Reprod *64*, 272-283.

Kurita, T., Lee, K.-A., Cooke, P., Lydon, J., and Cunha, G. (2000). Paracrine regulation of epithelial progesterone receptor by estradiol in the mouse female reproductive tract. Biol Reprod *62*, 831-838.

Kurita, T., Young, P., Brody, J., Lydon, J., O'Malley, B., and Cunha, G. (1998). Stromal progesterone receptors mediate the inhibitory effects of progesterone on estrogen-

induced uterine epithelial cell deoxyribonucleic acid synthesis. Endocrinology *139*, 4708-4713.

Lang, I., Chuang, T., Barbas, C. I., and Schleef, R. (1996). Purification of storage granule protein-23. A novel protein identified by phage display technology and interaction with type I plasminogen activator inhibitor. J Biol Chem *271*, 30126-30135.

Lee, K., and Demayo, F. (2004). Animal models of implantation. Reproduction *128*, 679-695.

Leung, C., Sun, D., Zheng, M., Knowles, D., and Liem, R. (1999). Microtubule actin cross-linking factor (MACF): a hybrid of dystonin and dystrophin that can interact with the actin and microtubule cytoskeletons. J Cell Biol *147*, 1275-1286.

Leyva, J., Bianchet, M., and Amzel, L. (2003). Understanding ATP synthesis: structure and mechanism of the F1-ATPase (review). Mol Membr Biol *20*, 27-33.

Lim, H., and Dey, S. K. (1997). Prostaglandin E2 receptor subtype EP2 gene expression in the mouse uterus coincides with differentiation of the luminal epithelium for implantation. Endocrinology *138*, 4599-4606.

Lim, H., Gupta, R., Ma, W.-G., Paria, B., Moller, D., Morrow, J., DuBois, R., Trzaskos, J., and Dey, S. (1999a). Cyclo-oxygenase-2-derived prostacyclin mediates embryo implantation in the mouse via PPAR-delta. Genes Dev *13*.

Lim, H., Ma, L., and Dey, S. (1999b). Hoxa-10 regulates uterine stromal cell responsiveness to progesterone during implantation and decidualization in the mouse. Mol Endocrinol *13*, 1005-1017.

Lim, H., Paria, B., Das, S., Dinchuk, J., Langenbach, R., Trzaskos, J., and Dey, S. (1997). Multiple Female Reproductive Failures in Cyclooxygenase 2-Deficient Mice. Cell *91*, 197-208.

Ma, L., Benson, G., Lim, H., Dey, S., and Maas, R. (1998). Abdominal B (AdB) Hoxa genes: regulation in adult uterus by estrogen and progesterone and repression in mullerian duct by the synthetic estrogen diethylstilbestrol (DES). Dev Biol *197*, 141-154.

Ma, X.-H., Hu, S.-J., Ni, H., Zhao, Y.-C., Tian, Z., Liu, J.-L., Ren, G., Liang, X.-H., Yu, H., Wan, P., and Yang, Z.-M. (2006). Serial analysis of gene expression in mouse uterus at the implantation site. J Biol Chem *281*, 9351-9360.

Marie-Josee Sasseville, A., Caron, A., Bourget, L., Klein, A., Dicaire, M., Rouleau, G., Massie, B., Langlier, Y., and Brais, B. (2006). The dynamism of PABPN1 nuclear inclusions during the cell cycle. Neurobiol Dis *23*, 621-629.

Matsumoto, H., Ma, W.-G., Daikoku, T., Zhao, X., Paria, B., Das, S., Trzaskos, J., and Dey, S. (2002). Cyclooxygenase-2 Differentially Directs Uterine Angiogenesis during Implantation in Mice. J Biol Chem *277*, 29260-29267.

Mericskay, M., Kitajewski, J., and Sassoon, D. (2004). Wnt5a is required for proper epithelial-mesenchymal interactions in the uterus. Development *131*, 2061-2072.

Miller, C., and Sassoon, D. (1998). Wnt-7a maintains appropriate uterine patterning during the development of the mouse female reproductive tract. Development *125*, 3201-3211.

Mishra, A., and Seshagiri, P. (2000). Heparin binding-epidermal growth factor improves blastocyst hatching and trophoblast outgrowth in the golden hamster. Reprod Biomed Online *1*, 87-95.

Morse, D., Cermakian, N., Brancorsini, S., Parvinen, M., and Sassone-Corsi, P. (2003). No Circadian Rhythm in Testis: Period1 expression is clock independent and developmentally regulated in the mouse. Mol Endocrinol *17*, 141-151.

Murthy, K., and Manley, J. (1995). The 160-kD subunit of human cleavage-polyadenylation specificity factor coordinates pre-mRNA 3'-end formation. Genes Dev *9*, 2672-2683.

Nagoshi, E., Saini, C., Bauer, C., Laroche, T., Naef, F., and Schibler, U. (2004). Circadian Gene Expression in Individual Fibroblasts, Cell-Autonomous and Self-sustained Oscillators Pass Time to Daughter Cells. Cell *119*, 693-705.

Nakamura, T., Moriya, T., Inoue, S., Shimanzoe, T., Wanatabe, S., Ebihara, S., and Shinohara, K. (2005). Estrogen differentially regulates expression of Per1 and Per2 genes between central and peripheral clocks and between reproductive and nonreproductive tissues in female rats. J Neuro Res *82*, 622-630.

Niklaus, A., and Pollard, J. (2006). Mining the mouse transcriptome of receptive enndometrium reveals distinct molecular signals for the luminal and glandular epithelium. Endocrinology *147*, 3375-3390.

Noda, N., Minoura, H., Nishiura, R., Toyoda, N., Imanaka-Yoshida, K., Sakakura, T., and Tashimich, Y. (2000). Expression of tenascin-c in stromal cells of the murine uterus during early pregnancy: induction of interleukin-1 alpha, prostaglandin E2 and prostaglandin F2alpha. Biol Reprod *63*, 1713-1720.

Oishi, K., Sakamoto, K., Okada, T., Nagase, T., and Ishidad, N. (1998). Antiphase Circadian Expression between BMAL1 and period Homologue mRNA in the Suprachiasmatic Nucleus and Peripheral Tissues of Rats. Biochem Biophys Res Comm *253*, 199-203.

Okada, H., Sanezumi, M., Nakajima, T., Okada, S., Yasuda, K., and Kanzaki, H. (1999). Rapid down-regulation of CD63 transcription by progesterone in human endometrial stromal cells.
Mol Hum Reprod *5*, 554-558.

Paria, B., Das, N., Das, S., Zhao, X., Dileepan, K., and Dey, S. (1998a). Histidine decarboxylase gene in the mouse uterus is regulated by progesterone and correlates with uterine differentiation for blastocyst implantation. Endocrinology *139*, 3958-3966.

Paria, B., Das, S., Andrews, G., and Dey, S. K. (1993). Expression of the epidermal growth factor receptor gene is regulated in mouse blastocysts during delayed implantation. Dev Biol *90*, 55-59.

Paria, B., Lim, H., Wang, X.-N., Liehr, J., Das, S., and Dey, S. (1998b). Coordination of Differential Effects of Primary Estrogen and Catecholestrogen on Two Distinct Targets Mediates Embryo Implantation in the Mouse. Endocrinology *139*.

Pavlova, A., Boutin, E., Cunha, G., and Sassoon, D. (1994). Msx1 (Hox-7.1) in the adult mouse uterus: cellular interactions underlying regulation of expression. Development, 335-346.

Raab, G., Kover, K., Paria, B., Dey, S., Ezzell, R., and Kagsbrun, M. (1996). Mouse preimplantation blastocysts adhere to cells expression the transembrane form of heparin-binding EGF-like growth factor. Development *122*, 637-645.

Rahman, M., Li, M., Li, P., Wang, H., Dey, S., and Das, S. (2006). Hoxa-10 deficiency alters region-specific gene expression and peturbs differetiation of natural killer cells during decidualization. Dev Biol *290*, 105-117.

Reese, J., Das, S., Paria, B., Lim, H., Song, H., Matsumoto, H., Knudtson, K., DuBois, R., and Dey, S. (2001). Global gene expression analysis to identify molecular markers of uterine receptivity. J Biol Chem *276*, 44137-44145.

Riesewijk, A., Simon, C., Martin, J., van Os, R., Horcajadas, A., Polman, J., Pellicer, A., and Mosselman, S. (2003). Gene expression profiling of human endometrial

receptivity on days LH+2 versus LH+7 by microarray technology. Mol Hum Reprod *9*, 253-264.

Rugh, R. (1990). The Mouse: Its Reproduction and Development: Oxford University Press).

Shah, B., and Catt, K. (2005). Roles of LPA3 and COX-2 in implantation. Trends Endocrinol Metab *16*, 397-399.

Sharkey, A., and Smith, S. (2003). The endometrium as a cause of implantation failure. Best Practice and Research Clinical Obstetrics and Gynaecology *17*, 289-307.

Sherwin, J. R. A., Freeman, T. C., J, S. R., Kimber, S., Smith, A. G., Chambers, I., Smith, S. K., and Sharkey, A. M. (2004). Identification of genes regulated by leukaemia inhibitory factor in the mouse uterus at the time of implantation. Mol Endocrinol *18*, 2185-2195.

Shin, H., Bargiello, T., Clark, B., Jackson, F., and Young, M. (1985). An unusual coding sequence from a Drosophila clock gene is conserved in vertebrates. Nature *317*, 445-448.

Sidhu, S., and Kimber, S. (1999). Hormonal control of H-type alpha(1-2)fucosyltransferase messenger ribonucleic acid in the mouse uterus. Biol Reprod *60*, 147-157.

Song, H., Lim, H., Das, S., Paria, B., and Dey, S. K. (2000). Dysregulation of EGF family of growth factors and cox-2 in the uterus during the preattachment and attachment reactions of the blastocyst with the luminal epithelium correlates with implantation failure in LIF-deficient mice. Mol Endocrinol *14*, 1147-1161.

Soundararajan, R., and Jagannadha Rao, A. (2004). Trophoblast 'pseudo-tumorigenesis': Significance and contributory factors. Reproductive biology and endocrinology *2*, http://www.rbej.com/contents/2/1/15.

Surveyor, G., Gendler, S., Pemberton, L., Das, S., Chakraborty, I., Julian, J., Pimental, R., Wegner, C., Dey, S., and Carson, D. (1995). Expression and Steroid Hormonal Control of Muc-1 in the Mouse Uterus. Endocrinology *136*.

Tong, B., Das, S., Threadgill, D., Magnuson, T., and Dey, S. (1996). Differential expression of the full-length and truncated forms of the epidermal growth factor receptor in the preimplantation mouse uterus and blastocyst. Endocrinology *137*, 1492-1496.

Tsitskov, E., Laouini, D., Dunn, I., Sannikova, T., Davidson, L., Alt, F., and Gera, R. (2001). TRAF1 is a negative regulator of TNF signaling: enhanced TNF signaling in TRAF-1 deficient mice. Immunity *15*, 647-657.

Wang, H., and Dey, S. (2006). Roadmap to embryo implantation: clues from mouse models. Nature Rev Gen *7*, 185-199.

Wang, H., Zhang, X., Qian, D., Lin, H., Li, Q., Liu, D., Liu, G., Yu, X., and Zhu, C. (2004). Effect of Ubiquitin-Proteasome Pathway on Mouse Blastocyst Implantation and Expression of Matrix Metalloproteinases-2 and -9. Biol Reprod *70*, 481-487.

Wang, X., Matsumoto, H., Zhao, X., Das, S., and Paria, B. (2003). Embryonic signals direct the formation of tight junctional permeability barrier in the decidualizing stroma during embryo implantation. J Cell Sci *117*, 53-63.

Wang, X.-N., Das, S., Damm, D., Klagsbrun, M., Abraham, J., and Dey, S. (1994). Differential Regulation of Heparin-Binding Epidermal Growth Factor-Like Growth Factor in the Adult Ovariectominsed Mouse Uterus by Progesterone and Estrogen. Endocrinology *135*, 1264-1271.

Welsh, D., Yoo, S.-H., Liu, A., Takahashi, J., and Kay, S. (2004). Bioluminescence Imaging of Individual Fibroblasts Reveals Persistent, Independently Phased Circadian Rhythms of Clock Gene Expression. Current Biology *14*, 2289-2295.

White, C., and Salamonsen, L. (2005). A guide to issues in microarray analysis: application to endometrial biology. Reproduction *130*, 1-13.

White, S., and Kimber, S. (1994). Changes in alpha(1-2)-fucosyl-transferase activity in the murine endometrial epithelium during the estrous cycle, early pregnancy, and after ovariectomy and hormone replacement. Biol Reprod *50*, 73-81.

Yamamoto, T., Nakahatu, Y., Soma, H., Akashi, M., Mamine, T., and Takumi, T. (2004). Transcriptional oscillation of canonical clock genes in mouse peripheral tissues. BMC Mol Bio *http://www.biomedcentral.com/1471-2199/5/18*.

Yamazaki, S., Numano, R., Abe, M., Hida, A., Takahashi, R., Ueda, M., Block, G., Sakaki, Y., Menaker, M., and Tei, H. (2000). Resetting Central and Peripheral Circadian Oscillators in Transgenic Rats. Science *288*, 682-685.

Yanaihara, A., Otsuka, Y., Iwasaki, S., Aida, T., Tachikawa, T., Irie, T., and Okai, T. (2005). Differences in gene expression in the proliferative human endometrium. Fertility and Sterility *83*, 1206-1215.

Yang, Z.-M., Das, S., Wang, J., Sugimoto, Y., Ichikawa, A., and Dey, S. (1997). Potential sites of prostaglandin actions in the peri-implantation mouse uterus: Differential expression and regulation of prostaglandin receptor genes. Biol Reprod *56*, 368-379.

Yoon, S.-J., Choi, D.-H., Lee, W.-S., Cha, K.-Y., Kim, S.-N., and Lee, K.-A. (2004). A molecular basis for embryo apposition at the luminal epithelium. Mol Cell Endocrinol *219*, 95-104.

Yue, L., Daikoku, T., Hou, X., Li, M., Wang, H., Nojima, H., Dey, S., and Das, S. (2005). Cyclin G1 and cyclin G2 are expressed in the periimplantation mouse uterus in a cell-specific and progesterone-dependent manner: evidence for aberrant regulation with Hoxa-10 deficiency. Endocrinology *146*, 2424-2433.

Zhao, X., Ma, W.-G., Das, S., Dey, S., and Paria, B. (2000). Blastocyst H2 receptor is the target for uterine histamine in implantation in the mouse. Development *127*, 2643-2651.

Zheng, B., Albrecht, U., Kaasik, K., Sage, M., Lu, W., Vaishnav, S., Li, Q., Sun, Z., Eichele, G., Bradley, A., and Lee, C. (2001). Nonredundant Roles of the mPer1 and mPer2 Genes in the Mammalian Circadian Clock. Cell *105*, 683-694.